THE DESIGN, CALIBRATION, AND COMMISSIONING OF A BENCHMARK HYPERSONIC WIND TUNNEL

by

Jason M. Solomon

A thesis submitted to the faculty of
The University of North Carolina at Charlotte
in partial fulfillment of the requirements
for the degree of Master of Science in
Mechanical Engineering

Charlotte

2021

Approved by:

_____
Dr. Peter T. Tkacik

_____
Dr. Russell G. Keanini

_____
Dr. Jerry L. Dahlberg

©2021
Jason M. Solomon
ALL RIGHTS RESERVED

ABSTRACT

JASON M. SOLOMON. The design, calibration, and commissioning of a benchmark hypersonic wind tunnel. (Under the direction of DR. PETER T. TKACIK)

In 2020, the United States Department of Defense requested $3.2 billion to fund research and development in hypersonic defense programs for the fiscal year of 2021. The demand for funding in hypersonic research directly responds to the increasing gap between hypersonic weapon capabilities between the United States and foreign entities. This gap in hypersonic research stems from a lack of specialized personnel, facilities, and hypersonic academic programs in the United States. I argue that the improvements in U.S. hypersonic programs rely on increasing the availability and implementation of hypersonic academic courses and labs in the collegiate curriculum. My thesis expands on these improvements by correlating the process of researching, designing, and constructing a benchmark blow-down hypersonic wind tunnel to create trained graduate students prepared to work within the hypersonic research field. This hypersonic wind tunnel, which was designed and built by a multidisciplinary team of senior year college students under my leadership, can train students to evaluate and measure changes in pressure, temperature, flow velocity, shock wave angles, boundary layers, and additional properties of hypersonic flow up to Mach 5 as it flows over a solid body. It provides these capabilities through the use of various pressure sensors, pitot tubes, Schlieren imaging, and thermocouples that have been integrated throughout the design of the system. The collected experimental data is validated using CFD and other numerical simulation programs. I conclude with a discussion on the potential impact of training and preparing graduate students to answer the national call for hypersonic researchers and facility personnel.

DEDICATION

This thesis is dedicated to my late mother, Barbara Ann Solomon. Thank you for supporting me throughout my life and never giving up on me, no matter the situation. I was fortunate to have a loving, caring, and outstanding role model such as yourself. Your hard work and efforts have allowed me to experience our family and ancestors' wildest dreams and aspirations. Thank you for being my Mom.

Figure 1: Me and my mother

ACKNOWLEDGEMENTS

I want to thank the Office of Naval Research (ONR) for providing the research and materials necessary for building the benchmark hypersonic wind tunnel. In addition, I would also like to thank them for providing financial aid, networking opportunities, and research opportunities.

I want to thank the Office of Adult Students and Evening Services (OASES) at UNCC for selecting me as the recipient of four scholarships and one fellowship. Your financial aid support allowed me to focus on my academic work without worrying about financial constraints.

I'd also like to acknowledge my graduate advisor, Dr. Tkacik. I appreciate your experience, knowledge, support, and patience in working with me. I've learned a lot from you over these past three years and look forward to improving and applying the skills and abilities you've taught me.

I also would like to thank my graduate mentor, Dr. Jerry Dahlberg, for his outstanding leadership, guidance, and encouragement. Your hard work and determination in assisting students are unparalleled. Thank you for your dedication to veterans and academic success.

I want to thank Dr. Russell Keanini for his technical advice, inspiration, and compassion for fluid mechanics. I will always admire your devotion to research.

Last but not least, I want to acknowledge the experience, determination, and teamwork of the members of my senior design team: Michael White, Christian Struckmeyer, Michael Allen, and Rollins Stewart. Thank you all for your hard work and support.

TABLE OF CONTENTS

LIST OF TABLES

LIST OF FIGURES

LIST OF SYMBOLS

γ	Fluid Specific Weight
ρ	Fluid Density
ρ_p	Plenum Density
β	Oblique Shock Angle
μ	Mach Angle
a	Speed of Sound
c_p	Specific Heat
h	Enthalpy
h_s	Stagnation Enthalpy
M	Mach Number
P_d	Dynamic Pressure
T_t	Stagnation Temperature
g	Gravity
m	Mass
P_d	Dynamic Pressure
P_t	Stagnation Pressure
p	Pressure
Q	Volume Rate of Flow
Re	Reynolds Number

R Gas Constant

U Local Free Stream Velocity

V Velocity

CHAPTER 1: INTRODUCTION

Research methods in hypersonic flow are being conducted at several different scientific hypersonic test facilities were hyper-velocity fluid behavior is experimentally simulated. Some examples of these hypersonic research facilities are: the Glen Research Center at NASA (Sandusky, OH, USA) [1], the Sandia National Laboratories at Sandia (Albuquerque, NM, USA) [2], the ICARE Laboratory at Institut de Combustion, Aérothermique, Réactivité et Environnement (ICARE) (Orléans, France) [3], and the Vikram Sarabhai Space Centre (VSSC),(Kerala, India) [4]. Professional scientific research facilities utilize large scale hypersonic wind tunnels that allow very close to real world experimental simulation of hypersonic flow. These tunnels can be scaled down to produce similar experimental simulations that allows institutions to train future researchers.

This thesis outlines the design, calibration and commissioning of a small scale benchmark hypersonic wind tunnel. Six chapters are provided to give a detailed overview on the construction of the benchmark hypersonic wind tunnel, it's purpose, and capabilities.

Chapter 2 provides a background into hypersonic-related research, hypersonic theory, the methodology of design for hypersonic wind tunnels, and the national need for hypersonic specialized researchers. The purpose of this chapter is to provide the foundational understanding of hypersonic research and purpose that was used in the construction of UNCC's benchmark hypersonic wind tunnel.

Chapter 3 outlines the design for all the subsystems of the benchmark hypersonic wind tunnel. The complete design of the hypersonic wind tunnel required extensive research in making sure every component, from the frame to the command center,

interacted favorably with each other. Important items of consideration were safety, temperature/pressure control, power supply, flow visualization, CD nozzle sizes, dimensions of the testing chamber, data acquisition, and control systems. Each subsystem plays a major role in providing a critical function in managing those listed important considerations.

Chapter 4 describes the process of calibrating and installing sensors, actuators and additional apparatuses. Software programs such as MathWorks MATLAB, National Instruments LabVIEW, and Automation Directs DirectSOFT6 were used for data acquisition and the control system. The purpose of this chapter is to highlight the systems calibration process that was used to obtain ideal and accurate testing conditions and results.

Chapter 5 goes over the commissioning process of the benchmark hypersonic wind tunnel and its future research goals. The purpose of this chapter is to give an overview of the system procedures, capabilities, future training, graduate research, and course lab-work initiatives.

The concluding chapter discusses potential instrumental implementations for the future, career opportunities, and the potential industry impact that this benchmark hypersonic wind tunnel can provide.

CHAPTER 2: BACKGROUND

Within the last decade, the U.S. Department of Defense (DOD) has increased its researching efforts into hypersonic weapons and vehicles in response to the growing developments of international hypersonic vehicles and weapons system programs [5]. Chinese and Russian hypersonic weapon programs have encouraged an arms competition with the U.S. in securing offensive and defensive hypersonic countermeasures where the U.S. may be trailing behind [6]. Hypersonic research dates back to the 1940's where scientist John Becker built an 11-inch wind tunnel capable of reaching operating speeds of Mach 6.9 [7]. These hypersonic research facilities provide analytical data that help in designing, testing and building hypersonic weapons and vehicles. With the ever-growing interest in hypersonic research, researchers will be needed to address the call for further development on this topic. The research of hypersonic flow aims to understand and redefine the principles of how compressible flowing fluid particles behave while moving within an environment or over the surface of a solid body at speeds exceeding Mach 5. The complexity of hypersonic compressible fluid flow requires an understanding of fluid mechanics. This knowledge is key in making an extensive analysis using Computational Fluid Dynamics (CFD) and real world wind tunnel for design validations.

Five engineering students (Jason Solomon, Michael White, Michael Allen, Christian Struckmeyer and Rollins Stewart) were selected to build a compact educational hypersonic wind tunnel for their senior design capstone project at UNCC. These students were given a budget of $40,000.00 dollars to design, construct, test and present the progression of their project at UNCC's bi-annually senior design exposition. On December 6, 2020, the students completed the design and construction of the compact

educational hypersonic wind tunnel capable of achieving Mach 3 and Mach 5. It was presented at the senior design EXPO and won 4^{th} place out of 56 project entries for overall best senior design project. Our project, is loosely modelled after the Virginia Tech's hypersonic wind tunnel [8] and uses compressed air that is released via a fast-actuated valve to initiate flow through a heater, plenum, and a specific convergent divergent (CD) nozzle to achieve a desired Mach number for testing. Utilizing the numerous tools, devices, and software for this system, UNCC's is able to train graduate level hypersonic researchers. In addition to research, this system will be used as lab equipment for an military technology advanced experimental methods course.

Figure 2.1: UNCC Charlotte hypersonic wind tunnel researchers, Michael Allen (left) and Jason Solomon (right).

Table 2.1: Components of the manifold system.

Name	Team Role	Subsystem 1	Subsystem 2
Jason Solomon	Team Lead	Control System	-
Michael White	Team Member	Test Chamber	Schlieren Imaging
Christian Struckmeyer	Team Member	Frame	Manifold
Michael Allen	Team Member	Plenum	CD Nozzles
Rollins Stewart	Team Member	Diffuser	Silencer

2.1 The History of Hypersonic-Related Research

After the surrender of the Nazis in World War II, the United States welcomed leading German rocket researchers to the US, whose research on the V-2 rocket would prove to be paramount for the beginning of U.S. hypersonic research [9]. The Germans introduced and used experimental specialized nozzles at extremely high horsepower facilities that could reach speeds from Mach 8.8 to Mach 10. During this time, supersonic flow was the primary focus of ongoing research at Langley. However, several American researchers wanted to go beyond this flow regime.

Conducting high speed tunnel research on flow velocities exceeding Mach 4.5 proved to be problematic. One main issue was that air passing through the tunnel would experience liquefaction, which would cause errors in flow parameters. An aero-physics researcher from New York University had several ideas to deal with this issue so that we could reach true hypersonic testing flow velocities.

2.1.1 The Father of the X-15 and The American Hypersonic Wind Tunnel

Figure 2.2: NACA and NASA Chief Aero-Engineer, John V. Becker. Credit: NASA

Regarded as the father of the X-15, John Vernon Becker shown in figure 2.2, designed and built America's first hypersonic wind tunnel. Born in Albany, New York, 1913, John earned his bachelors degree in mechanical engineering with a focus in aero in 1935 from New York State University where he also earned his masters of science in aero engineering in 1936 [10].

2.1.1.1 The First American Hypersonic Wind Tunnel

In 1947, he built the first U.S. hypersonic wind tunnel, with a test section that was 11 inches square and capable of reaching Mach 6.6 [11]. Its high pressure tank could hold up to a maximum operating pressure of approximately 735 psi which incorporated an electric resistance heater to fight against liquefaction from initial low temperatures by raising its charging temperate to **900 degrees Fahrenheit**. In

figure 2.3, a diagram is shown of all the components used in this tunnel. This was a groundbreaking advancement into hypersonics. His wind tunnel was considered a blow down facility in that it was not continuous and could only provide a 45 second testing window [12]. This facility was operational for 20 years up until 1973, where it was disassembled and donated to Virginia Polytechnic Institute and State University (VT) [9].

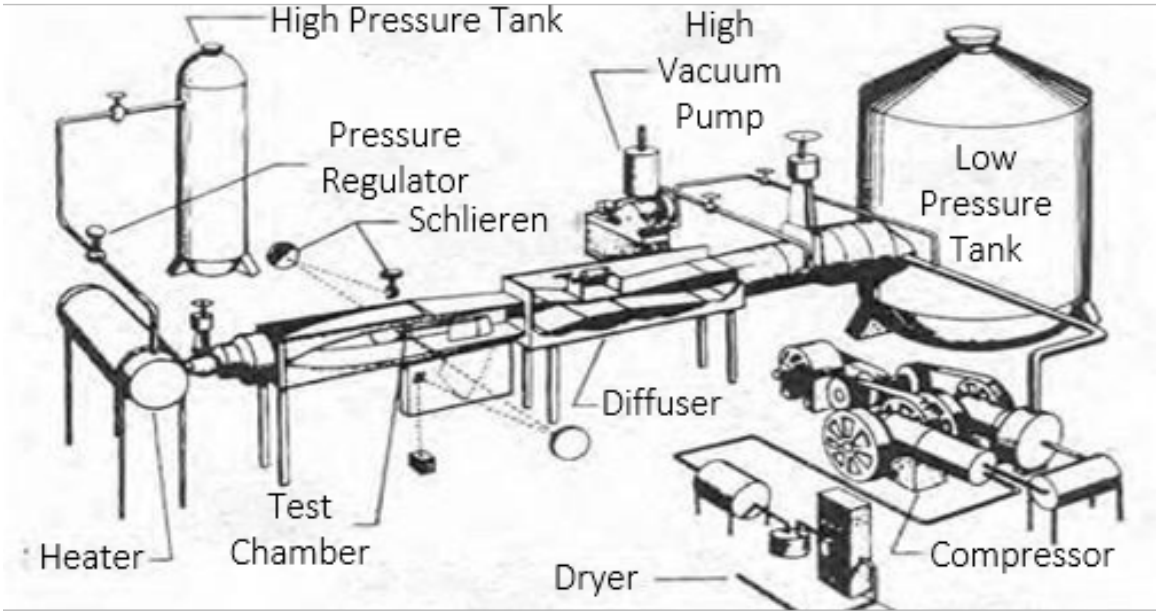

Figure 2.3: John Becker's 11-inch hypersonic wind tunnel. Credit: NASA

2.1.1.2 Influence Of Diversity in Aerospace Engineering

Around this time, Becker was preparing for retirement so he could focus on consulting. Several years earlier, a young African-American mathematician woman, named Christine Darden was hired at NASA to work in computer programming. Darden, shown in figure 2.4, faced workplace discrimination of being passed up on promotions because of her ethnicity and primarily her gender while working in the computer rooms of NASA. Growing tired of being passed up on promotions by her male counterparts, she requested to be transferred to an engineering section at NASA, which inadvertently almost cause her to be fired. At the time, Becker was the chief of

Aero-Physics Research Division, ad aerospace engineering division that Darden was requesting to be transferred to. Becker took on Darden and promoted her to aerospace engineering position. A position that was rarely occupied by women. Darden went on to excel as an aerospace engineer and earned her PhD in engineering at George Washington University while working at NASA. She would go on to author over 50 publications, receive numerous awards, featured as a researcher in the movie "Hidden Figures" and became the first African-American woman to be promoted into Senior Executive Service at NASA's Langley Research Center.

Figure 2.4: American mathematician, data analyst, and aeronautical engineer Christine Darden in Langley's Unitary Plan Wind Tunnel, 1975. Credit: NASA

2.2 Hypersonic Vehicles

Hypersonic aircraft are vehicles that travel significantly faster than the speed of sound. Most combat jets fly at supersonic speeds, which is slightly faster than the speed of sound. The difference between combat jets and hypersonic aircraft is that hypersonic aircraft travel at speeds where fluid molecules, such as oxygen and nitrogen, dissociate from the increasing flow temperature. The increasing temperature

changes the fluid's viscosity and causes several issues for designing vehicle aerodynamics and flight controls for a hypersonic aircraft. I have listed several hypersonic research vehicles below and some of their statistics.

2.2.1 North American X-15

The North American X-15 is an X-series rocket-propelled hypersonic aircraft [13]. Built by North American Aviation and operated by NASA and the United States Air force, the X-15 set multiple altitudes and speed records during the 1960s [14]. It was able to bring valuable flight data from reaching the edge of outer space and safely returning. As seen in table 2.2, the highest speed recorded was at Mach 5.9 at an altitude of 19.3 miles by the pilot, William J. Knight [15]. John V. Becker led the initial program to develop and test the X-15 [16].

Figure 2.5: North American X-15 pulling away. Credit: U.S Air Force

Table 2.2: Components of the manifold system.

Date	Top Speed	Altitude	Pilot
July 26,1962	Mach 5.20	18.7 mi	Neil Armstrong
December 5, 1963	Mach 5.24	19.1 mi	Robert A. Rushworth
November 9, 1961	Mach 5.33	19.2 mi	Robert M. White
June 27, 1962	Mach 5.35	23.4 mi	Joseph A. Walker
October 3, 1967	Mach 5.90	19.3 mi	William J. Knight

2.2.2 X-20 Dyna-Soar Program

The X-20 Dyna-Soar, short for Dynamic Soarer, was a one-pilot experimental space vehicle designed by the United States Air Force for space missions [17]. The X-20 never took flight as this program was canceled on December 10, 1963, shortly after its construction [18]. This vehicle was designed to briefly experience space flight, resulting in hypersonic-re-entry speed back into the earth's atmosphere. It would use a rocket stage booster to reach its suborbital yet outer atmosphere altitude [19]. It would use its wings to create an aerodynamic lift that would allow it to glide long distances to its destination or target. Figure 2.6 shows the X-20 model on display with two people for a scaling reference.

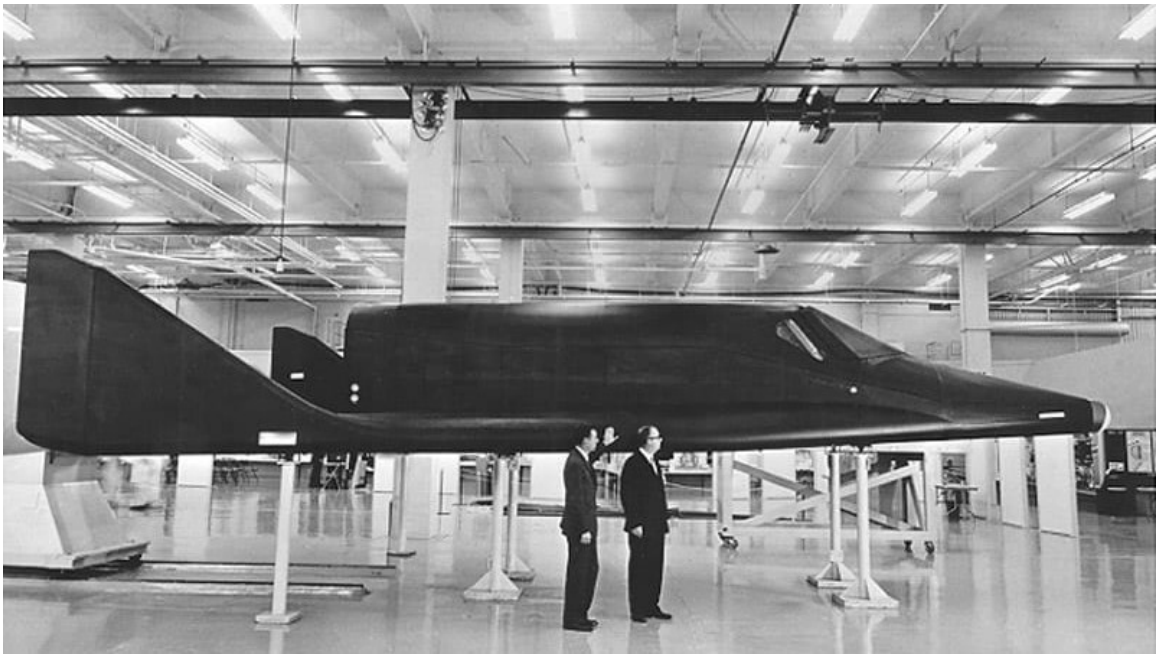

Figure 2.6: North American X-20 model on display. Credit: U.S Air Force

2.2.3 NASA X-43 X Hyper Scramjet

The X-43 was designed by NASA, who commissioned Micro Craft to build the airframe and General Applied Science Laboratory (GASL) to build the engine [20]. The X-43 is an experimental crewless rocket-boosted hypersonic scramjet aircraft with three variant scaled sizes (X-43A, X-43B, and X-43C) [21]. The X-43A has set the record as the fastest aircraft, reaching approximately Mach 9.6 (7365.78 mph) on November 16, 2004 [22]. The X-43 is "stacked" on top of a winged booster rocket launched mid-flight from a B-52 aircraft. Once the winged booster reaches its targeted speed and altitude, the X-43 detaches and reaches its maximum velocity via its scramjet engine [23]. Figure 2.7 shows the X-43 being prepared for test flight atop its booster rocket [24].

Figure 2.7: North American X-15 being prepped for a test flight. Credit: U.S Air Force

Table 2.3: Components of the manifold system.

Date	Top Speed	Altitude	Pilot
November 16, 2004	Mach 9.6	20.8 mi	X-43A

2.3 The Theory Behind Hypersonic Flow

To explain the dynamics of hypersonic flow, first, we should begin to understand what it means for an object to travel at hypersonic speed. Hypersonic flow occurs when a solid object or fluid flow moves at an extremely high speed or velocity [25]. This instance could be a high-speed object moving through a fluid or a high-speed fluid flow passing over a solid body. A hypersonic flow can range between 3,800 mph to 32,000 mph. At this range of speed, the fluid's temperature, density, and molecular properties undergo significant changes. Hypersonic wind tunnels measure, observe and analyze these property changes. A hypersonic wind tunnel typically holds a solid-bodied object stationary in a test chamber while the fluid flow passes over the

object. During testing, pressure, temperature, density, and many other fluid property measurements are collected and analyzed to improve hypersonic applications and discoveries. *Hypersonic flow research* is a critical science used in aerospace and defense programs. This research revolves around four classifications of fluid flow regimes that develop around solid aerodynamic bodies [26]. The flow regimes or classifications are: subsonic, transonic, supersonic, and hypersonic. These classifications are used to design and test re-entry space vehicles, race cars, golf balls, long distant weapon systems, and wind tunnel testing systems. They are characterized by a unit of measure called a Mach number. Named after the 19^{th} century, Austrian physicist Ernst Mach [27], the Mach number of a fluid flow can be determined by the number of times the speed of sound an object or flow is moving [28]. Therefore, the Mach number, M, is equal to the local velocity, U, divided by the speed of sound, a, as depicted in equation 2.1.

$$M = \frac{U}{a} \tag{2.1}$$

2.3.1 Incompressible Flow and Compressible Flow

Incompressible flow is a fluid flow that cannot be compressed from an external pressure application [29]. The volume of this flow cannot be reduced, nor will the density change due to a change in pressure. The range of velocity as it pertains to incompressible flow is $0 > M > 0.3$ [30]. *Compressible flow* is a fluid flow that can compress from external pressure applications. Here, the volume of this flow can vary for a change in pressure, resulting in a change in density. The range of velocity for compressible flow is $0.3 < M < \infty$ and becomes more dominant the larger the Mach number [31]. Hypersonic research is primarily concerned with compressible flow because of the abrupt fluid property changes.

2.3.2 Subsonic Flow

Figure 2.8: Schematic of subsonic flow.

Subsonic flow occurs when an object or flow moves at a relatively lower speed than the speed of sound [32]. A flowing velocity with a range from $0 < M < 1$ is considered a subsonic flow. Both incompressible and compressible flows can occur separately or simultaneously within a subsonic flow [33]. A bullet, car, and a golf ball typically travel at subsonic speeds.

2.3.3 Transonic Flow

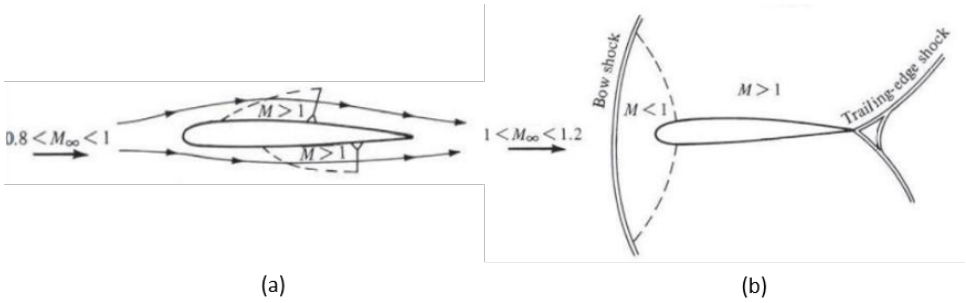

Figure 2.9: Schematic of transonic flow.

At the transonic flow regime, the sonic flow around a solid body can be greater than or less than that of the speed [34]. The result is that the solid body experiences subsonic and supersonic flows at different locations within the flow. Transonic flow usually takes place at $0.8 > M > 1.2$, however, for simplification, it is commonly classified as being $M \approx 1$ [35].

2.3.4 Supersonic Flow

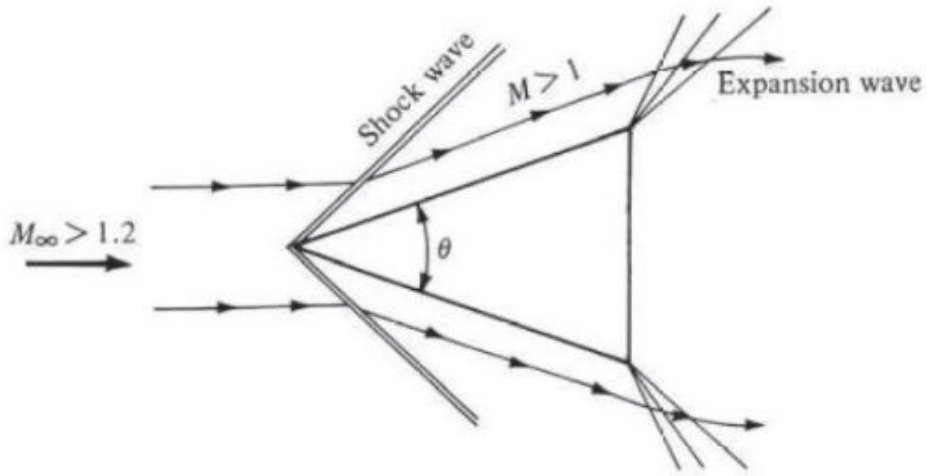

Figure 2.10: Image of John Becker with Hypersonic Wind Tunnel.

When an object is traveling at a velocity above the speed of sound, $M > 1$, it is said to be supersonic [36]. Shock waves form in a supersonic flow due to an abrupt change in pressure, density, and nearly discontinuous temperature. The abrupt change in fluid properties generates an enormous sound called a sonic boom. Shock waves are irreversible propagating disturbances that carry energy and dissipates quickly as distance increases [37]. Similar to the circular waves that form when a pebble dropped into a still body of water. **Here, energy is preserved; however, entropy increases**.

2.3.5 Hypersonic Flow

Figure 2.11: Image of John Becker with Hypersonic Wind Tunnel.

A hypersonic flow typically occurs when an object or fluid flow moves at $5 > M > 42$. Strong shock waves are produced that create significantly high gas temperatures [38]. At Mach 5, molecular bonds vibrate within the fluid at an approximate temperature of 800^oC and begin to alter the magnitude of forces acting on the solid body. As the Mach number increases from Mach 5, the flow temperature increases, and oxygen and nitrogen molecules dissociate into oxygen and nitrogen atoms. The result is the creation of shock waves that cause variations in density and pressure. At Mach 5, research regarding sonic flow will have to be considered substantially different from previous sonic flows [39]. Some examples of hypersonic objects are NASA's X-43 experimental scramjet aircraft and the U.S. Air Forces X-51 scramjet engine demonstrator.

It is important to remember these foundational properties of flow regimes so that proper fluid mechanic equations and formulas are used while conducting research. Table 2.4 below lists the flow classifications of these flow regimes.

Table 2.4: Sonic Flow Classifications

Flow Regime	Mach Number	Velocity m/s	Density Gradient	Shock Waves
Subsonic	$0 > M > 1$	$102.9 > 343$	Small	None
Transonic	$M \approx 1$	≈ 343	Significant	First Appear
Supersonic	$1 > M > 5$	$343 > 1715$	Significant	Significant
Hypersonic	$5 > M > 42$	$1715 > 4802$	Dominant	Dominant

2.3.6 Shock Waves

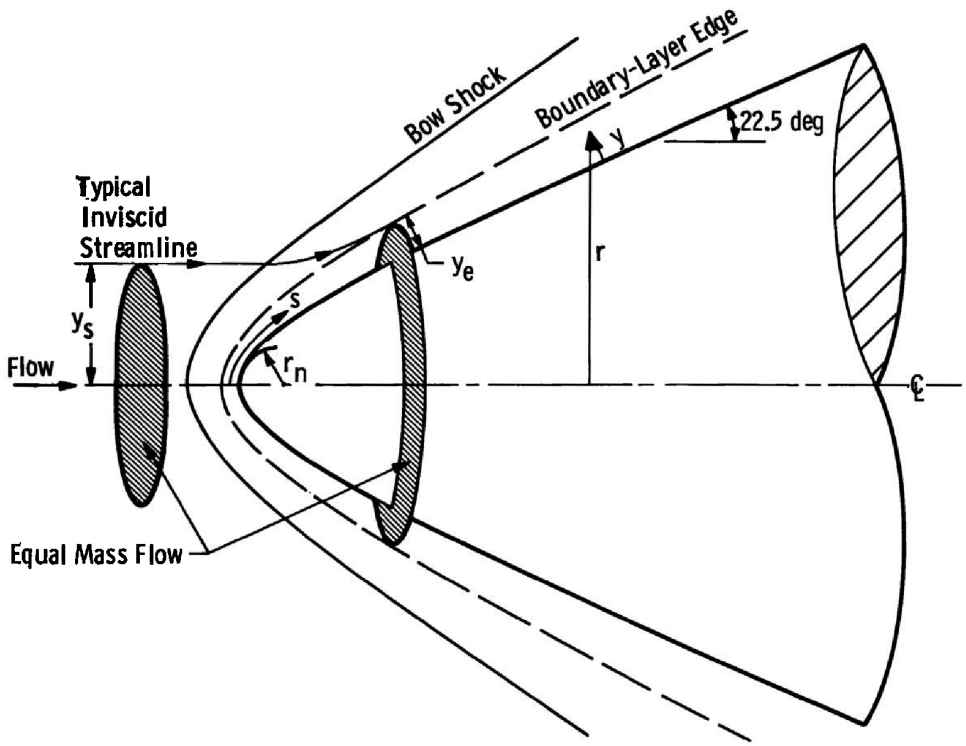

Figure 2.12: Image of shock wave phenomena at hypersonic speed.

The shock waves that cause thermal effects on a solid body in hypersonic flow are significant in hypersonic research [40]. Consider a wedged-shaped solid body. When this wedged-shaped passes through a supersonic flow, a shock wave, or oblique shock, will attach and form a shock cone at the sharp tip of the wedge. As the Mach number increases, the angle of the oblique shock will decrease, which reduces the distance between the shock wave and the surface of the wedge. At hypersonic speeds, the shock wave can become extremely thin and inviscid [41]. The area between the wedge surface and the shock wave is called the shock layer.

When this solid body passes through air at subsonic speeds, a thin region close to the surface, called a boundary layer, is formed. At this speed, this boundary layer will decrease in thickness due to an inverse relationship between boundary layer thickness, δ, and the Reynolds number, Re_x, as shown in equation 2.2.

$$\delta \propto \frac{x}{\sqrt{Re_x}} \tag{2.2}$$

Compressible flow behaves differently in that the boundary layer thickness expands with an increase of speed that causes an increase in flowing temperature from frictional heat. The viscosity and the density in the air are the primary driving forces for the boundary layer's increase in thickness. Therefore, when experiencing high-velocity compressible flow, the variance in boundary layer thickness is due to the square of the Mach number:

$$\delta \propto \frac{M^2}{\sqrt{Re_x}} \tag{2.3}$$

An enormous amount of drag can form when this boundary layer rapidly increases in size at high Mach numbers. If the boundary layer becomes too thick, a viscous interaction can occur where the boundary layer interfaces with the shock wave, creating a shock layer and an inviscid layer within the shock wave. The flow field within the inviscid layer can affect skin friction and surface pressure distributions. Engineers have to consider aerodynamic design on changes in thermal properties, drag, lift, and overall vehicle stability.

2.4 Hypersonic Wind Tunnel Type and Design Methodology

There are several design regimes for hypersonic wind tunnels. Many hypersonic wind tunnels cannot simulate all physical properties, such as real gas effects, concerning hypersonic flow no matter its design [42]. However, heat transfer data, force, and pressure data can be obtained and manipulated to produce additional information about the testing flow. Most high-speed wind tunnels utilize an air compressor, high-pressure air storage, heater, starting valve, CD nozzle, test section, diffuser, vacuum valve, low-pressure vacuum tank, and a vacuum pump for its operation. However, some high-speed tunnels attempt to reach hypersonic flow using other methods and

components.

2.4.1 Quiet Tunnel - Purdue-Boeing

In 2001, Boeing and the Air Force Office of Scientific Research (AFOSR) funded Purdue University to design and develop a Mach-6 Quiet Tunnel [43]. This quiet tunnel utilizes a Ludwieg tube concept, named after its inventor and German professor, Dr. Hubert Ludwieg, that produces high-speed flow at short increments. The driver tube is 122 feet with a diameter of 18 inches that feeds into a 9.5-inch convergent-divergent (CD) nozzle. High pressure is held downstream of the tube and the nozzle by a thin double-diaphragm. The diaphragm is ruptured by a piercing tool or by a vacuum valve, as shown in figure 2.13. Once the diaphragm is ruptured, shock waves will propagate into the 4000 cubic foot vacuum chamber, while an expansion wave will propagate back towards the nozzle and driver tube. The unsteady expansion wave creates a steady flow into the CD nozzle that will accelerate the flow to supersonic and hypersonic speeds. This high Reynolds number operating quiet tunnel is currently the largest facility globally.

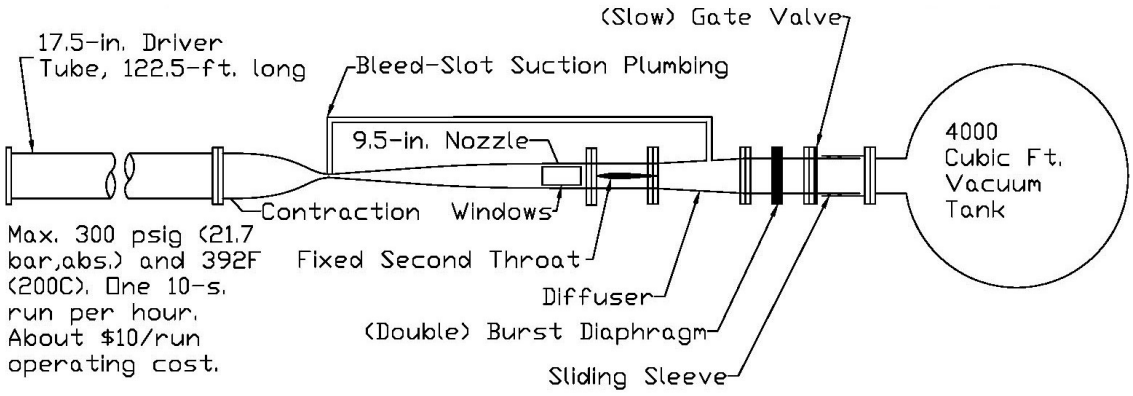

Figure 2.13: Schematic of Boeing Mach-6 Quiet-Flow Ludwieg Tube. Credit: Purdue Engineering-Purdue University

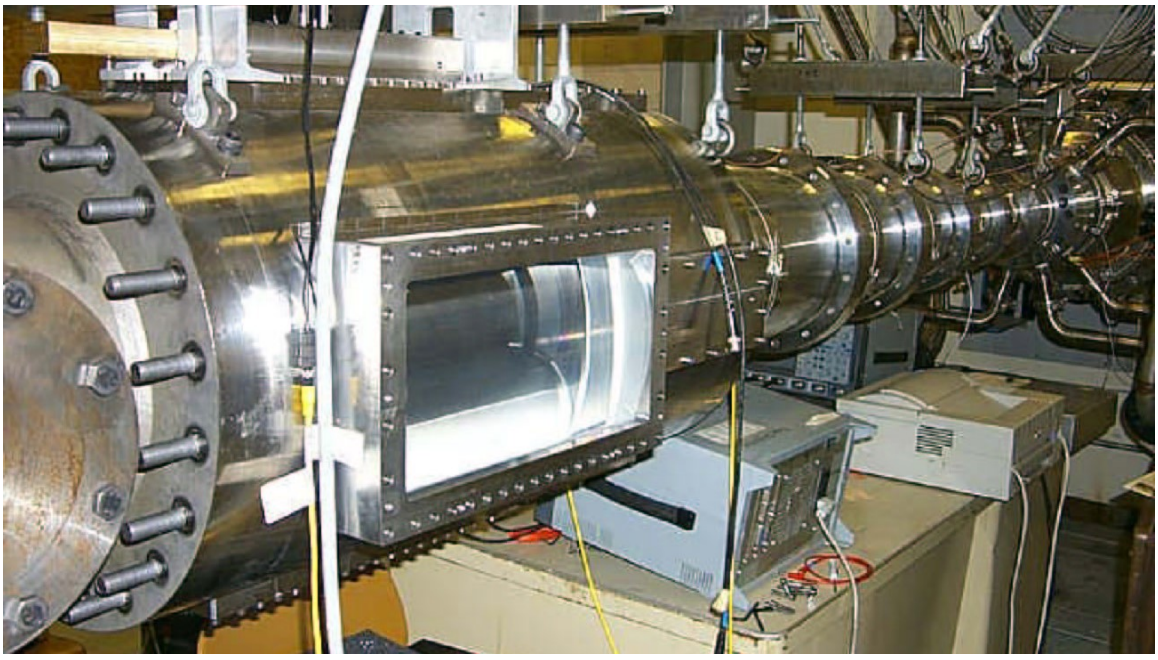

Figure 2.14: The Boeing Mach-6 Quiet-Flow Ludwieg Tube. Credit: Purdue Engineering-Purdue University

2.4.2 Shock Tunnel - AMES Electric Arch Shock Tube

The AMES Electric Shock Tube (EAST) is a research facility that analyzes radiation data from hypersonic flow created by simulating shock-heated gas environments encountered by re-entry space vehicles. It's flow velocity range is from Mach 1.3 (997.5 mph) to Mach 134 (102,814 mph) at a pressure range of $1.93x10^{-3}$ psi to 76.87 psi for a variety of planetary atmospheres [44]. It is the only shock tube facility capable of collecting this specialized data used in the validation of computational fluid dynamics (CFD) and design for hypersonic vehicles. It works similar to the quiet tube used at Purdue; however, EAST uses a driver tube is 29.5 feet and a conical arc driver to pierce its diaphragms. In figure 2.16 the conical diver is seen at the right side with numerous wires connected.

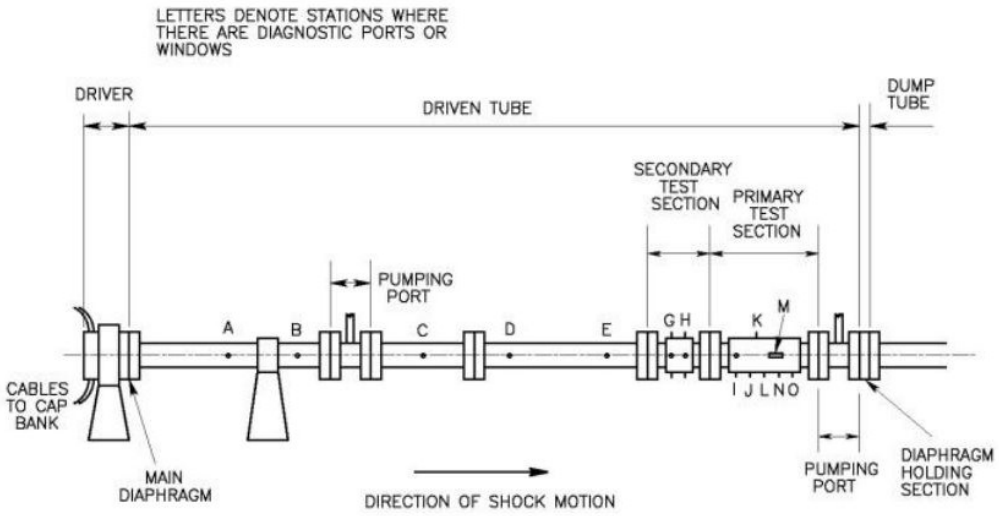

Figure 2.15: Schematic of NASA's AMES Research Center's electric arc shock tube. Credit: ELORET Corporation/David W. Bogdanoff

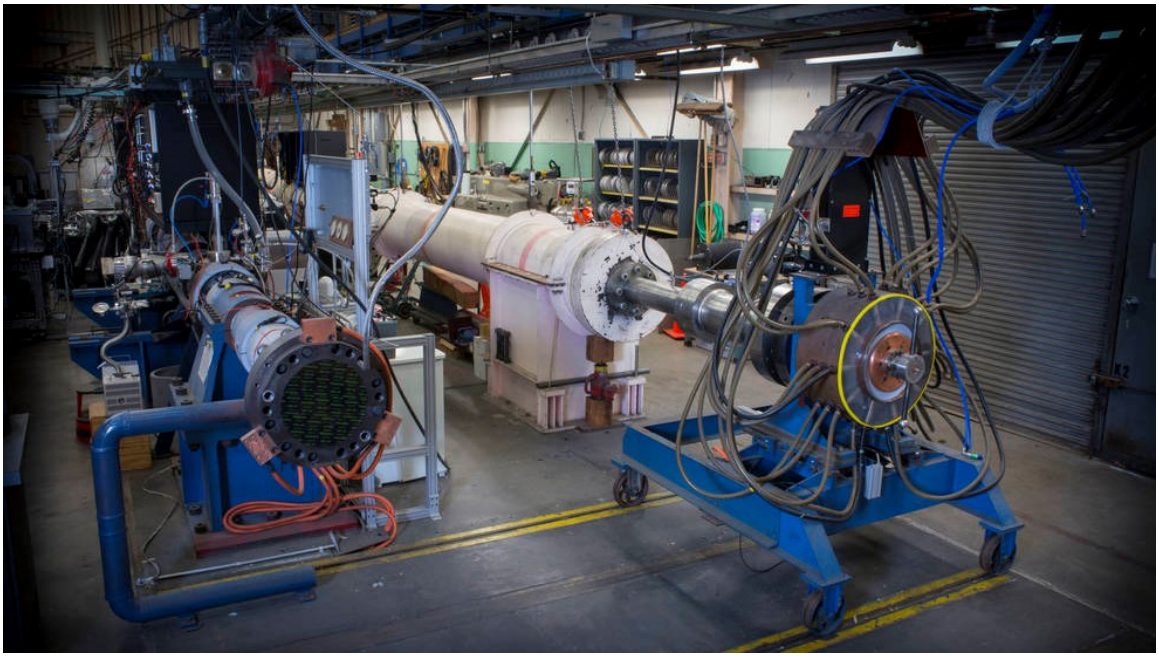

Figure 2.16: NASA's AMES Research Center's electric arc shock tube. Credit: NASA

2.4.3 Blowdown Tunnel - Sandia National Laboratories

The most common hypersonic wind tunnel is the blowdown variant. Sandia National Laboratories utilizes a blowdown hypersonic wind tunnel with 18-inch modular test sections capable of reaching Mach 5, Mach 8, and Mach 14. Test runs take place for 45 seconds at 45-minute intervals [45]. Test models can be mounted in the testing section with a series of angles of attack. This system uses high-pressure air for Mach 5 test runs and nitrogen for Mach 8 and Mach 12 test runs. It utilizes compressed air heated up to 2500°F with an electric heater and released through a nozzle that converts high-pressure low-velocity gas to hypersonic speeds. A valve upstream of the nozzle and a vacuum valve are instantly opened simultaneously to release the high-pressure flow. Some of these components are in the schematic shown in figure 2.17 below.

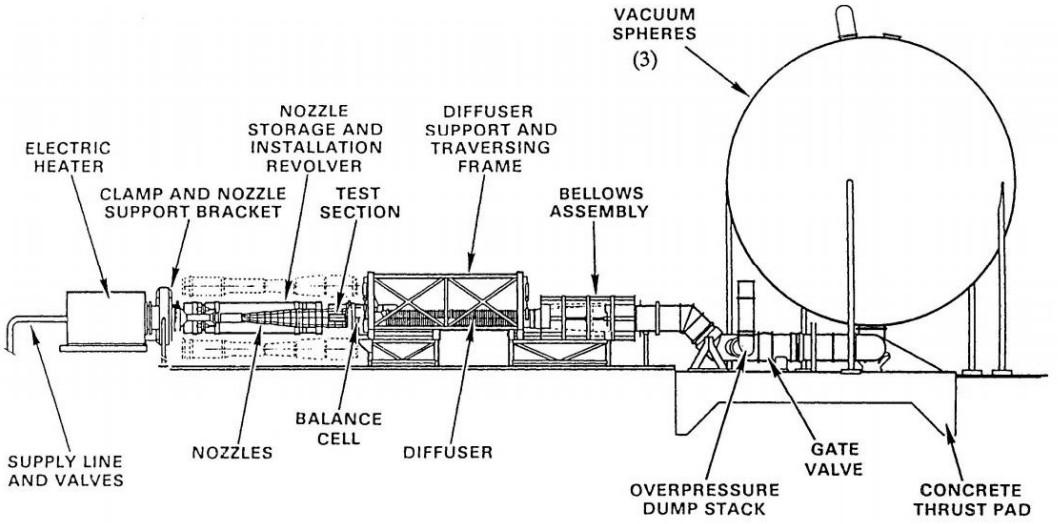

Figure 2.17: Schematic of the Sandia HWT in its modern configuration from 1977 until the present. Credit: Sandia National Laboratories

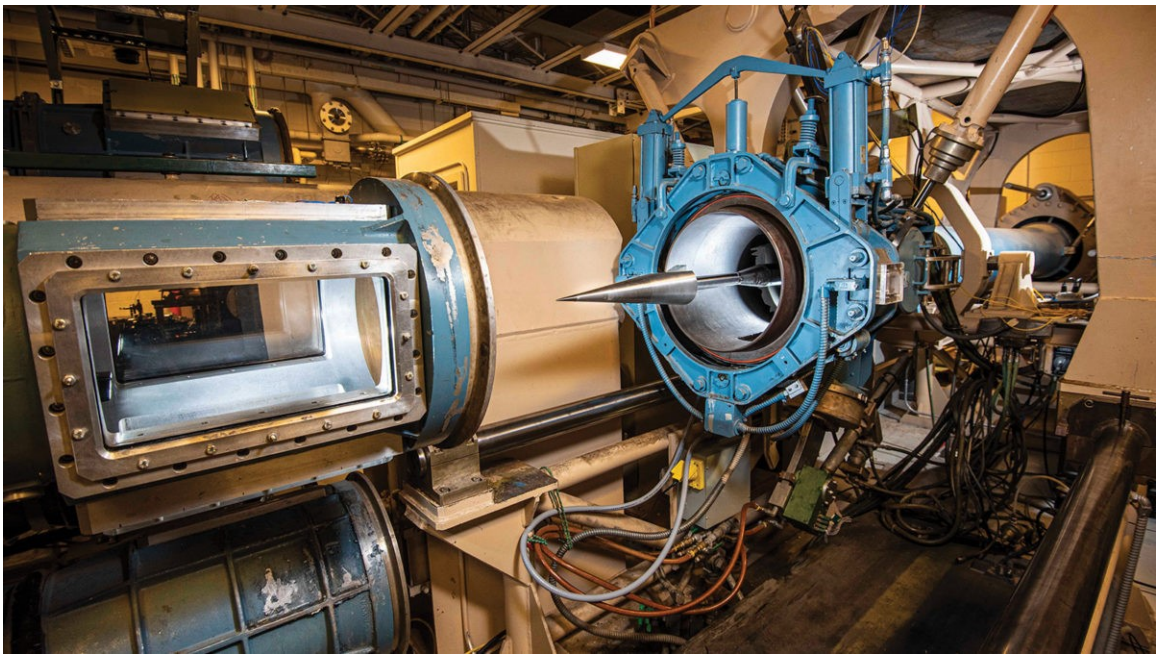

Figure 2.18: The Sandia blowdown hypersonic wind tunnel, capable of reaching Mach 5, 8, or 14. Credit: Sandia National Laboratories/Randy Montoya

2.5 The National Call for Hypersonic Researchers

International states are constantly competing for offensive and defensive weapon capabilities. Hypersonic weapons have been **identified** as a critical component for national defense as it pertains to future wars by The National Defense Strategy in 2018 *ADDREFERENCE*.

2.5.1 International Competition

The increasing development of hypersonic weapon programs in Russian and China has urged the US department of defense (DOD) to strengthen a hypersonics weapon program that can complete. The Pentagon issued a total of $2.6 billion to the DOD for hypersonic research in 2020. As of 2021, an additional request for $3.2 billion has been fulfilled, which included a $206.8 million request for a hypersonic defense program [5]. This funding of hypersonic-related research is intended to help provide equipment, materials, research facilities, and new hire researchers for academic institutions and government research facilities. Unfortunately, the United States is trailing behind China and Russia in hypersonic-related research and testing while other countries, such as India, Germany, France, and Australia, are developing their hypersonic research initiatives. According to a published article from the Atlantic Council, Russia tested a hypersonic glide vehicle (HGV) reported to reach speeds above Mach 20 in 2018.

Figure 2.19: The Russian Zircon hypersonic cruise missile is launched from the Admiral Groshkov frigate on Oct. 7, 2020, in the White Sea. Credit: Russian Defense Ministry Press Service via AP

China conducted 20 times more hypersonic tests than the United States in 2018, as reported in a CRD report [6]. Their hypersonic wind tunnel is said to have the capability to reach Mach 25.

Figure 2.20: Chinese military vehicles carrying DF-17 ballistic missiles rolled through Beijing during in a parade to commemorate the 70th anniversary of Communist Party power.

In the United States, there are approximately 48 specialized test facilities for hypersonic-related research where the number of personnel and research initiatives are falling behind its competitors. USAF Chief Scientist Richard J. Joseph has stated that the number of specialized personnel available to carry out hypersonic efforts is insufficient in the United States [46]. A 2020 Government Accountability Office (GOA) document mentions that the DOD lacked documentation on roles and responsibilities for the development of hypersonic-related research. The challenges of managing human capital in this field revolve around gender, age, lack of diversity, new hires, and hypersonic-focused academic programs for college students. In the conclusion of this thesis, A discussion of how aerospace and hypersonic-related research and academic programs can help close the gap in hypersonics human resources.

2.5.2 The Joint Hypersonic Transition Office

The Joint Hypersonic Transition Office (JHTO) was established on October 15th, 2020 [47]. Its purpose is to form policies to advance hypersonic technologies, transition them to operational purposes, coordinate in international partnerships, and reinforce the hypersonics workforce. To address the nation's academic community and call for hypersonics researchers, JHTO has established a university consortium initiative for hypersonic-related research and workforce development [DoD Establishes JHTO SEFA at NSWC Crane]. Texas A&M University is one of the first universities to support the JHTO university consortium. Their Engineering Experiment Station was awarded $ 20 million per year for five years to help manage the University Consortium for Applied Hypersonics (UCAH) program under the JHTO. This program will create research pathways between government organizations, national colleges, and industry partners to improve future hypersonic research initiatives. Many colleges and institutions such as the Massachusetts Institute of Technology, University of Arizona, University of Tennessee Space Institute, and Morgan State University will provide the UCAH with a fantastic board of experts in its initial operations. These collegiate entities will team up with government and industry partners to encourage significant engagements to prepare academic institutions to contribute to the nation's call for hypersonic-related research [DoD Awards UCAH Contract]. Currently, the UCAH accommodates over 100 universities and 500 researchers that provide the workforce and hypersonic-related research crucial for these programs.

The collaboration between universities, researchers, and industry partners was created to reduce research inefficiencies by fostering opportunities for non-traditional performers (collegiate and foreign ally researchers) while balancing a healthy workforce to meet national threats immediately and discover groundbreaking scientific phenomena [Leveraging University Expertise to Accelerate Hypersonic Technology Dev]. Because the primary vision for the UCAH is to provide high-speed flight capa-

bilities to war-fighters, industry combat vehicle experts such as Lockheed Martin are closely tied in support. Lockheed Martin shares hypersonic-related research facilities with Texas A&M. This proximity of collaborative research can provide a workforce recruitment funnel for Texas A&M students working on hypersonic projects to transition into Lockheed Martin researchers as interns or after graduation [The Hypersonics Force Multiplier] [48]. Additionally, the UCAH also provides funding to universities for hypersonic-related research project papers if the applicant is a university-affiliated UCAH member through its Project Call initiative. [UCAH Project Call]. The JHTO helps answer the nation's call for specialized hypersonic researchers and research facilities through programs such as the UCAH that bridge the gaps between government, collegiate, and industry hypersonic-related research. To get involved, universities with aerospace programs must establish hypersonics-related curriculum, projects, and research initiatives to assist in the nation's call for research.

CHAPTER 3: DESIGN

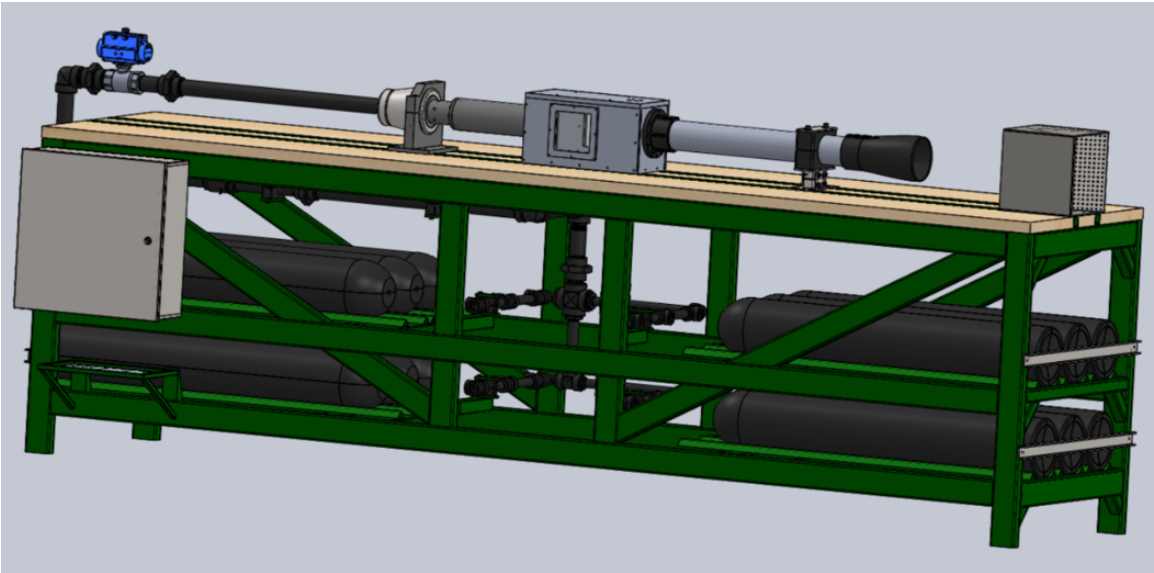

Figure 3.1: CAD image of the UNCC benchmark hypersonic wind tunnel

Virginia Tech's operational hypersonic tunnel heavily influenced the benchmark hypersonic wind tunnel at UNCC. They call the Model Aerodynamic Facility (MAF). Their frame was donated to their lab from the Russian Academy of Sciences Division Institute of Theoretical and Applied Mechanics. Our senior design team was invited to visit this lab and witness a demonstration of MAF operating at Mach 2. They allowed us to collect images and measurements and provided us with documents that outlined its operating procedures, test results, and capabilities. Figure 3.2 shows an image of their initial setup, while figure 3.3 shows engineering drawings of the Virginia Tech hypersonic wind tunnel. In that design, it initially used eight pressure vessels. In 2019 they increased the number of pressure vessels from eight to sixteen larger capacity tanks and replaced a small high air compressor with two larger, high-powered compressors to charge their system with air.

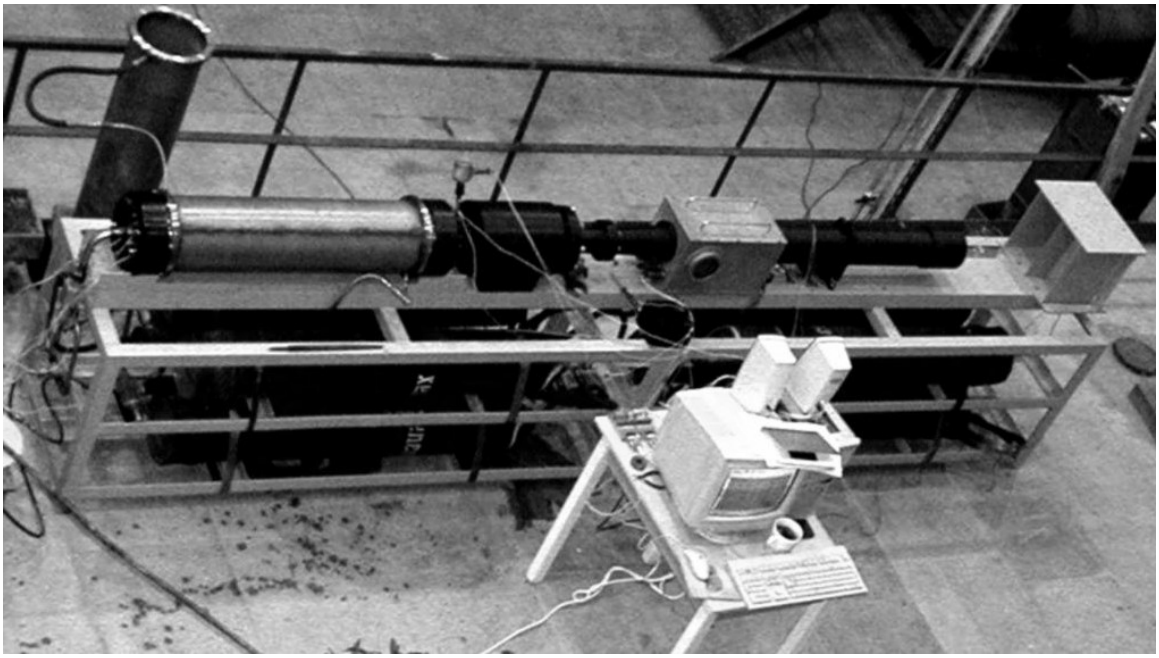

Figure 3.2: Virginia Tech Hypersonic Wind tunnel. Credit: Russian Academy of Sciences Siberian Division Institute of Theoretical and Applied Mechanics.

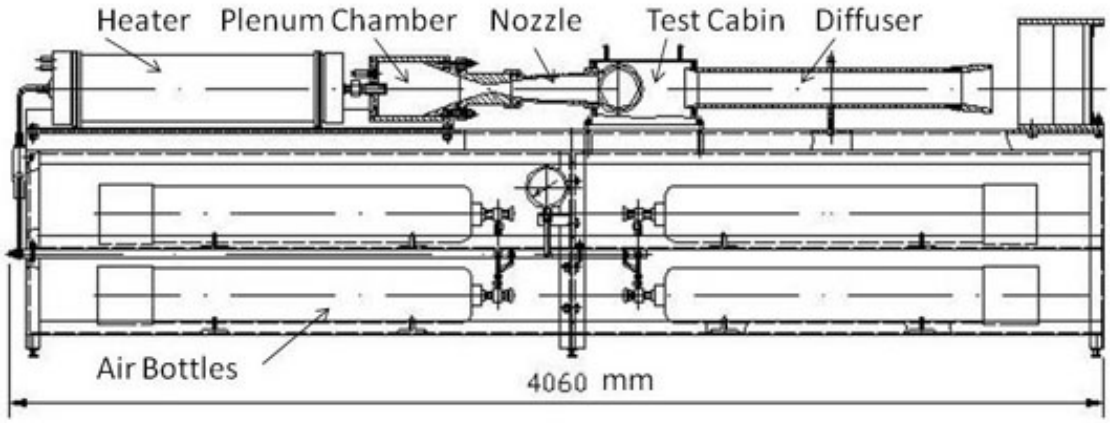

Figure 3.3: Virginia Tech Hypersonic wind tunnel drawing. Credit: Russian Academy of Sciences Siberian Division Institute of Theoretical and Applied Mechanics.

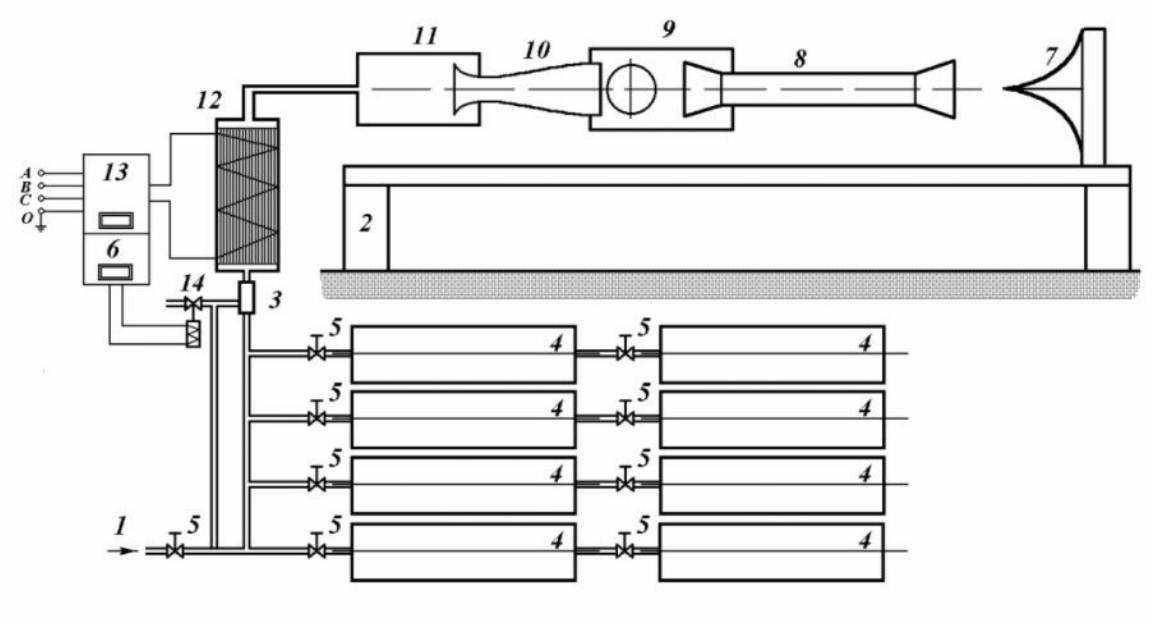

Figure 3.4: Sketch of the Model Aerodynamic Facility MAF for student's research and instructions. Credit: Russian Academy of Sciences Siberian Division Institute of Theoretical and Applied Mechanics.

Table 3.1: Item numbers for the VT HSWT parts in figure 3.4

Item Number	Component	Item Number	Component
1	Air Supply	8	Diffuser
2	Frame	9	Working Section
3	Main Valve	10	CD Nozzle
4	Pressure Vessel	11	Plenum
5	Manual Valves	12	Heater
6	Timer Control	13	Power Supply
7	Silencer	14	Control Valve

The frame of the VT tunnel is made mainly from steel angle iron coated in grey paint. Its dimensions are approximately 13-feet long, 2.5-feet wide, and 3.5 feet tall. The sixteen pressure vessels are stored upright off approximately five feet to the rear

of their frame and are secured using custom aluminum-built t-slotted framing rails. Its manifold is constructed from high-pressure steel pipes and high-pressure steel-woven flex lines fed from the sixteen pressure vessels into the fast actuated valve. The fast valve was fed directly into the heater via a one-inch pipe, and the heater fed into the plenum/settling chamber with a one-inch pipe. In order to reach specific Mach numbers, they have individual steel CD nozzles specifically designed to reach Mach 1 through Mach 8. The test section is also made of steel with dimensions 9" x 9" x 15". Two 1.2-inch optical windows are located on both sides of the test chamber for process visualization. The diffuser is made of steel and has an approximate length and diameter of 36 inches and 6 inches, respectively. Between the inlet and the diffuser outlet, there is a variable working zone of approximately four to ten inches. This four to ten inches working zone helps provide hypersonic flow without a vacuum chamber. The silencer-deflector has a height of 1 foot, while the width is about 1.25 feet. It utilizes a 30-degree wedge with a knife-edge perpendicularly mounted towards the exhaust jet from the diffuser to reduce noise and vibrations. This design is very similar to the 11-inch hypersonic wind tunnel that John Becker designed in 1947, shown in figure 2.3.

3.1 Frame

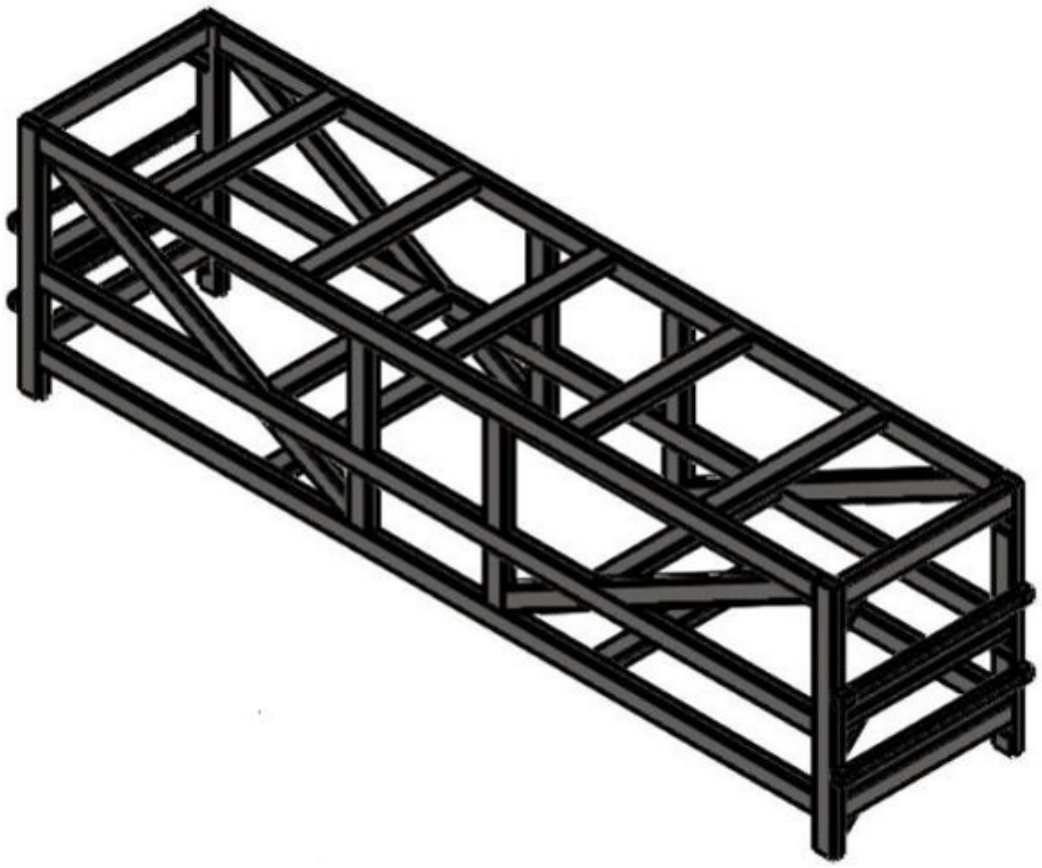

Figure 3.5: CAD image of the benchmark hypersonic tunnel frame.

A frame is a load resisting subsystem of structural materials that provides an engineering system with structural support by transferring loads through interconnected joints or members. In order to build a compact and mobile wind tunnel system that could house the majority of the subsystems, a frame had to be designed to provide safety and convenience. The frame provides a durable and rigid foundational support for all the completed benchmark hypersonic wind tunnel subsystems. It allows all subsequent subsystems to connect and work together to function correctly. The frame contacts the ground at four points; each point has an adjuster to account for the uneven ground to guarantee that the frame will not be able to shift under load. The air compression tanks are used to provide pressure to the system are fixed and

secured within the frame. Each tank has an individual tray to keep the tank from rolling. The manifold system is mounted inside the frame. The remaining components (Valve, Heater, Plenum, Nozzle, Test Chamber, Diffuser, and Silencer) are bolted to the top of the frame. The top of the frame incorporates a rail system that allows components to be adjusted for each nozzle since they vary in length. A control panel that houses all the electronics used to operate and compile data is attached to the frame's side.

At Virginia Tech, the MAF frame is designed to secure all parts of the HSWT. The frame configuration consists of two related supports with 23.6"x27.5"*78.7 inches. The guide rails in the channel are fixed on the support's top surface, and the central device units are mounted to them [49]. The supports have regulating screws to guarantee the horizontal position of the guide rails at assembling. For convenient transportation, the supports are separated from each other. Inside both sides of the body, there are four pressure vessels for collecting and storing working gas. Here, a manifold collector is connected to the pressure vessel and a manometer for pressure control. The basement must be electrically grounded. A diagram of the MAF frame is shown in figure 3.6.

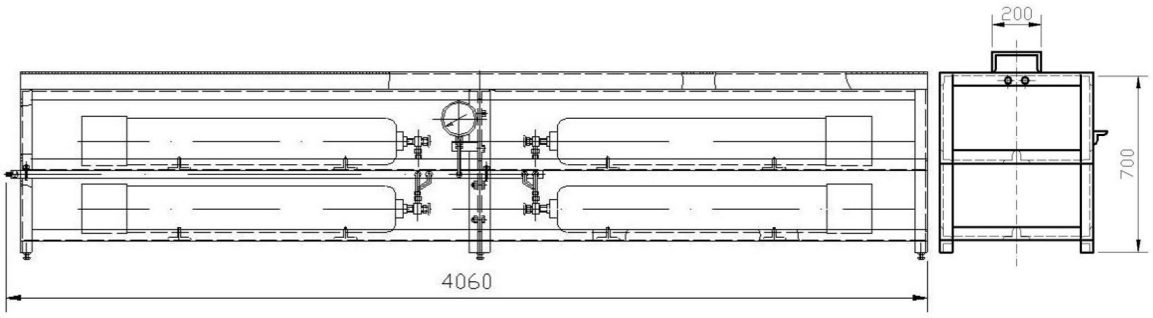

Figure 3.6: Drawing of the MAF HSWT frame. Credit: Russian Academy of Sciences Siberian Division Institute of Theoretical and Applied Mechanics.

The initial design for the frame was done using SOLIDWORKS CAD software. The frame dimensions were loosely borrowed and modified from the MAF hypersonic wind tunnel at Virginia Tech. Visiting Virginia Tech's advanced propulsion lab allowed our

senior design team to examine how their frame was built physically to understand its design purposes. They provided us with documentation and allowed us to take pictures to have a scheme reference for our project. The two critical components of the frame that we wanted to improve from the Virginia Tech reference were accessibility and safety. For accessibility, we increased the overall height from 2.3-feet to 4-feet, which would put the upper part of the wind tunnel right below eye level for the average user. A uni-strut railing was also used on the top portion of the tunnel to allow modulation and adjustability to the upstream clamps and subsystems and ease of maintenance. Safety walk adhesive strips are installed to allow users to climb onto the frame, minimizing slipping/falling safely. There are hangers for hearing protection located at the rear of the frame. Mounting clamps, as shown in figure 3.7, are used to secure the upstream and downstream piping components with rubber clamps that also help minimize pipe vibration during operation. At both ends of the frame, steel C-channels are bolted directly behind the pressure vessels to keep them from gaining momentum should they fail as shown in figure 3.8. These pressure vessels sit between two bars of angle iron welded to the frame. Ratchet straps are used to secure the pressure vessels to the frame. The top side of the frame has a butcher block installation to provide a workspace for maintenance or removing/installing CD nozzles.

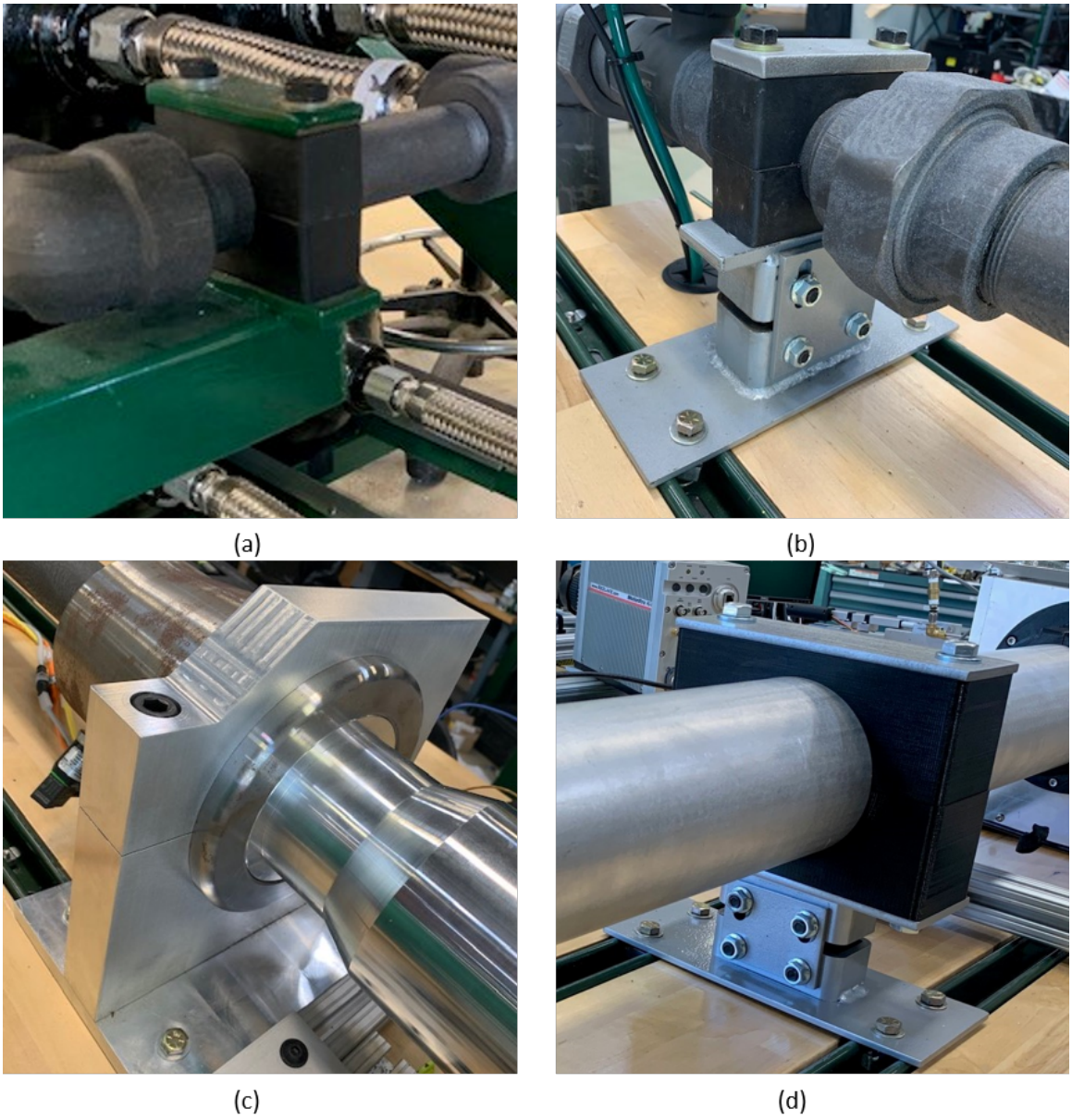

Figure 3.7: Image of mounting clamps on the UNCC HSWT: (a) manifold collector clamp, (b) fast valve clamp, (c) plenum clamp, and (d) diffuser clamp.

Figure 3.8: Image of the UNCC HSWT frame retention C-channel safety bars.

The frame is made from approximately 165 feet of 2x4 A36 steel rectangular tubing, 1.75-inch thick butcher block, 60 feet of angle iron, and one-inch 90° fiberglass, 28 feet of Uni-strut, 29 feet of 2-inch channel, and additional plates and clamps. The frame's net weight capacity is approximately 1,060 lbs when the additional subsystems are not installed. The dimension for the frame 3.95'x 3.2' x 14' and contacts the ground at four points sitting at the corners of a rectangular area of 3.2' x 14'. The 165 feet of A36 steel rectangular tube was cut into 42 parts, and MIG welded together to form its rigid skeletal shape and structure. These components were constructed so that the frame is capable of supporting the vertical load up to 7,500 lbs. Each significant load supporting member is MIG welded together to form a permanent rigid body. The bare frame is shown in figure 3.5 right after it was finished being painted.

Figure 3.9: Image of the UNCC HSWT frame.

3.2 Manifold

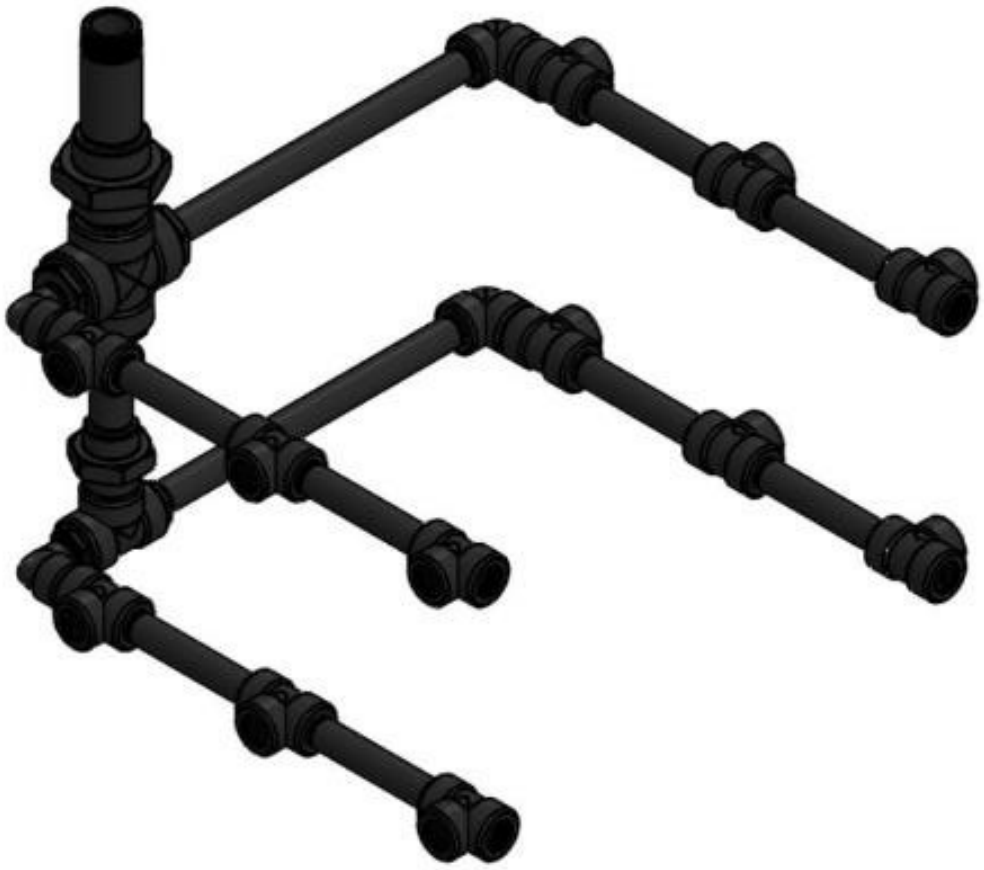

Figure 3.10: CAD image of the benchmark hypersonic tunnel manifold.

The UNCC HSWT manifold system collects and stores high-pressure compressed air within an airtight sealed system of high-pressure pipes and pipe fittings until it is ready for testing usage. The majority of the various system components are secured within the frame with the mounting clamps mentioned in the previous section. Having the manifold components staged within the frame decreases the chance of bodily harm to the user. In the event of a bursting pipe or exploding connection, a launched damaged part will hit the interior frame before discharging out into the lab. The manifolds pressure can be monitored using its integrated mechanical valve, and

storing the pressure is done using several ball valves.

The volume capacity of the MAF pressure vessels at Virginia Tech is $1.57 - in^3$ and is used to collect and store compressed air [49]. The pressure vessels specified at 2204 psi but have been tested at the pressure of 3306.5 psi. The pressure vessels have been updated. This update consisted of increasing the diameter of the handle valve throat from 0.157 inches to 0.216 inches. This increased throat diameter provides a sufficient flow rate of the compressed air. The total open area of all eight pressure vessels is $7.5 - in^2$. A diagram of the manifold apparatus is shown in figure 3.11.

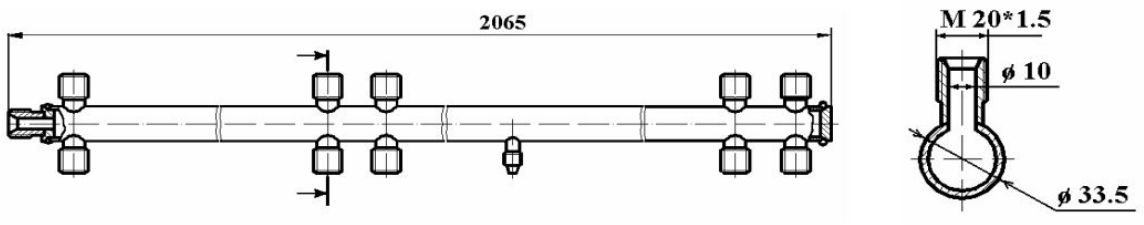

Figure 3.11: Diagram of the MAF manifold apparatus. Credit: Russian Academy of Sciences Siberian Division Institute of Theoretical and Applied Mechanics.

The manifold system consists of thirty-five feet of various sized steel pipe secured within the frame that connects the twelve pressure vessels to the CD nozzle. The pipes connect through a series of connectors until a single pipe enters a high-pressure fast valve, which controls the flow from the pressure vessels/compressed air tanks. The fast valve is held in a normally closed position, allowing the tanks to be charged through a separate ball valve by an external air compressor. The complete manifold system is rated at a maximum working pressure of 3,000 psi; however, all tests are executed at pressures below 2,400 psi. Each pressure vessel has a total volume of $300 - ft^3$ and is suitable for storing air, argon, nitrogen, and helium. Several of the critical components of the manifold system are shown in figure 3.12.

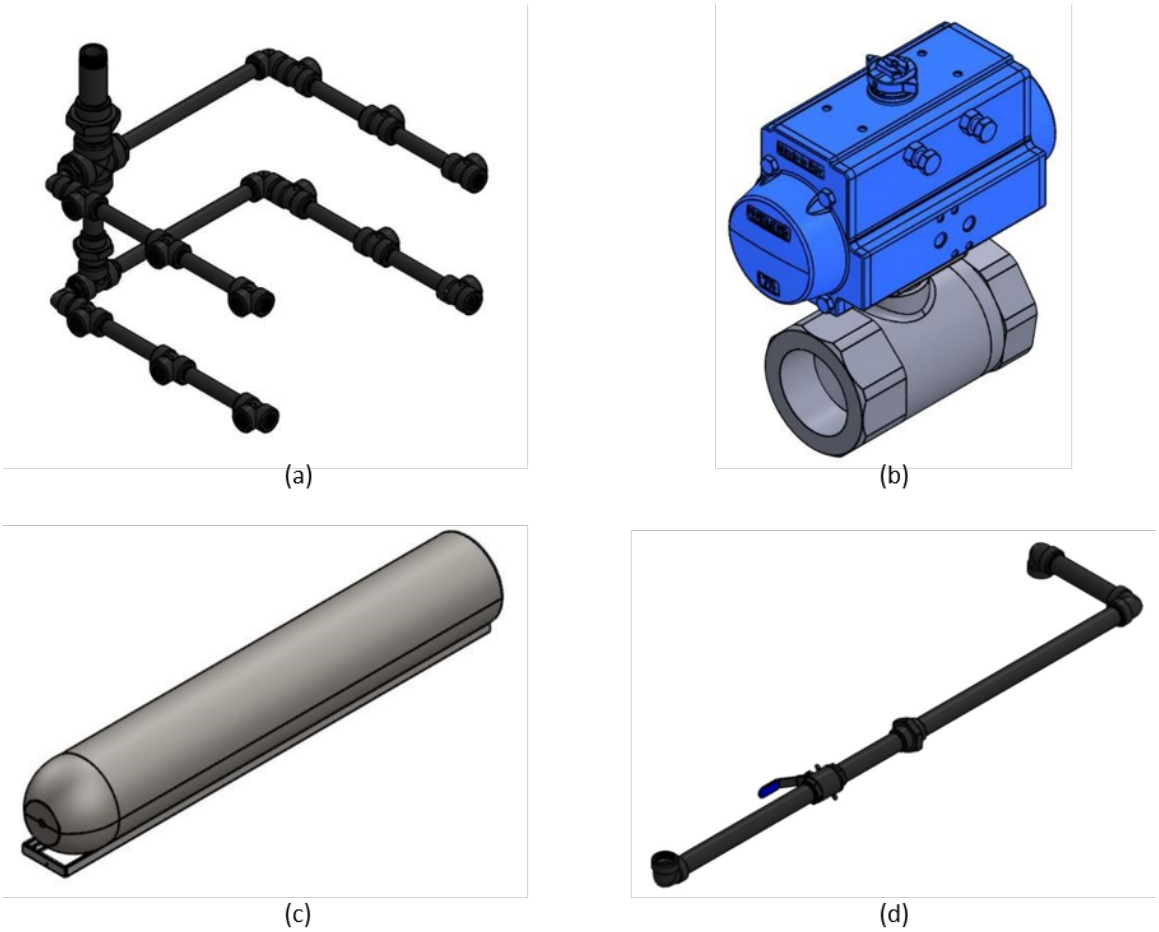

Figure 3.12: CAD images of the UNCC HSWT manifold components: (a) manifold collector, (b) fast valve, (d) pressure vessel, (e) downstream pipe with pre-fast valve, ball valve.

An MCH13/ET Standard Nuvair air compressor is used to charge the manifold system. It has a maximum operating pressure rating of 5,000 psi and is set to a working pressure of 4,700 psi. It utilizes a 5.5 HP electric motor powered that requires a 440 volt 7 amp power supply to operate. The UNCC HSWT compressor has an integrated dryer to keep condensation from forming inside the pressure vessels. The compressor connects to the manifold via a high-pressure to a quick-disconnect port. An image of the compressor can be seen below in figure 3.13 and figure 3.14 the pressure vessels can be seen nested and secured within the frame.

Figure 3.13: Image of UNCC HSWT Nuvair air compressor.

Figure 3.14: Image of UNCC HSWT pressure vessels within the frame.

The manifold system consists mainly of high pressurized steel pipe. For perspective, 94 of the components are high-pressure pipe components, and the remaining 18 are the fast valve, upper ball valve, lower ball valve, air compressor, and the 12 pressure vessels. The 94 components of high-pressure steel pipe make up the manifold collector. Because there are so many connections within the manifold collector, special attention was given to sealing each connection to ensure there were no leaks while the system was charged. In figure 3.15 the central portion of the manifold collector is shown. This portion routes the compressed air in and out of the pressure vessels. The air compressor routes compressed air into the manifold collector via the charging port (figure 3.16 (a)). There is a lower ball valve at the charging port used to hold the system pressure once the compressor is turned off. The compressed air will flow through the manifold collectors, fill the pressure vessels and stop at the upper ball (3.16(b)). The upper ball valve is used to hold high pressure before the fast valve to minimize wear to the fast valve. The manifold system pressure can be monitor by a mechanical gauge (3.17 installed on the lower right-hand side portion of the manifold collector.

Figure 3.15: Image of the UNCC HSWT manifold collector.

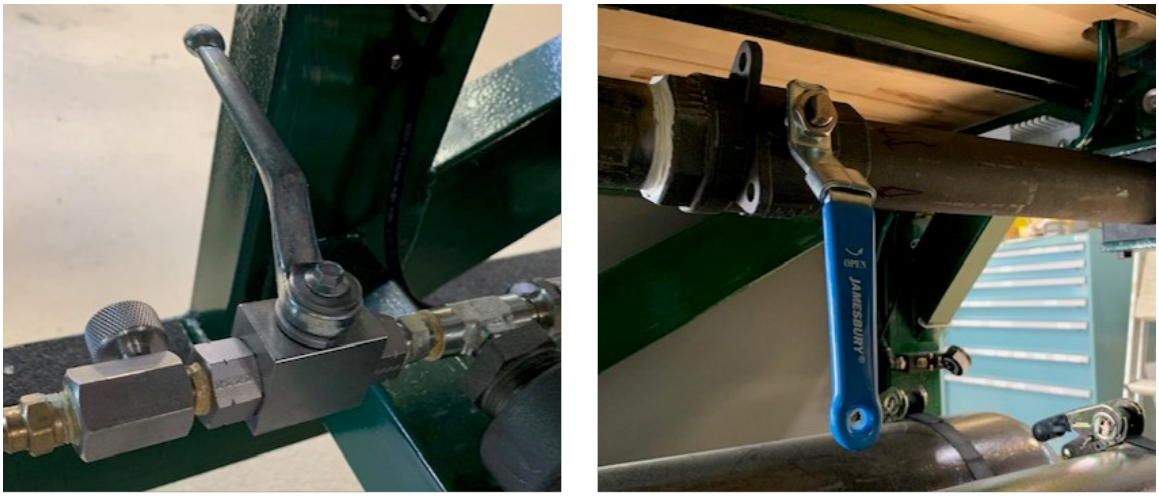

Figure 3.16: Images of the pre-fast valve, ball valves: (a) lower ball valve (charging port/bleeder valve/ ball valve), (b) Upper ball valve.

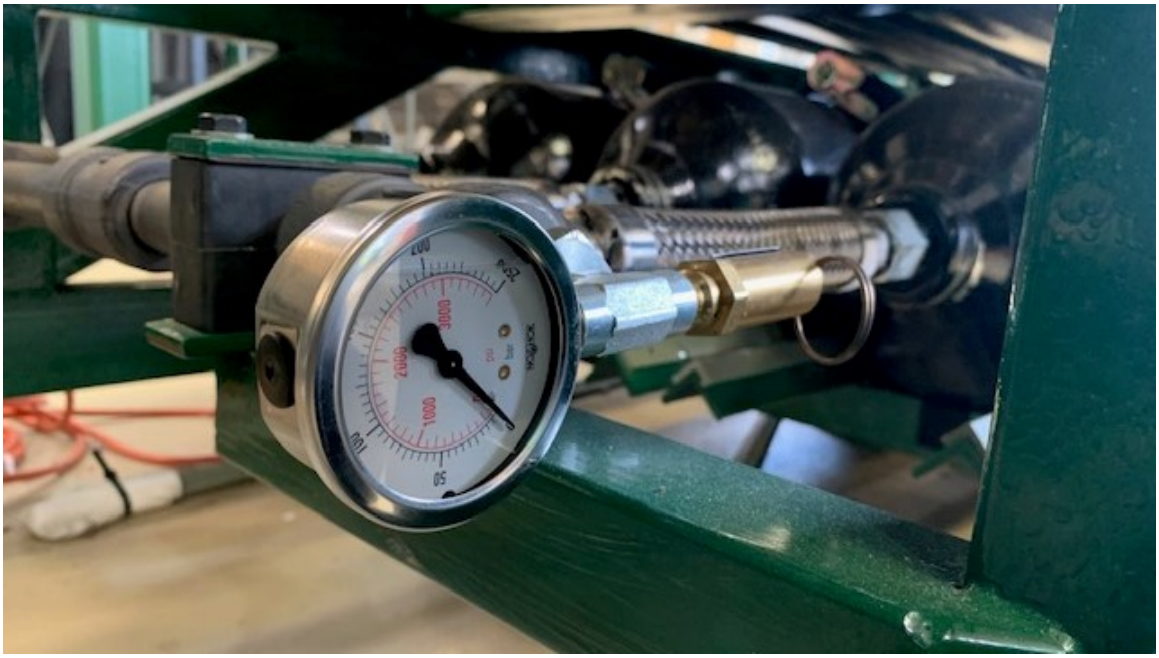

Figure 3.17: Image of the UNCC HSWT mechanical pressure gauge.

The fast valve is a 2-inch Bonomi 8P3000 series direct mount, 2-way, carbon steel ball valve with a double-acting actuator to quickly release the charged flow from the 12 pressure vessels and route it into the plenum. It has a maximum pressure rating of 3000 psi, a temperature range of -20$^{c}ircF$ to 185$^{c}ircF$, and utilizes a double-acting pneumatic actuator to open the ball valve immediately. The fast valve is the last component of the manifold system and connects to the high-pressured steel pipe with a 2-inch NPT threaded connection. Compressed air is supplied from the Motorsports Research Lab to activate the pneumatic actuator. The left and right sides of the fast valve can be seen in figure 3.18.

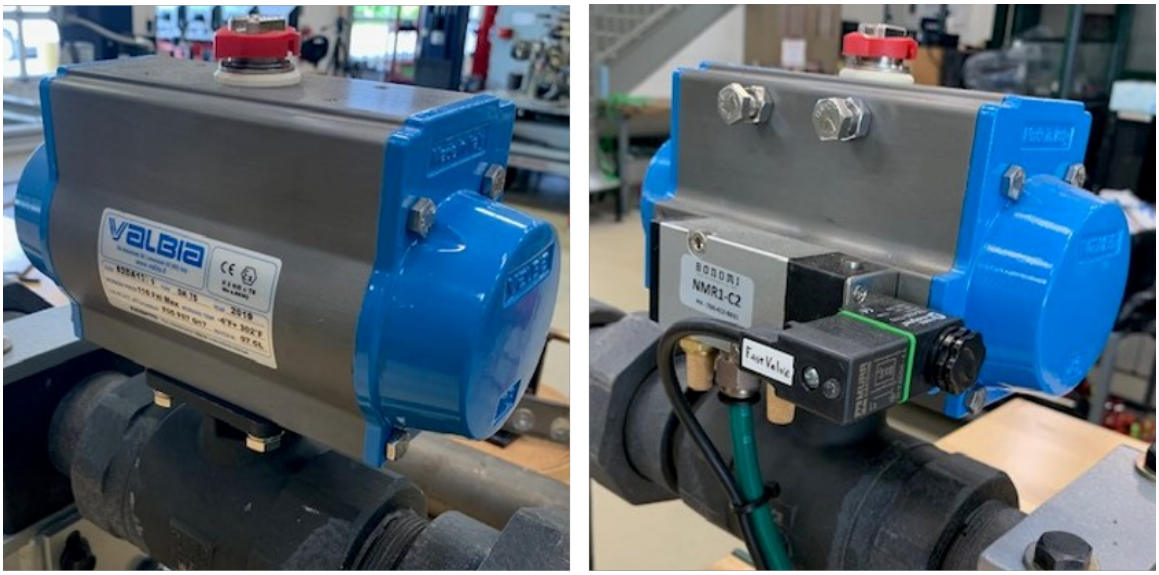

Figure 3.18: Image of the UNCC HSWT fast valve: (a) left side and (b) right side.

Table 3.2: Components of the manifold system.

Component	Outer Diameter D	Inner Diameter d	Length l	Quantity
Pipe	2 in	1.675 in	8 in	12
Elbow	2 in	1.675 in	3 in	30
Union	4 in	3.675 in	8 in	2
Reducers	- in	- in	- in	2

3.3 Plenum

Figure 3.19: CAD image of the benchmark hypersonic tunnel plenum.

A *plenum* is a device used to capture the turbulent unsteady fluid flow and route it into a steady flow. In blowdown high-speed wind tunnels, plenums, sometimes called settling chambers, are used to steady any possible turbulent flow before entering the CD nozzles. Some plenums use a complex design that uses throttling holes to help settle turbulent flow, while other plenums use a tapered interior for a similar effect.

The plenum used in the MAF facility is made of a steel tube with an outer diameter of 9.5 inches, an inner diameter of 8.6 inches, and a length of 11.8 inches [49]. Two nuts with thread fix the flanges of this cylinder. The tightness of thread affords

for the rubber seals. A gas supply tube is fed into one of the flanges. This tube terminates with several flow throttling holes to reduce and settle any turbulent flow. A contoured subsonic nozzle mates at the opposing flange with an exit diameter of approximately four inches. The inner cavity of the plenum was pressure tested in water under pressure for 10 minutes at 2,900 psi. A drawing of the MAF facility plenum is shown in figure 3.20.

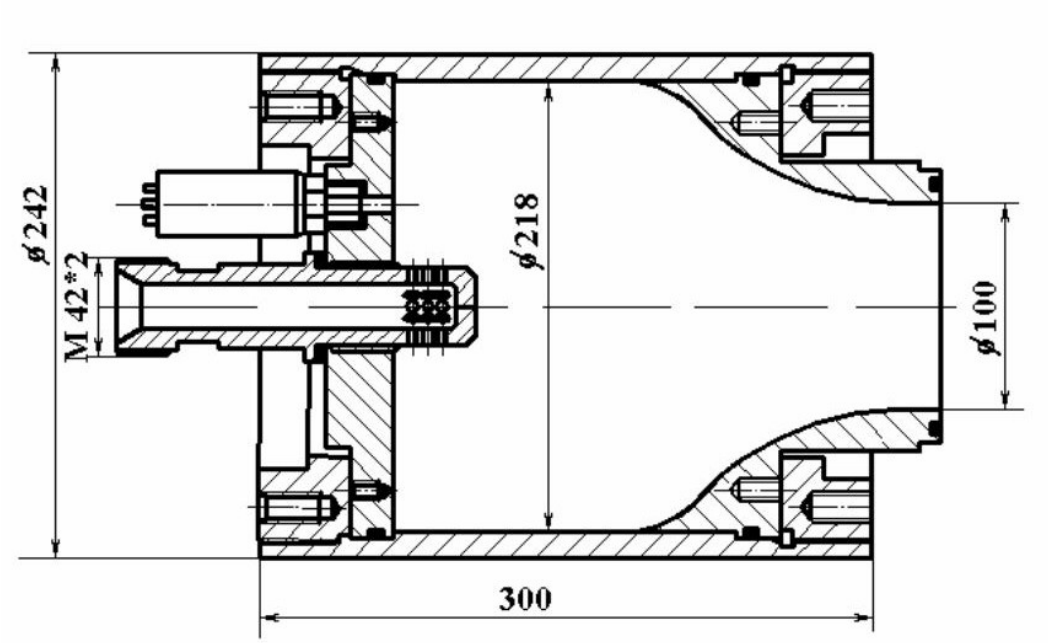

Figure 3.20: Drawing of the MAF plenum. Credit: Russian Academy of Sciences Siberian Division Institute of Theoretical and Applied Mechanics.

The UNCC HSWT plenum equalizes any path restrictions from the manifold and provides a large volume buffer from pressure changes. It is connected to the heater on its inlet end and the CD nozzle on its outlet end. An eight-inch-long steel round bar was machined to make the plenum. The plenum increases its inner diameter from two inches to four inches to match the inner diameter of each CD nozzle precisely. The plenum has a pressure sensor for measuring downstream pressure before entering the CD nozzle and a K-type thermocouple to measure ambient temperature. The plenum interfaces with the UNCC HSWT tabletop via c-channel rails, and a custom

aluminum mount allow its position to be adjusted for installing CD nozzles or performing maintenance, as shown in figure 3.21. The plenum to CD nozzle interface is shown in figure 3.25 while the figure A.8 shows a drawing of the plenum for better visualization.

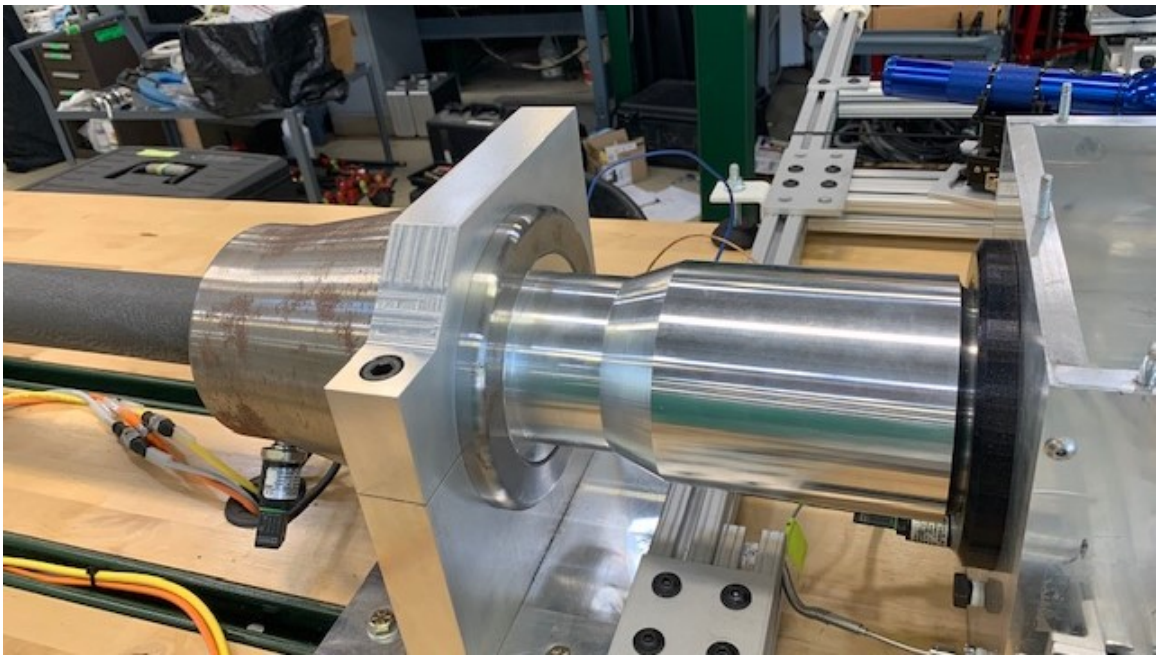

Figure 3.21: Image of the UNCC HSWT plenum with the Mach 3 nozzle installed.

3.4 Convergent Divergent Nozzles

Figure 3.22: CAD image of the Mach 3, 5, and 7 CD nozzles.

A de Laval nozzle, commonly known as a convergent-divergent (CD) nozzle, is represented by a tube having a pinched middle creating an asymmetric hourglass shape. A CD nozzle is used to accelerate pressurized gases to supersonic flow from a high-pressure low-velocity state by creating kinetic energy from heat energy.

The MAF facility forms supersonic flow with axisymmetric contoured nozzles with an exit diameter of about four inches. The method of flow turning around a corner point was used to contour the profiles of the CD nozzles. These CD nozzles accelerate

flow up to the necessary velocity around a point located immediately after the nozzle throat. Then a profiled smoothing segment follows, which converts the stream into a steady flow parallel to the nozzle axis [49]. All of the CD nozzles are made of steel. The nozzle contour was observed with accuracy up to $7.87x10^{-4} - in$. The CD nozzles with Mach number M $\geq$ 4 were made as a composite of two parts. All nozzles have a similar paired design.

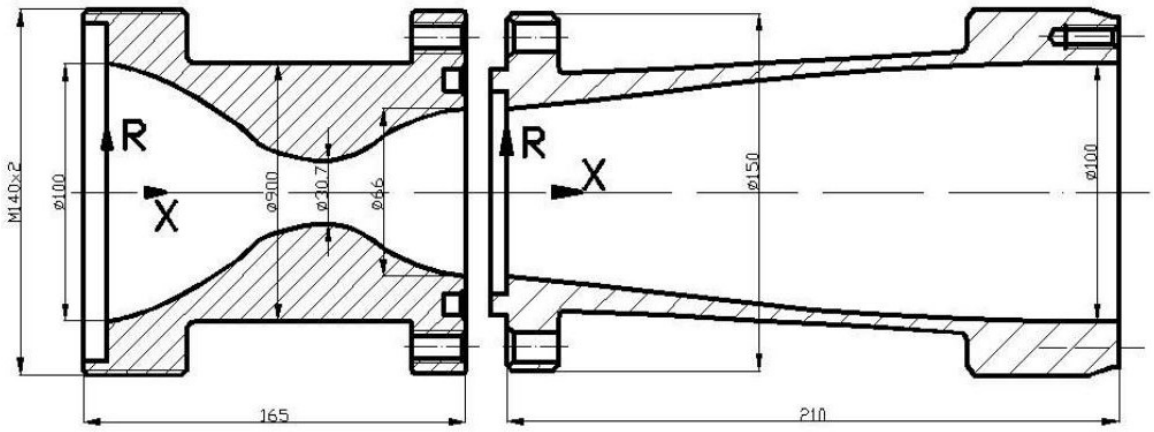

Figure 3.23: Cross-sectional drawing of the MAF facility CD nozzle assembly. Credit: Russian Academy of Sciences Siberian Division Institute of Theoretical and Applied Mechanics.

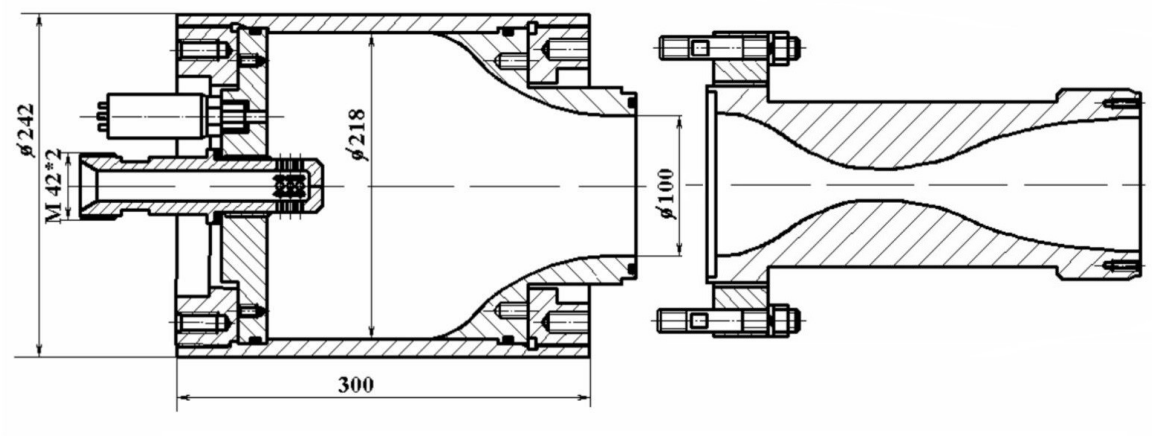

Figure 3.24: Cross-sectional drawing of the MAF facility plenum interfacing with a CD nozzle. Credit: Russian Academy of Sciences Siberian Division Institute of Theoretical and Applied Mechanics.

The UNCC HSWT uses three 6061 aluminum CD nozzles that have been designed and machined to achieve Mach 3, 5, and 7 based on our operating pressure of 2400 psi. Each CD nozzle has a four-inch diameter inlet that converges to a smaller diameter at the nozzle's throat to accelerate airflow and then diverges to a four-inch diameter outlet where fluid velocity radically increases. Threads outside the inlet allow the nozzles to be interchangeably fastened to the plenum. The asymmetric designs for the profiles of the nozzles were provided through a collaborative effort with Virginia Tech. Each nozzle is designed to achieve its specific Mach number based on its profile characteristics. The nozzles designed to reach Mach numbers greater than 3 had to be built in two parts to simplify the machining carried out by Brian Dutterer.

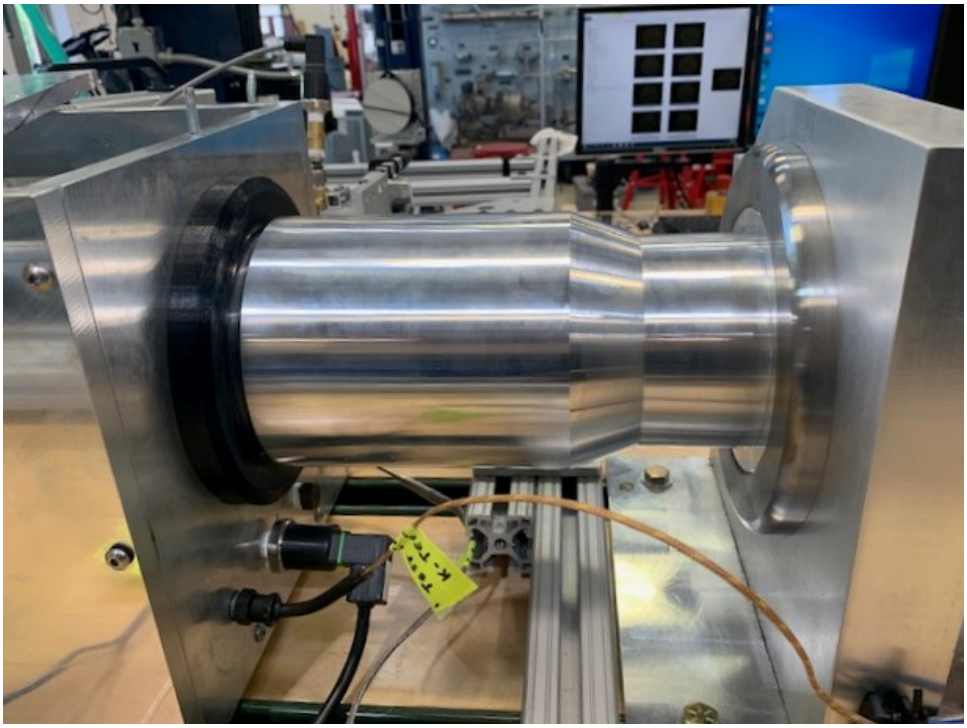

Figure 3.25: Image of the UNCC HSWT Mach 3 nozzle screwed into the plenum (on the right) and resting in the test section (on the left).

3.5 Testing Chamber

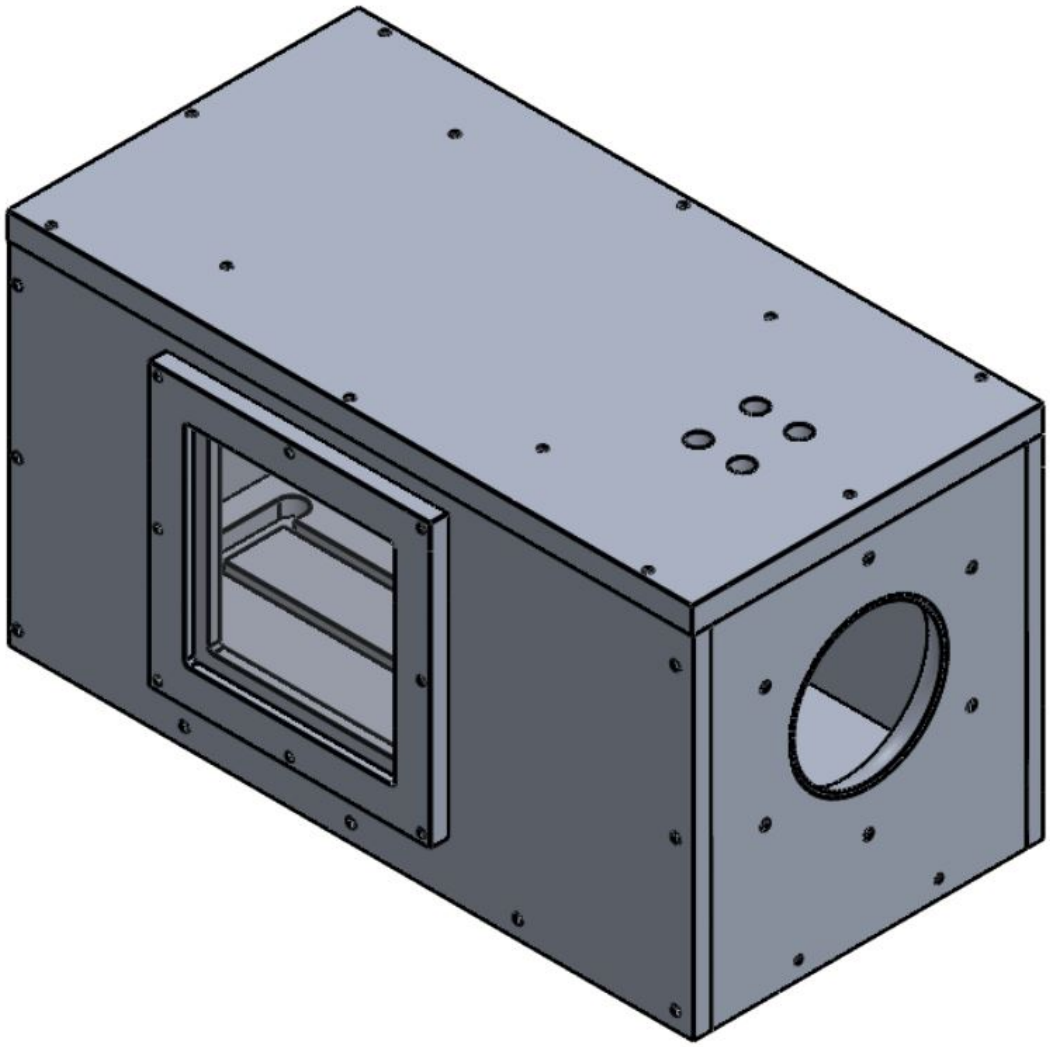

Figure 3.26: CAD image of the benchmark hypersonic tunnel test chamber.

The test section of the MAF facility is a rectangular chamber with inner dimensions 14"x9"x8". It was designed to fit test samples and measuring devices. The chamber walls are 0.4-inch plates of steel, and the upper lid is removable to provide accessibility for maintenance of the internal tools and devices. The working surfaces of the test section are the front and back walls. These walls are normal to the streams axis and have two opposing 5.5-inch diameter holes for the passage of the nozzle and

diffuser. Optic windows with a sight diameter of 100 mm are set in side walls for flow visualization inside the working part. A stinger is utilized to secure test models within the working area of the test section [49]. The stinger is fastened into the bottom part of the test section slots. There are special 24-prong connectors installed into the working section wall for the outlet of the electric line. Four sleeves are integrated into the exhaust sidewall to supply gases to the model necessary for the experiment. A drawing of the MAF facility test section is shown in figure 3.27.

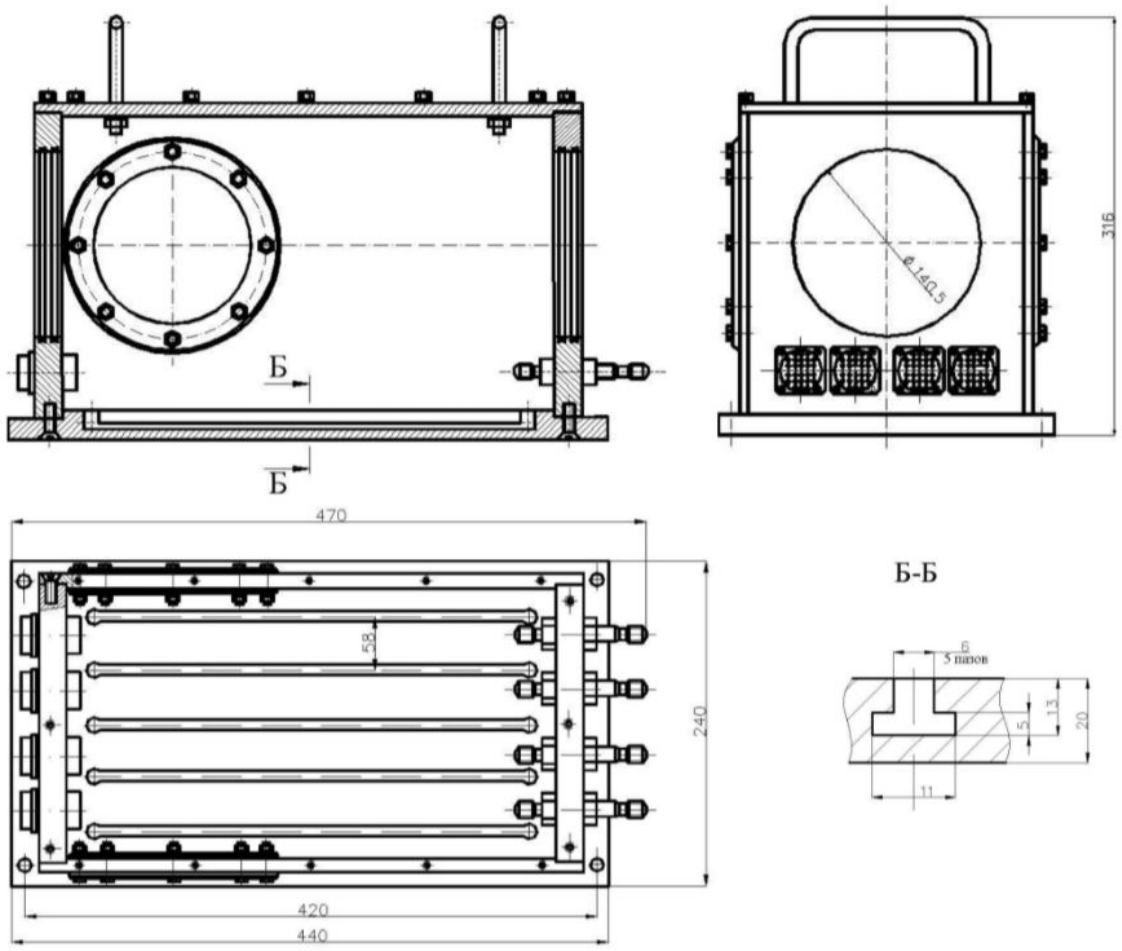

Figure 3.27: Drawing of MAF test section. Credit: Russian Academy of Sciences Siberian Division Institute of Theoretical and Applied Mechanics.

The UNCC HSWT testing chamber was designed to monitor pressure differences, temperature changes, and flow visualization techniques, such as Schlieren imaging,

to gather and examine high-speed flow as it moves around test models. The UNCC HSWT test chamber base is made from 6061 aluminum with the following dimensions: 19.75" x 10" x 1". In order to integrate measuring devices and tools, the base plate design incorporates two T-slots that will run across the length of the base. The remaining dimensions of the test chamber are as follows:

- 2 Sidewalls: 19.75" x 11" x 0.75" (0.75-inch thick)
- 1 CD Nozzle Inlet Wall: 11" x 10" x 0.75" (1-inch thick)
- 1 Diffuser Exhaust Wall: 11" x 10" x 1" (1-inch thick)
- 1 Lid: 19.75" x 10" x 0.5" (0.75-inch thick)

The test chamber has a demountable top plate (lid) with a recessed lip to facilitate the secure, straightforward installation of test models onto a stinger suspended from the top plate. The stinger's angle of attack can be adjusted for high-speed flow analyses of test models at different attack angles. The test chamber uses one low-pressure sensor and two thermocouples (one K-type and one T-type) to monitor upstream pressure and temperature. A port in the sidewall of the test chamber was made for the installation and removal of a pitot tube that can traverse 6 inches across the CD nozzle outlet. The CD nozzle mates with the inlet side of the test chamber, and the diffuser properly mates with the exhaust sidewall of the test chamber via a 3D printed flange, allowing airflow to exit to atmospheric pressure. Both side walls have 4"x 4" glass windows to allow for Schlieren flow visualization. The UNCC HSWT test chamber image is shown in figure 3.28.

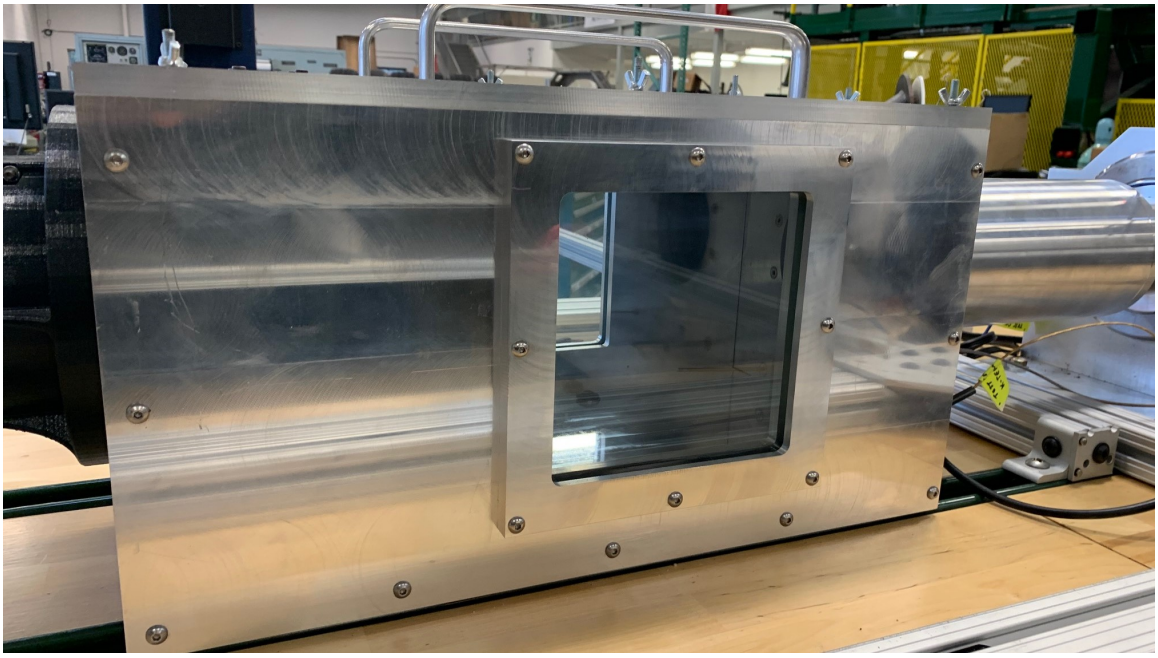

Figure 3.28: Image of the UNCC HSWT test chamber.

3.6 Schlieren Imaging

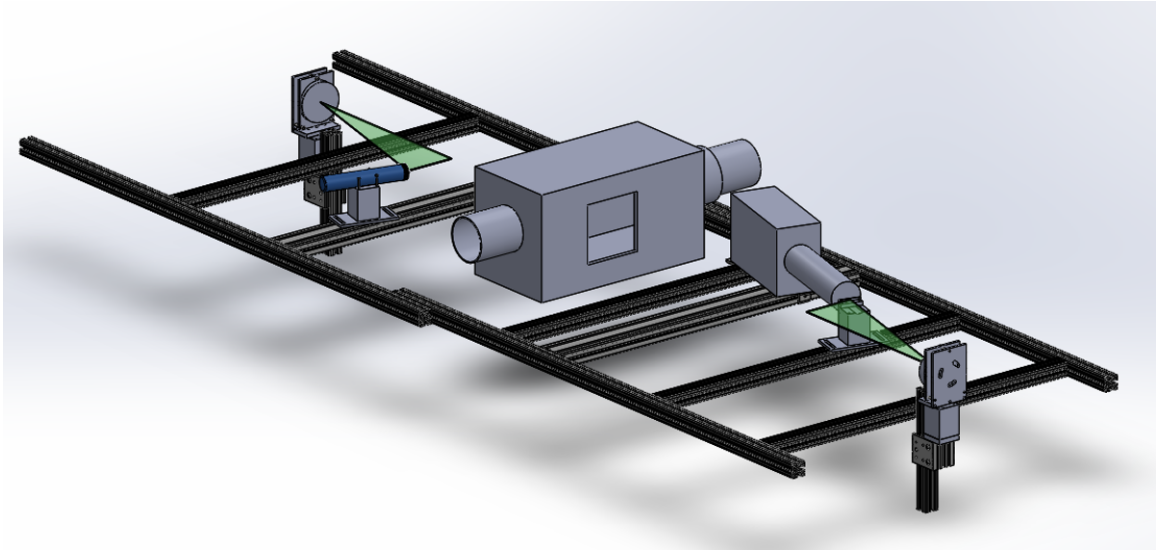

Figure 3.29: CAD image of the UNCC HSWT Schlieren System. Credit: Michael J. White, University of North Carolina at Charlotte.

Schlieren imaging or Schlieren photography is a flow visualization process use to produce images of varying fluid densities [50]. Schlieren imaging relies on refracting

or bending light rays that have interacted with different densities of fluid flow. The setup of a Schlieren imaging system usually involves concave mirrors, a light source, a knife-edge, and a recording device. There are several types of Schlieren system setups, such as the lens system, double-pass mirror system, and the z-type two-mirror system.

The UNCC HSWT uses the z-type two-mirror system depicted in figures 3.29 and 3.32. An incandescent lamp bulb from a high-powered flashlight is used as light a light source. The light passes through a slit that is positioned so that parallel rays pass through the test section form from the reflected light of the incandescent bulb. A knife-edge is used as a focal point so that the secondary mirror can collect the parallel light rays. A high-speed camera records bending light rays of the varying fluid density.

In figure 3.31, a schematic of the z-type two-mirror Schlieren setup is shown. In the "test region," shock waves will form thin regions of high-pressure gradients, temperature, and density. The dashed line in the figure 3.31 represents a ray of light as it would pass through a shock wave located in the test section. The knife-edge stops the ray of light from passing through the focal point. The camera will record shaded lines that occur where density gradients take place. The model will be shown as a black image or shadow from completely blocking the light rays as they pass through the test section. However, the shaded lines will visualize how the shock waves interact with the test model as shown in figure 3.32.

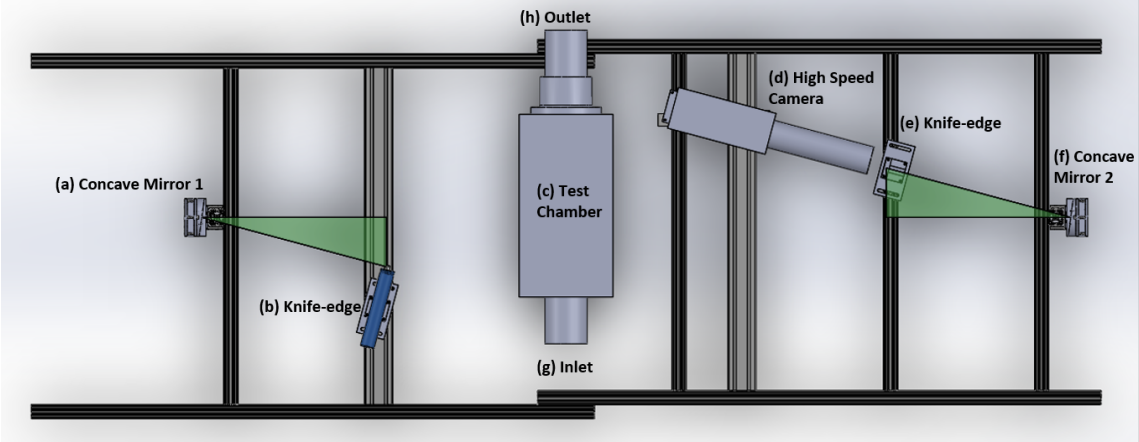

Figure 3.30: Top view CAD image of the UNCC HSWT Schlieren System. Credit: Michael J. White, University of North Carolina at Charlotte.

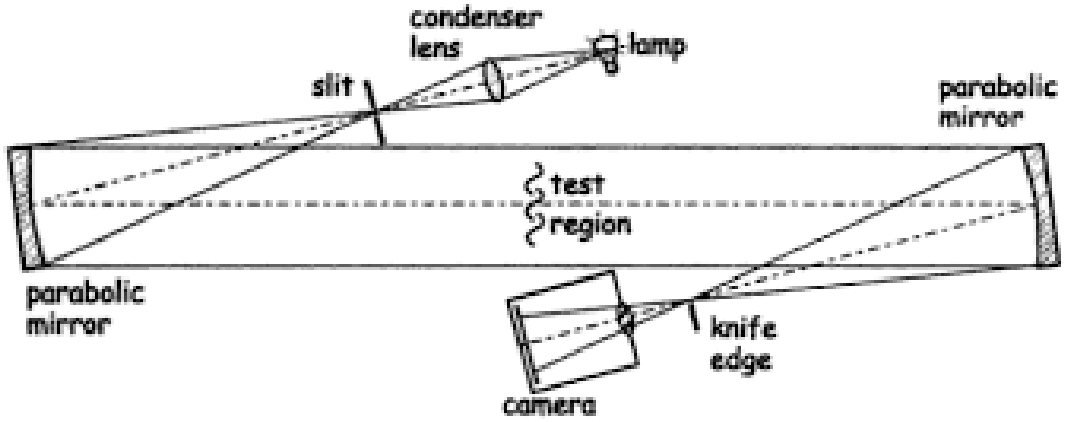

Figure 3.31: Schematic of a general z-type two-mirror Schlieren setup. Credit: Dr. Carlo Angelo Borghi, University of Bolonga|UNIBO.

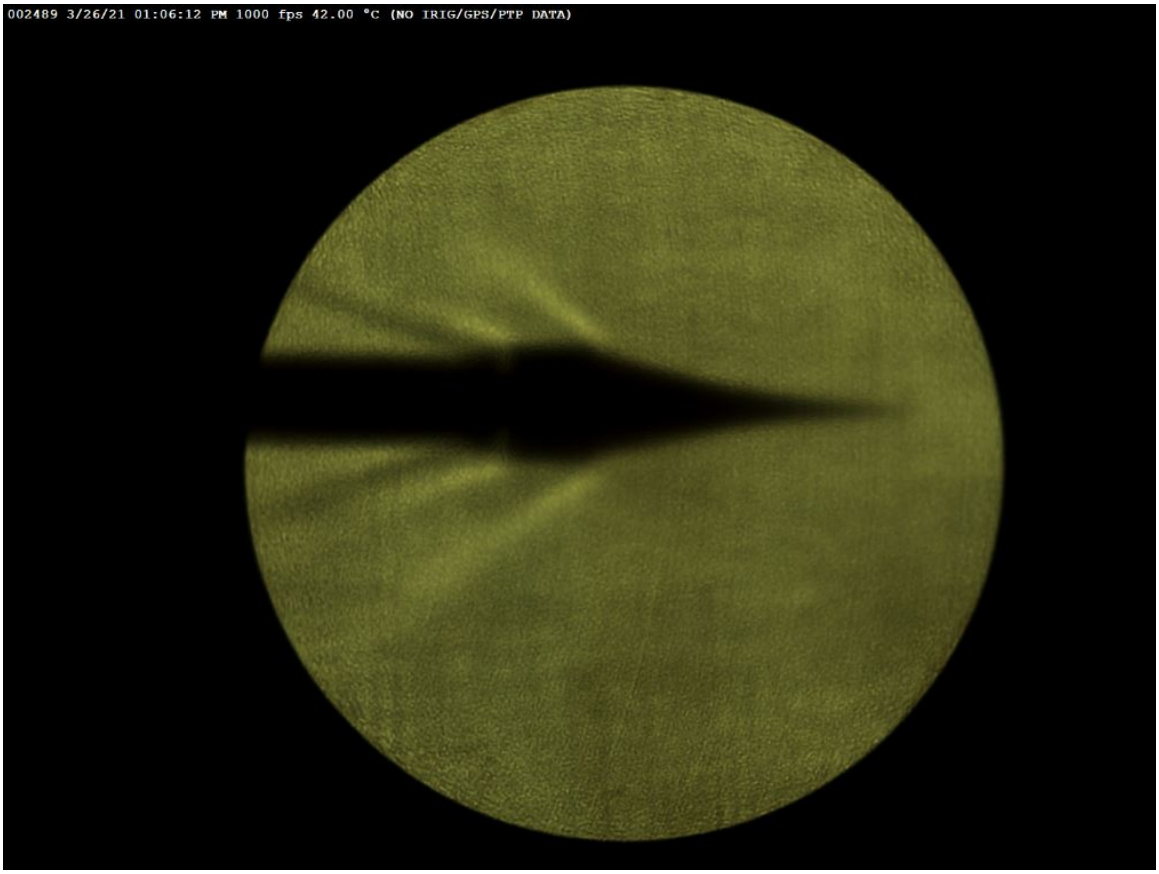

Figure 3.32: UNCC HSWT captured Schlieren image of a flared cone within a Mach 5 flow. Credit: Michael J. White, University of North Carolina at Charlotte.

3.7 Diffuser

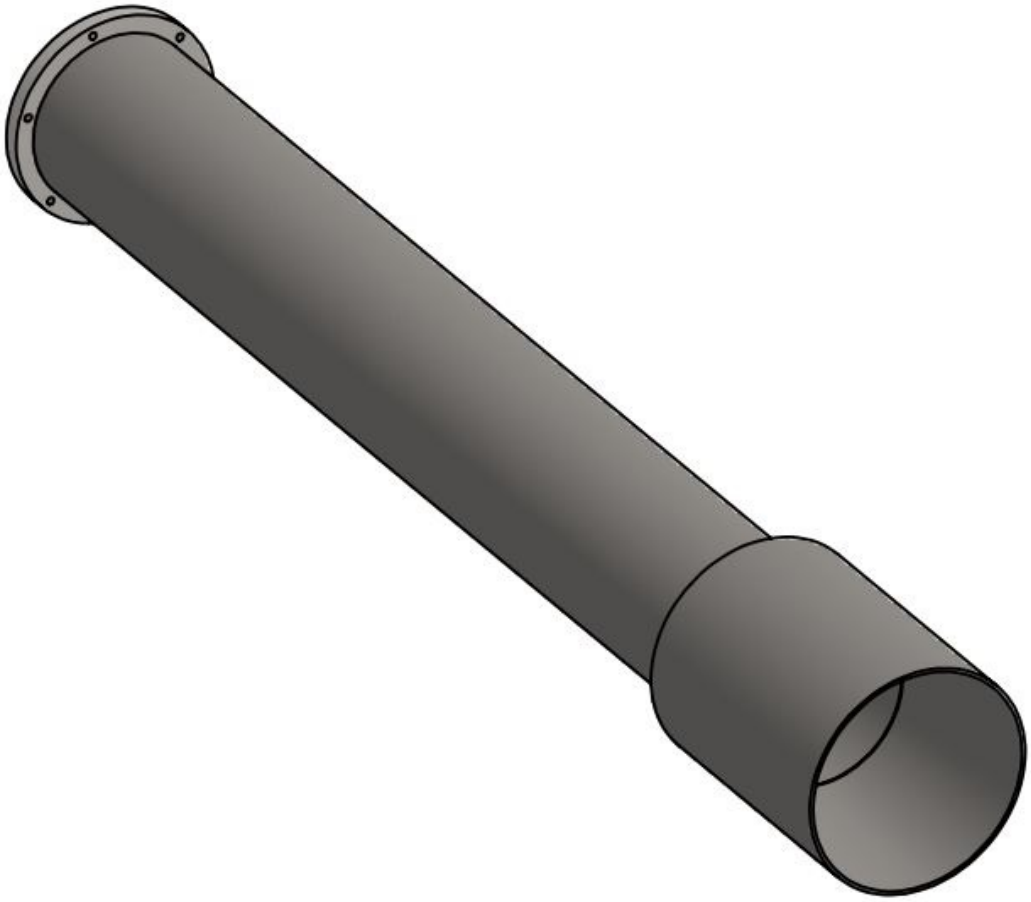

Figure 3.33: CAD image of the UNCC HSWT diffuser.

A diffuser is used to manipulate fluid flow to gain an aerodynamic advantage that can be used for an aero-systems performance. The diffuser used in the UNCC HSWT is accompanied with a silencer. The two components work together to reduce the flow velocity as it exits the test chamber and diffuses the pressure losses to reduce loud exhaust noises [51].

The diffuser at Virginia Tech's MAF facility is designed to decrease total pressure losses and decelerate the supersonic stream passing through the test section. The diffuser is approximately 32 feet long with an inlet diameter of 5.5 inches and has a

7-degree angle of generation inclination. There is a varying distance of 4 inches to 12 inches between the CD nozzle outlet and the diffuser inlet, depending on the size of the test model arrangement. The diffuser outlet also sports a cone-shaped generation inclination of 7 degrees. The ratio is nearly one-to-one of throat area to nozzle area at 1.56, with a diffuser throat diameter of 5 inches. A drawing diagram of the MAF facility diffuser is shown in in figure 3.34.

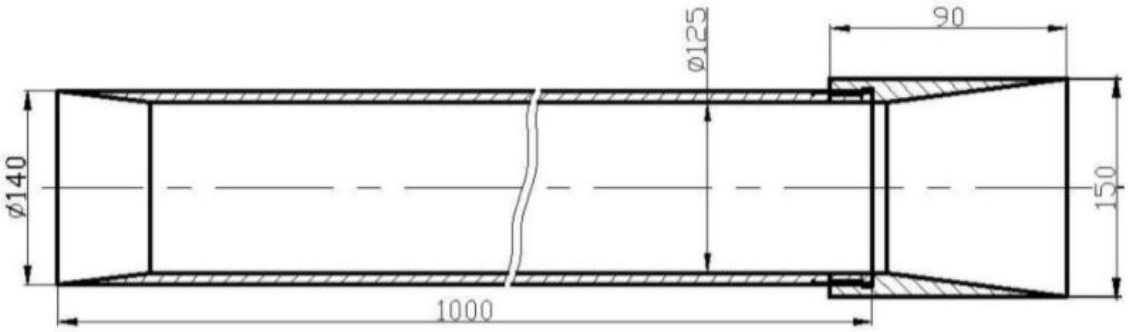

Figure 3.34: Drawing of MAF facility diffuser. Credit: Russian Academy of Sciences Siberian Division Institute of Theoretical and Applied Mechanics.

The UNCC HSWT diffuser is made from a three feet aluminum pipe. It is four inches in diameter and allows the supersonic flow to decelerate smoothly and efficiently through the test section and out the exhaust end. It does so without causing any adverse effects such as vacuums or unwanted turbulence in the testing chamber. The diffuser is held in place by a custom mounting clamp made of steel and abs 3d printed plastic. The diffuser and its mount are shown in figure 3.35.

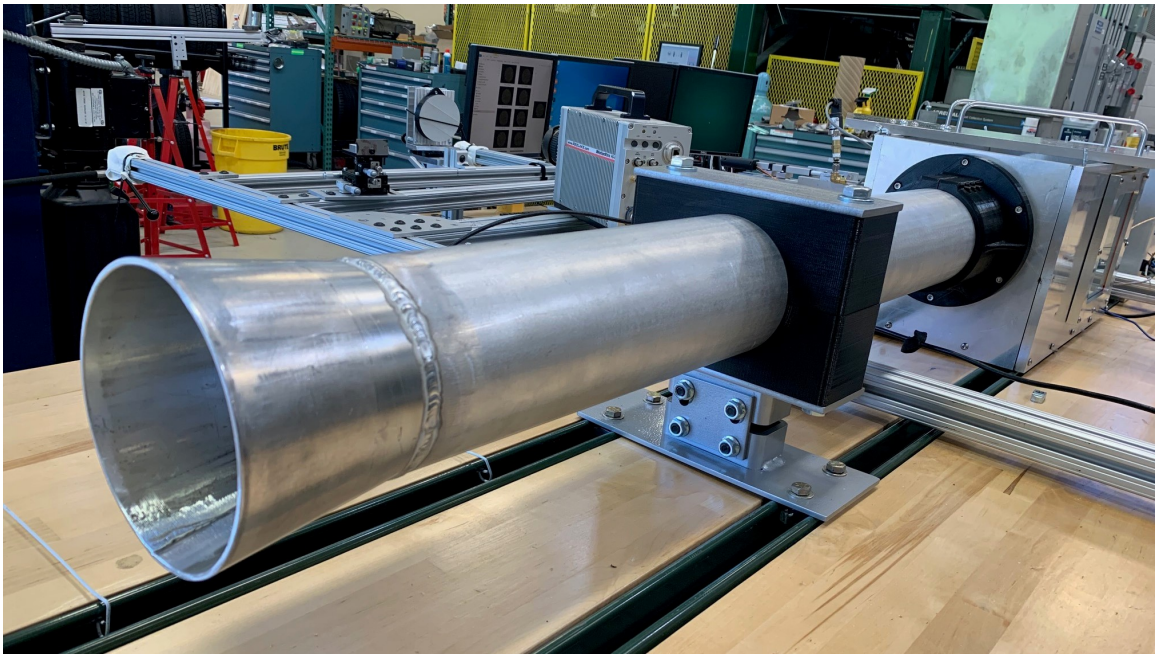

Figure 3.35: Image of the UNCC HSWT diffuser.

The silencer used in the MAF facility at Virginia Tech has a 30-degree wedge that is mounted normal to the exhaust port of the diffuser. This silencer deflects exhaust jets into two streams and into a perforated sheet that decreases the acting forces on the MAF facility during operations. The perforated sheets assist in splitting up hydraulic resistant pressure losses, which help decrease the flowing velocity and associated noise. A drawing of the top view of the MAF silencer is shown in figure 3.36.

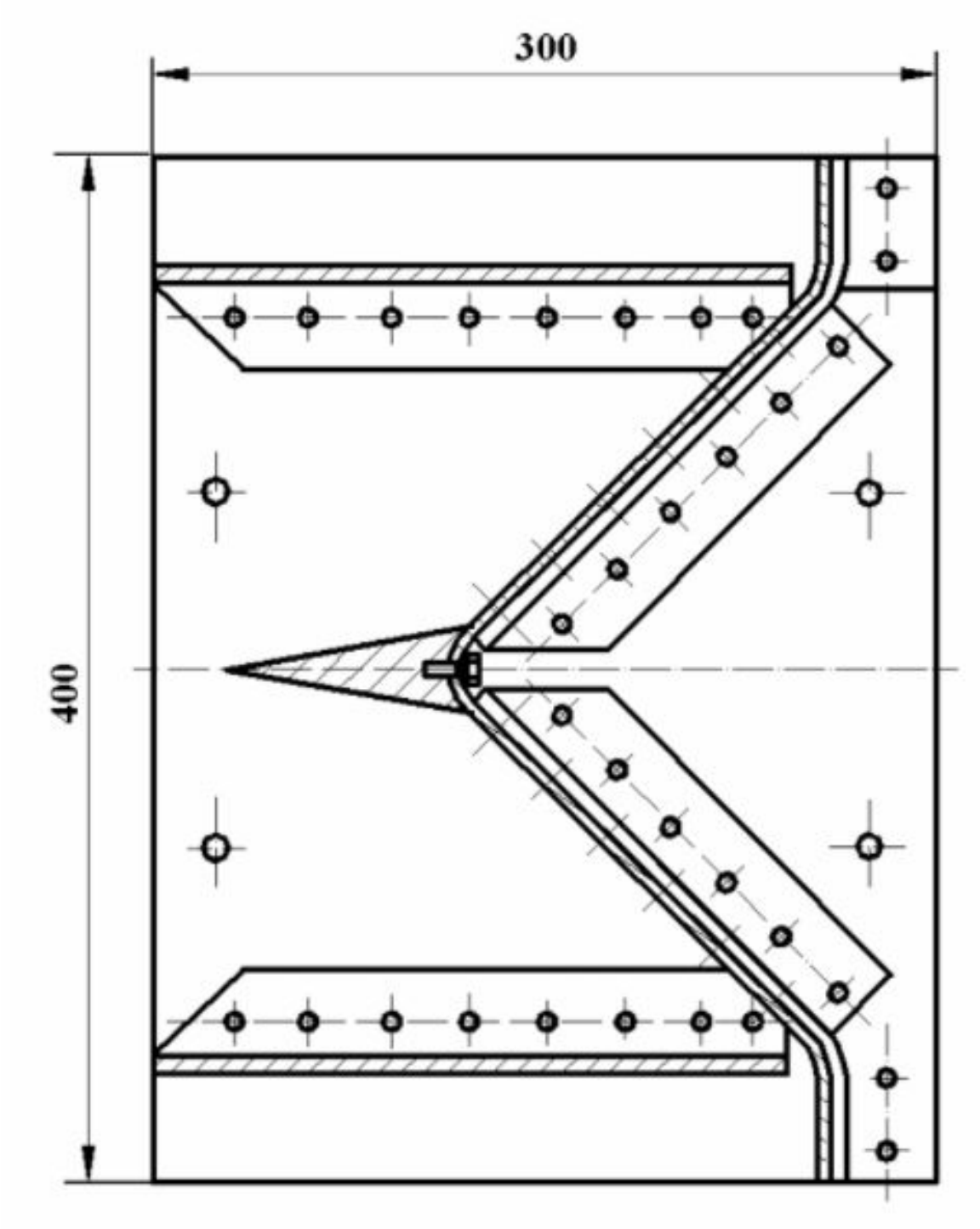

Figure 3.36: CAD image of the Mach 3, 5, and 7 CD nozzles.

The UNCC HSWT silencer moderates and reduces loud sound produced during operation. It is positioned so that the performance of the wind tunnel is not affected.

These two components safely return the hypersonic flow to the atmosphere by reducing the flow velocity. The governing dimensions of the silencer are 12" x 12" x 12". A Conceptual CAD image and live image are shown in figures 3.37 and 3.38.

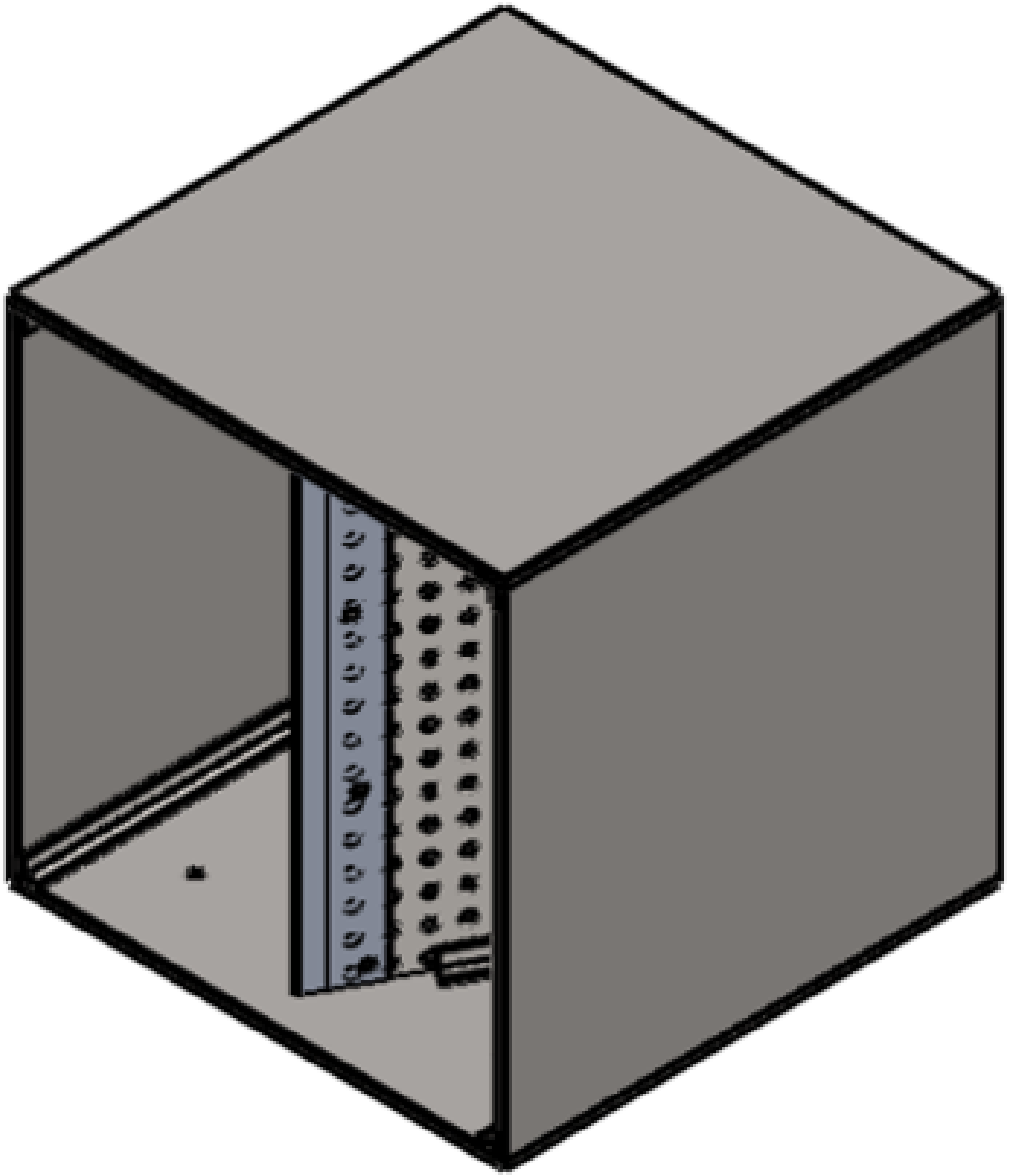

Figure 3.37: Conceptual CAD Image of the UNCC HSWT silencer.

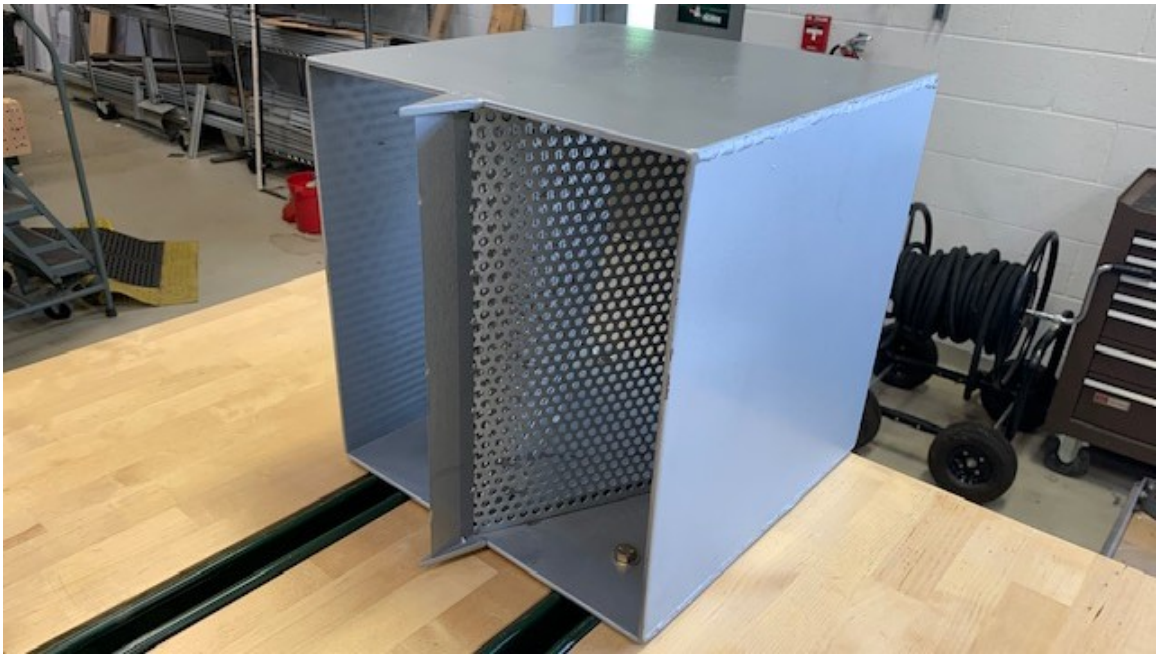

Figure 3.38: Image of the UNCC HSWT silencer.

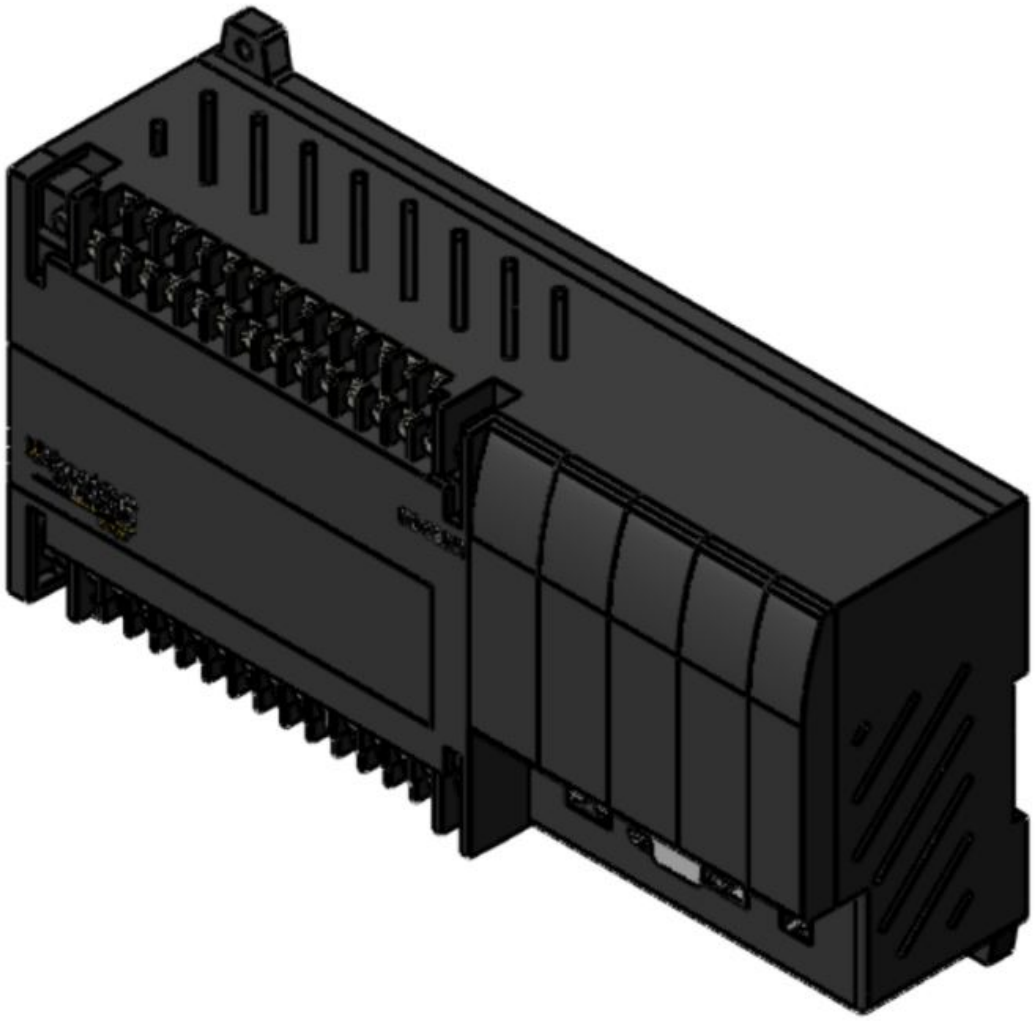

Figure 3.39: CAD image of the UNCC HSWT PLC.

The control panel is tethered to a mobile command center (Figure 3.41 where system programming and monitoring take place. The data acquisition setup allows users to monitor the pressure and temperature data needed to validate flow parameters. Data acquisition is facilitated using NI-SCXI-1000 hardware in conjunction with NI LabVIEW software. The NI-SCXI-1000 houses an SCXI-1300 and an SCXI-1303 terminal block [52]. The SCXI-1300 has 32 channels, with five channels currently being

used to monitor five separate pressure sensors. The SCXI-1300 also has 32 channels in which five channels are being used to monitor five thermocouples. The SCXI and all sensors and controls are wired through a single control panel attached to the side of the frame as shown in figure 3.42.

(a) (b)

Figure 3.40: Main components of the control system: (a) PLC and (b) National Instruments SCXI 1000 with integrated 1300 and 1303 modules.

Figure 3.41: Image of the UNCC HSWT command center.

(a) (b)

Figure 3.42: Image of the control panel of the UNCC HSWT: (a) with panel closed and (b) with panel open.

To power the command center computers, devices, and air compressor, the UNCC HSWT uses two separate power supplies. A 3 phase 480 V supply is used to power

the air compressor, while the 3 phase 460 V power supply is used for the entire control system. Images of both power supplies are shown in figure 3.43.

Figure 3.43: Image of the UNCC HSWT power supplies: (a) air compressor and (b) control system.

The Direct 6 PLC enables the operator to control the state of several output devices integrated into the UNCC HSWT [53]. Currently, the PLC controls and arms the fast valve, system LED's, compressor while also providing power to our command center computers and SCXI data acquisition interface. The SCXI will collect data from three pressure sensors (one low pressure (30 psi) and two high pressure (3000 psi)) and two thermocouples. The SCXI is also set up to accept additional instrumentation. The command center houses two PCs. One is used to program the PLC using Directsoft

6 software, while the other is used to collect data and operate the system utilizing NI LabVIEW. More information about the control system components will be given in the following chapter.

CHAPTER 4: CALIBRATION

The primary construction of the UNCC HSWT was completed on December 2, 2019. Several test runs have been conducted at low system pressures to ensure that data acquisition is collecting correctly. Leaks within the manifold were detected and corrected by re-tightening the couplings where leaks were discovered. Voltage readings from the PLC/SCXI were showing errors within LabVIEW. It was discovered that the resistors used on our voltage divider were too high, resulting in lower than expected values. We installed lower ohm resistors and our voltage data appropriately displayed. All other subsystems have operated as intended, and this system is now being used for graduate-level research.

4.1 Pressure Sensors

Figure 4.1: Pressure sensors that were used for the UNCC HSWT. Ratings: (a) -14.7 - 30 psig, (b) 3000 psig, and (c) 150 psig.

Currently, the UNCC HSWT utilizes four pressure sensors to collect specified pressure data. Two high-pressure sensors are rated at 0 to 3,000 psi. One of these pressure sensors is located on the manifold collector to monitor charged pressure in addition to the mechanical gauge in figure 3.17. The other high-pressure sensor is located in the plenum to monitor pressure changes downstream of the CD nozzles. A low-pressure sensor capable of reading pressures within the range of -14.7 to 30 psi is installed inside the testing chamber to monitor static pressure. The fluctuation in plenum pressure and test chamber static pressure is used in calculating the Mach number utilizing a static and stagnation pressure ratio formula. A fourth mid-range pressure sensor measures stagnant pressure from a pitot tube. Its pressure range is from 0 to

150 psi. Images of these pressure sensors and their locations are shown in figures 4.1 and 4.2.

Figure 4.2: Locations of pressure sensors: (a) test chamber (low pressure), (b) plenum (hi pressure), (c) pitot tube (mid-pressure), (d) manifold pressure (high pressure).

Pressure sensors use a diaphragm and a strain gauge to write pressure data [54]. As pressure enters the inlet of the pressure gauge, the diaphragm deforms, which agitates the strain gauge, allowing it to send a voltage signal to the data acquisition (DAQ) system [55]. A general schematic of a pressure sensor is shown in figure 4.3.

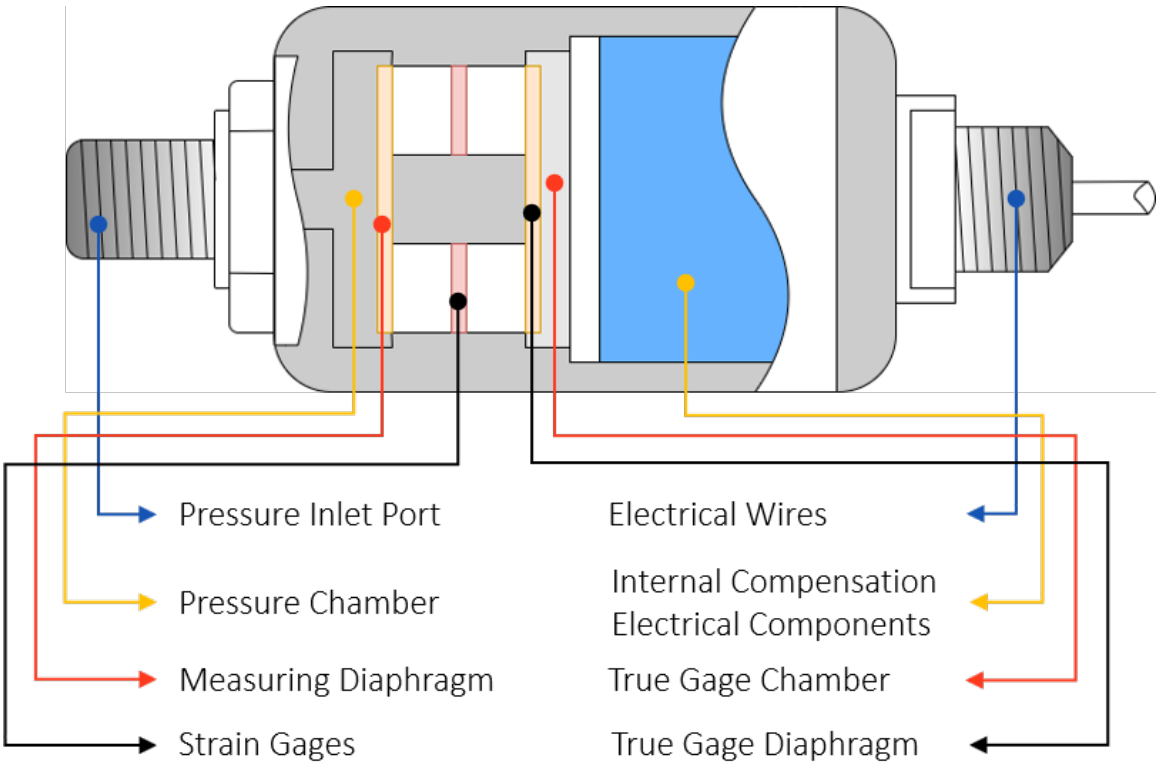

Figure 4.3: General schematic of a pressure transmitter.

4.2 Thermocouples

The UNCC HSWT utilizes six thermocouples of two types to monitor system temperatures, a T-type and a K-type [56]. There are two T-type thermocouples, one is installed in the base of the test chamber, and the other is installed in the plenum. These two are used for temperature ratio calculations. Three of the remaining thermocouples (K-type) are installed outside of the system to monitor the ambient temperature [57]. The remaining K-type thermocouple was installed in the test chamber. Figure 4.4 gives a general idea of what these thermocouples look like, while figure 4.5 shows their mounting locations.

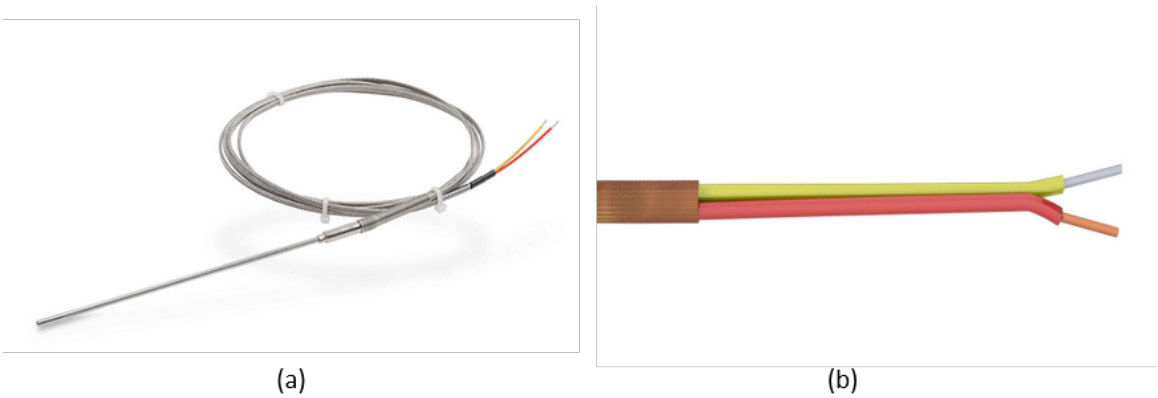

Figure 4.4: Thermocouples used on the UNCC HSWT: Types: (a) T-type (low pressure), (b) K-type.

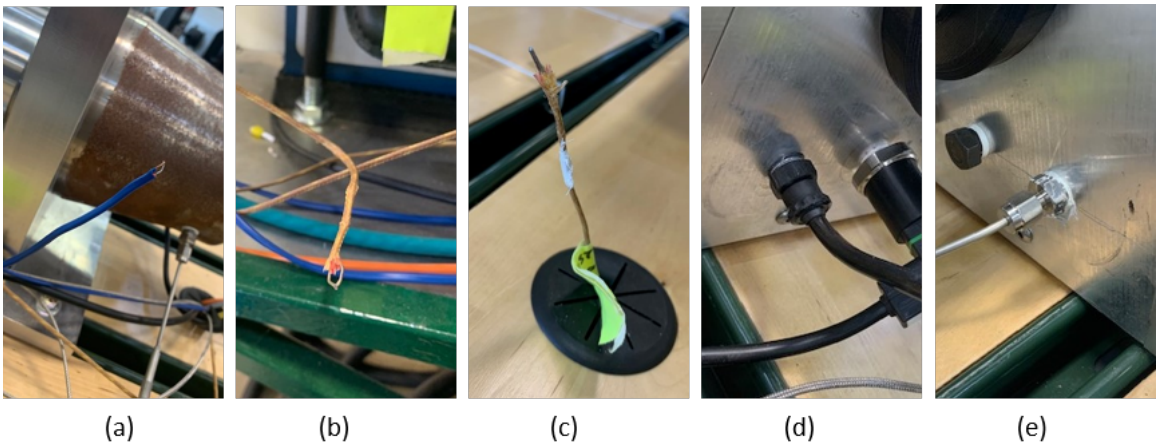

Figure 4.5: Locations of thermocouples: (a) plenum (ambient temperature), (b) SCXI (ambient temperature), (c) diffuser (exhaust temperature), (d) test chamber (static temperature), and (d) test chamber (stagnant temperature).

Thermocouples are used to measure temperature. They are constructed from two different metals soldered together at one end. When the soldiered junction is cooled or heated, voltage is carried to a DAQ system, where it can be converted to a temperature reading. Figure 4.6 shows a schematic of a thermocouple detailing how it operates.

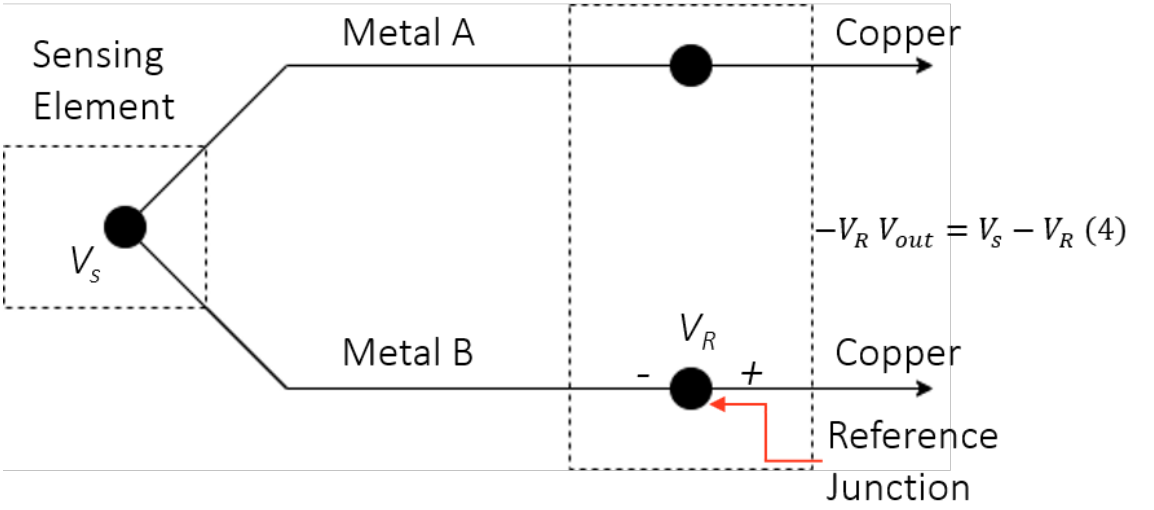

Figure 4.6: Schematic of a general thermocouple.

4.3 Linear Actuated Pitot Probe

Figure 4.7: Image of the pitot tube linear actuator assembly, (a)left side and (b) right side.

The linear actuated pitot probe system is shown in figure 4.7. This system uses a linear actuator, pitot probe, aluminum T-slot rail, and two limit switches for its main functionality. The limit switches keep the linear actuator motor from bottoming out

and burning up while maintaining a desired range of motion. The linear actuator sweeps the pitot probe across the high-speed low-pressure flow exiting the CD nozzle. The T-slot aluminum rail serves as a mount for the circuit panel, limit switches, and a slider bearing to slide the pitot probe steady in a linear fashion. The circuit panel routes all the pressure sensor and linear actuator wires through the DIN rail out to the PLC in the control panel. The inside of the circuit panel is shown in figure 4.8. Our pitot tube had to go through several design iterations due to more miniature diameter pitot probes. The final pitot probe used is durable, custom-made, and had an outer diameter of 3/8ths of an inch.

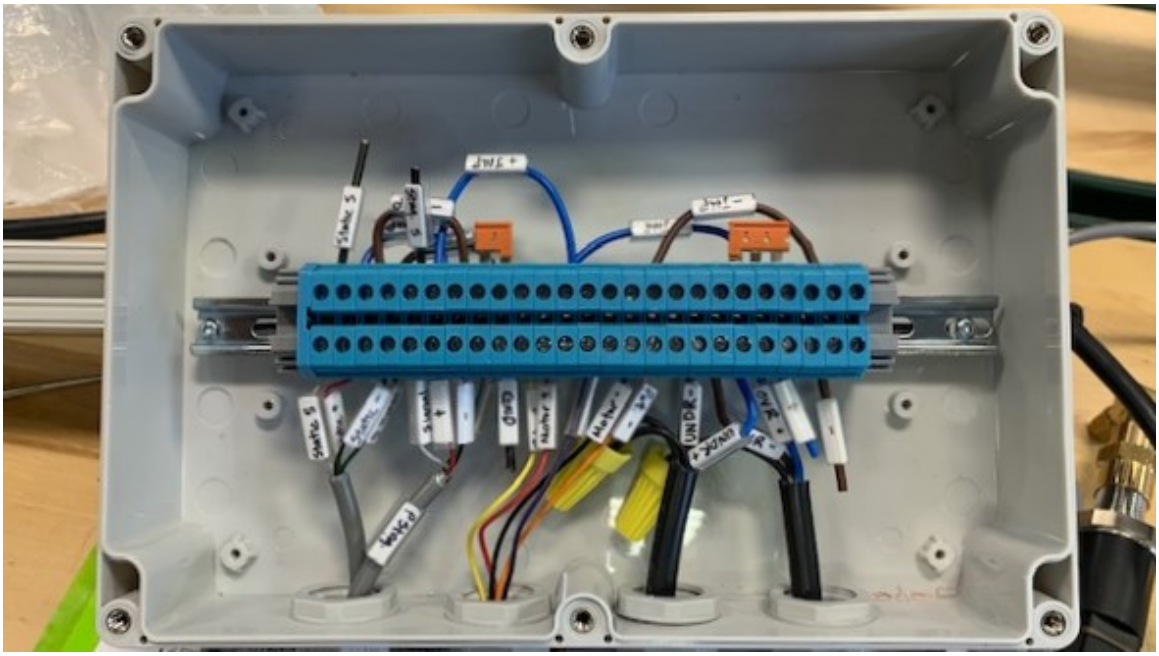

Figure 4.8: Image of the pitot tube linear actuator circuit panel.

Figure 4.9 shows a general pitot tube and manometer schematic. A pitot probe or tube is usually installed into a duct with the tip pointed towards the flowing body of fluid [58]. The hole at the tip of the pitot probe is connected to the stagnant /positive portion of the manometer. The hole along the tip of the tip is connected to the manometer's static or negative portion. When a fluid flow passes over the pitot probe, variances in pressure will change the fluid level in the manometer that is then relayed

back to a DAQ and converted into velocity [59]. In the case of the UNCC HSWT, the manometer would replaced by the diaphragm strain gauge combination. Bernoulli's equation is used in calculating total pressure, P_t. A simplified Bernoulli's equation is shown below in equation 4.1 using static pressure, P_s and dynamic pressure, P_d to solve for stagnant or total pressure, P_t.

$$P_t = P_s + P_d \tag{4.1}$$

To sovle for dynamic pressure, multiply the squared velocity by the density and divide by 2:

$$P_d = \frac{\rho V^2}{2} \tag{4.2}$$

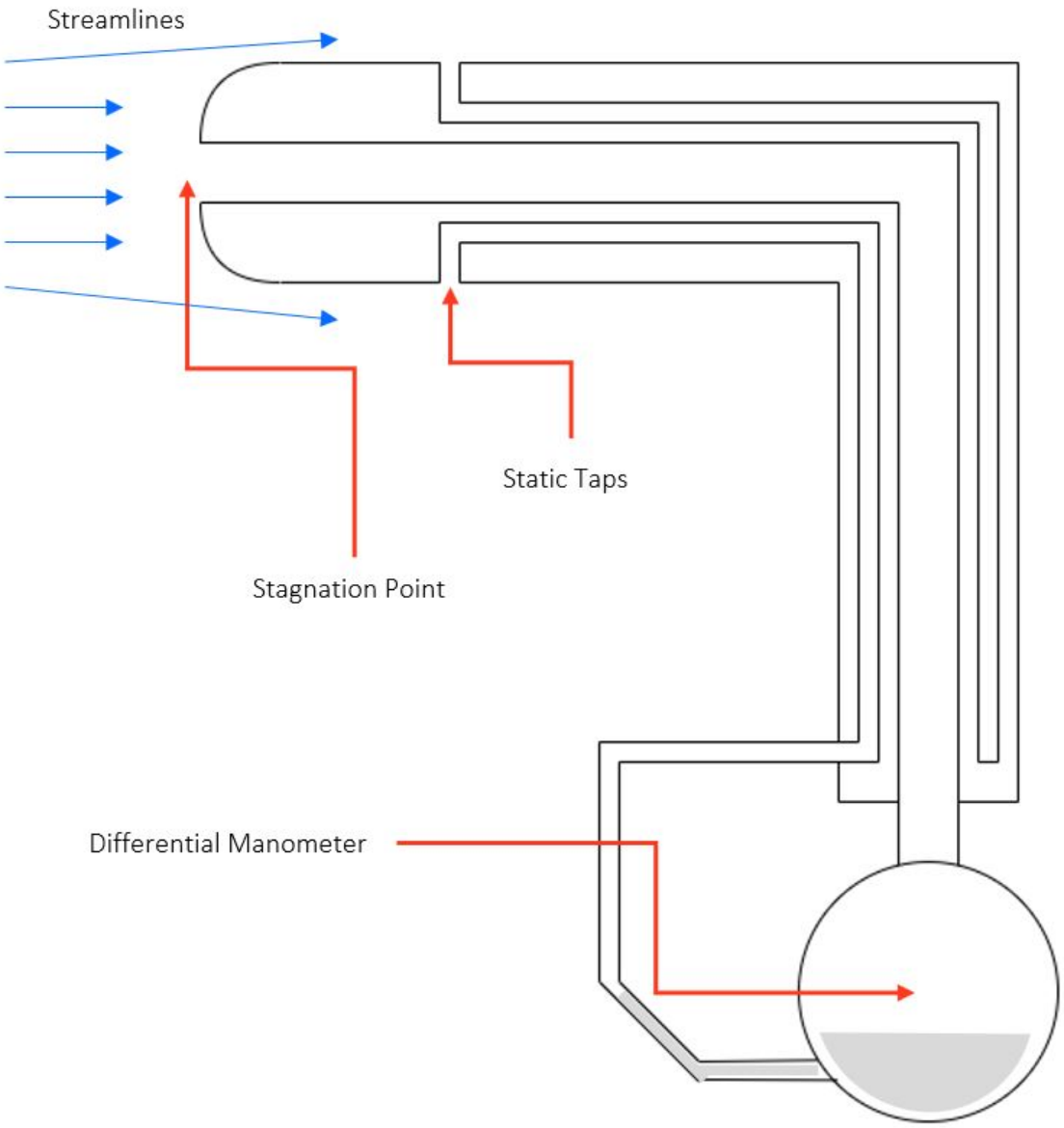

Figure 4.9: Schematic of the workings of a general pitot tube and manometer.

4.4 Programmable Logic Controller

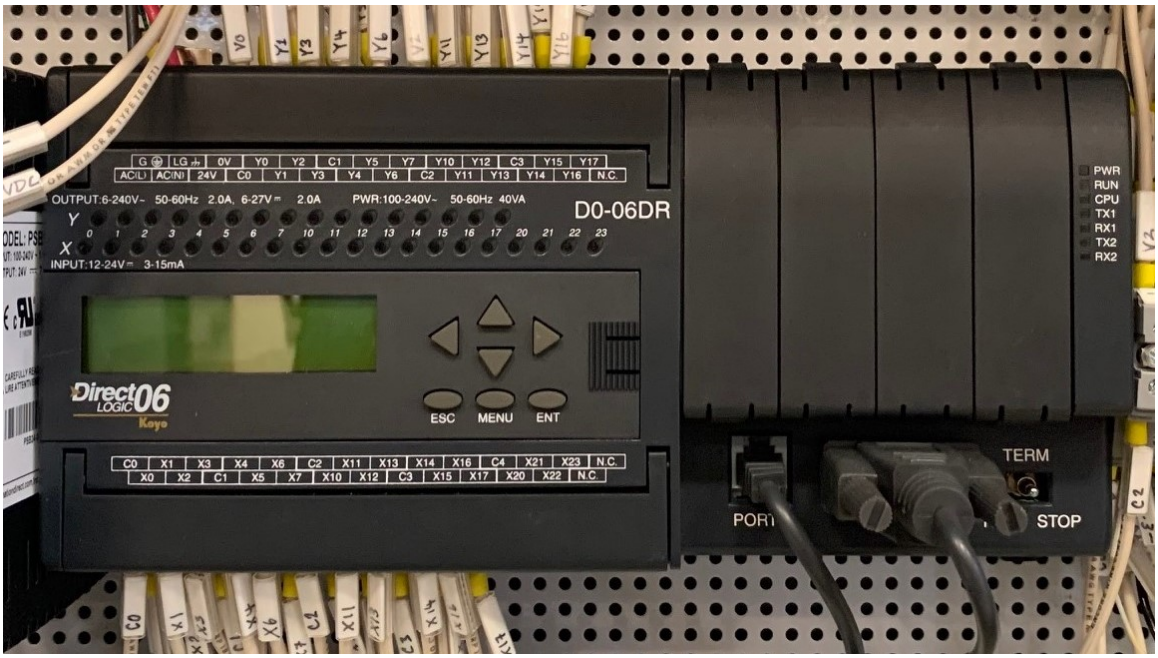

Figure 4.10: Image of the Direct6 programmable logic controller.

The UNCC HSWT uses a Automation Direct programmable logic controller (PLC) to facilitate the functionality of the fast valve, linear actuator, control panel LED's, and emergency stop currently [60]. It has 20 discrete inputs and 16 discrete outputs. Since only a few are used, future instruments can be implemented without concern. It utilizes a Direct6SOFT ladder logic software for programming. An image of the installed PLC is shown in figure 4.10. Images of the ladder logic software can are located in figure C.1 through C.8 in Appendix C.

Currently, there are manual control panel buttons for:

- Emergency Stop
- Main Power
- Heating Chamber
- Heater At Temp

- Retract Actuator
- Extend Actuator
- Camera Trigger
- Fast Valve
- Schlieren Light Power
- Compressor Power
- Compressor Compressing
- Cycle Actuator
- Test Light

4.5 Data Acquisition

Figure 4.11: Image of the National Instruments SCXI 1000.

Data acquisitions are carried out using a National Instruments SCXI 1000 chassis with an integrated SCXI 1300 and SCXI 1303 modules. Pressure and temperature data are captured by several pressure sensors and thermocouples installed through the UNCC HSWT. The SCXI 1300 is used to process pressure sensor data, and the SCXI 1303 is used to process temperature data delivered from the thermocouples.

Both of the integrated modules have 32 channels each. This allows for a connection of 64 devices total if needed. The SCXI chassis also has an additional vacant module bay. If another 1300 series SCXI was installed, a maximum of 96 devices could be connected. National Laboratories LabVIEW software is used to collect the testing data [61]. Once this data is collected, it is saved as a txt file and uploaded into Microsoft Excel to create data plots that will be discussed in the following chapter. The LabVIEW block diagram and front panel is shown in figures D.1 through D.3 in Appendix D.

CHAPTER 5: COMMISSIONING

Four senior-year multi-discipline engineering students built the UNCC hypersonic wind tunnel under my leadership. Each team member, including myself, was assigned a subsystem to design, manage, and construct. The hypersonic wind tunnel works by charging twelve pressure vessels with compressed air up to a maximum of 1000 psi. Once 1000 psi is reached, a fast actuated valve releases this pressure and flows into a specific convergent-divergent nozzle, designed to reach a designated Mach number. High-pressure low-velocity flow enters the inlet of the CD nozzle below Mach 1. At the throat of the CD nozzle, the flow increases to Mach 1. As the flow exits the CD nozzle, the velocity dramatically increases above Mach 1, and the pressure reduces. The flow passes through a testing chamber where test samples can be analyzed with pressure sensors, thermocouples, and Schlieren imaging. The flow then exits the testing chamber into the diffuser, where it will be evacuated to the atmosphere.

5.1 Capabilities

The UNCC HSWT possesses many functional capabilities. However, its primary functions are to collect supersonic and hypersonic pressure and temperature data and record Schlieren images. Having the capability to record accurate hypersonic flow properties would allow student research to replicate/simulate their experimental test using a CFD or FEA program. This type of validation will set student researchers up to work within the aerospace research industry to contribute to the growing demand for hypersonic-related research.

We converted pressure ratio Mach equations to solve for the Mach number. We specifically used the Rayleigh pitot probe equation, 5.7 using the static pressure

data from the pressure sensor in the test chamber and the stagnate pressure from the sweeping pitot probe for a pressure ratio. The following sections show some of the governing fluid equations that we used in conjunction with the MAF facility for comparison.

5.2 Working Calculations

The plenums maximum pressure was calculated using a dynamic pressure value of $P_s \geq 29.4$ psi.

$$P_d = 0.7 * M^2 * P_s \tag{5.1}$$

$$P_s = \frac{P_d}{0.7 * M^2} \tag{5.2}$$

Using an isentropic relationship between stagnant and static pressure, we get

$$\frac{P_t}{P_s} = \left(1 + \frac{\gamma - 1}{2} * M^2\right)^{(\frac{\gamma}{\gamma - 1})} \tag{5.3}$$

The dependency for isentropic flows is what defines the stagnation temperature values [62].

$$\frac{T_s}{T_t} = \left(1 + \frac{\gamma - 1}{2} * M^2\right)^{-1} \tag{5.4}$$

The equation of state is used to solve for the gas density, ρ_p, in the plenum [63].

$$\rho_p = \frac{P_t}{R * T_t} \tag{5.5}$$

The isentropic relation between the plenum density and the test chamber working density can then be used to find the flow density.

$$\frac{\rho}{\rho_p} = \left(1 + \frac{\gamma - 1}{2} * M^2\right)^{\left(\frac{-1}{\gamma - 1}\right)} \tag{5.6}$$

Raleigh Pitot Tube Formula can be found in equation 5.7 [64]. This is the governing equation used in excel to calculate our Mach numbers from the data collected from the sweeping pitot probe.

$$\frac{P_t}{P_s} = \left[\frac{(\gamma + 1)^2 M^2}{4\gamma M^2 - 2(\gamma - 1)}\right]^{\left(\frac{\gamma}{\gamma - 1}\right)} \left[\frac{1 - \gamma + 2\gamma M^2}{\gamma + 1}\right] \tag{5.7}$$

5.3 Observations

While operating the UNCC HSWT, specific tests were conducted with arbitrary system pressure values ranging from 500 psi to 1500 psi. The results showed that specific pressures paired with specific Mach numbers yielded acceptable results. Further testing should occur with defined parameters to ensure the validation of the collected data. This is the approach taken with the MAF at Virginia Tech.

5.3.1 Data Comparison

The MAF data plots in figure 5.1 so consistent reoccurring test at set system pressures and temperatures. With the UNCC HSWT, the operating temperature was often room temperature, as there was no heating chamber installed into the system. In figure 5.1(a), (c), and (d), the temperature is increased from 80^oF to 620^oF and finally 980^oF while using their Mach 2 nozzle. The impact of temperature change is present in each of these plots showing an increase in pressure as temperature increases. In figure 5.1(b), the pressure in the test chamber falls as soon as the test begins, and in figure 5.1(d), the stagnation pressure increase and decreases simultaneously as the test chamber falls and rises. In figure 5.1(f), the pitot rake shows a nearly consistent Mach 2 flow while using the Mach 2 nozzle across 4 inches of the high-speed flow.

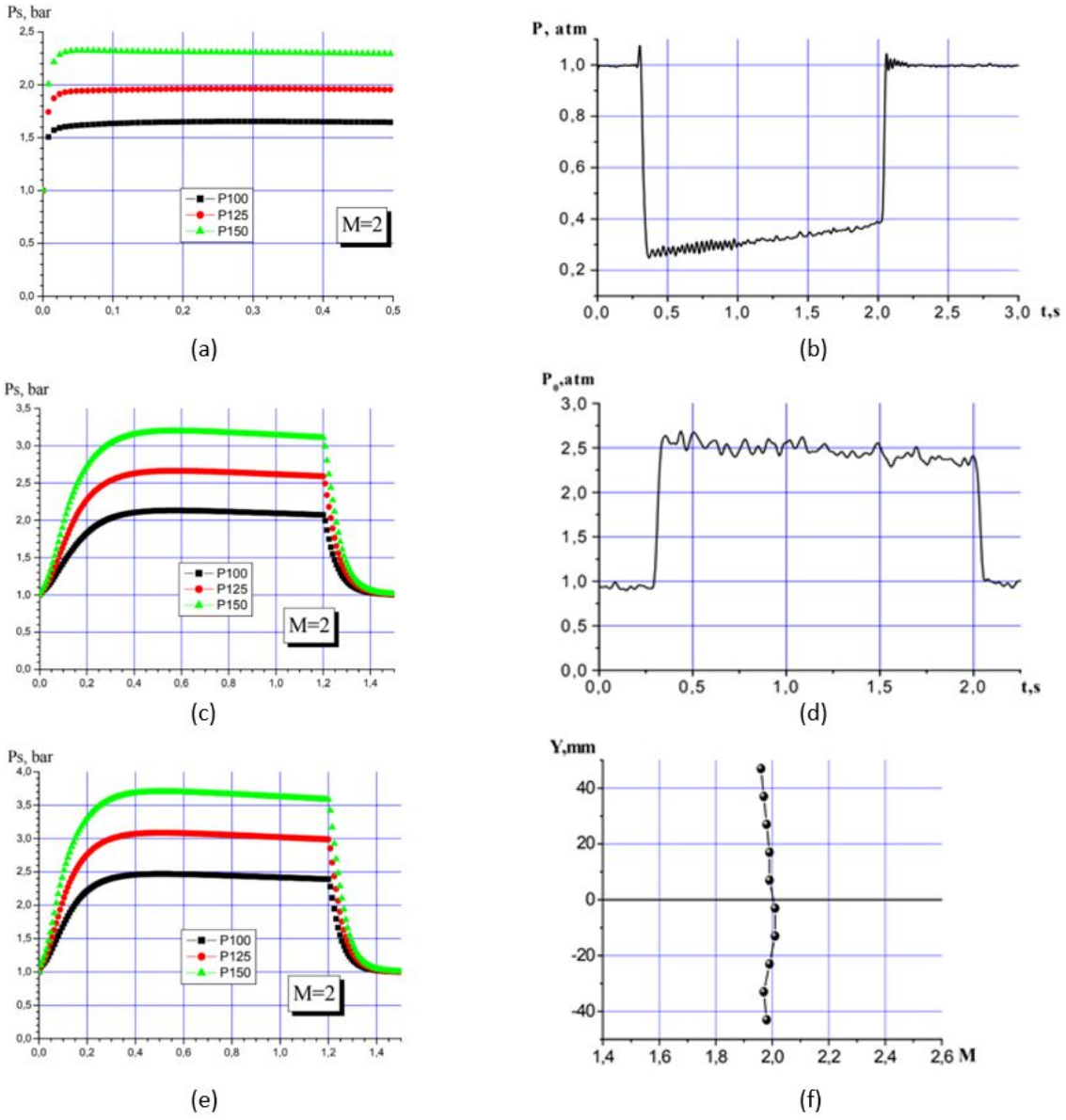

Figure 5.1: VT Data Charts:(a) Mach 2 nozzle pressures at 80^{o}F,(b) Mach 2 working section pressure,P_b = 2204 psi, 62.33^{o}F, (c) Mach 2 nozzle pressures at 620^{o}F,(d) Mach 2 stagnation pressure P_b = 2204 psi, 62.33^{o}F, (e) Mach 2 nozzle pressures at 980^{o}F, (f) Mach number collected from pitot rake with Mach 2 nozzle. Credit: Russian Academy of Sciences Siberian Division Institute of Theoretical and Applied Mechanics.

In figure 5.2 shows the UNCC HSWT wind tunnel data operating with a Mach 5 nozzle with low pressure. Figure 5.2(a) shows a filtered plot of Mach number values against the traverse position. This data was obtained using a sweeping pitot tube

apparatus, compared to the MAF pitot rake. In figure 5.2(b), the Mach number plot is calculated using the data from the plenum downstream pressure sensor and the test chamber upstream pressure sensor. It shows that the Mach number immediately climbs to a little over Mach and slowly decreases over 10 seconds. The profiles between figure 5.2(a) and figure 5.2(b) show similar behavior; however, their Mach Values are greatly skewed, and neither of the results reaches the intended Mach 5 value of the nozzle. Figure 5.2(c) shows that the pitot stagnation pressure increased up to 80 psi, which is not consistent with the test chamber pressure in figure 5.2(d) or the static pitot pressure in figure 5.2(d). As mentioned in the initial observations, consistent, structured tests need to occur to validate and confirm testing results similar to the methods used in the MAF facility documentation. Once this is established, a grounded comparison can be made between both systems.

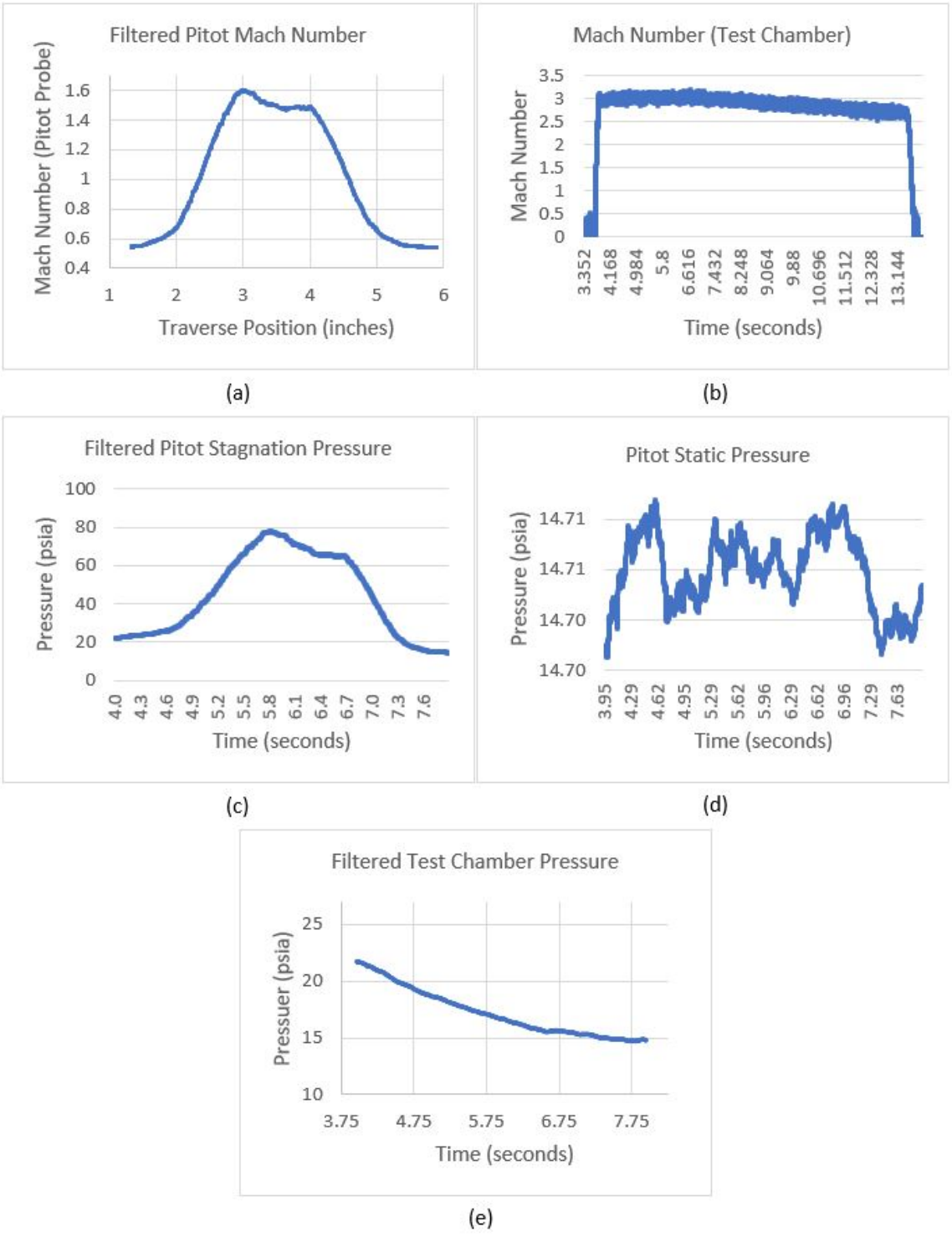

Figure 5.2: UNCC Data Charts using Mach 5 nozzle:(a) Filtered pitot Mach number, (b) Mach Number using static and stagnant pressure from the test chamber, (c) Filter pitot stagnation pressure, (d) Pitot static pressure, (e) filtered test chamber pressure.

Figure 5.3 shows a superimposed comparison of pitot Mach data between the UNCC HSWT and the MAF facility. The test ran with the MAF facility used a Mach 2 nozzle while the UNCC HSWT used a Mach 5 nozzle. Immediately the performance from the data of the MAF facility 4-inch pitot rake with ten pitot ports shows a more consistent range of values between Mach 1.96 to Mach 2.01, which is indicative of the Mach 2 nozzle in use. The sweeping pitot tube of the UNCC HSWT had a broader range and more data points. Although it did not reach its targeted Mach 5 value during this test, from the three to four-inch position mark, there is a nearly consistent value range of Mach 1.6 to 1.5. The MAF facility documentation alludes to completing test runs with specified values. The initial parameters used for the UNCC HSWT may have been too low for it to reach Mach 5. In the future, a comparison could be made between both HSWT's Mach 3, 5, and 7 nozzles under the same conditions. For this to occur, a heating chamber will have to be implemented.

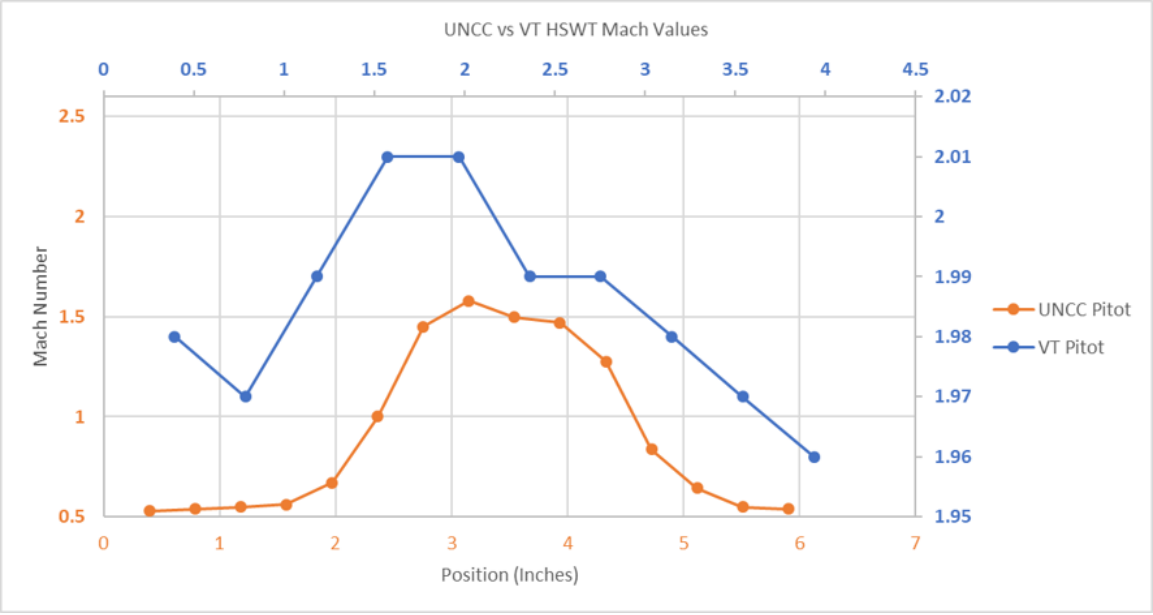

Figure 5.3: Mach value comparison between MAF Mach 2 nozzle and UNCC Mach 3 nozzle.

CHAPTER 6: CONCLUSIONS

In conclusion, the hypersonic wind tunnel at UNCC is a functional aerospace research equipment that could use some improvements. The initial pitot probed used a diameter of 3/16 inches and could not hand the force exerted on it from the supersonic flow. In order to truly consider the UNCC HSWT a "hypersonic" wind tunnel, our testing chamber and test models will have to change thermal properties. Because we do not have a heating chamber, liquefaction will lower the temperature of flow during testing. As it stands, the UNCC HSWT can work as a bridge for students looking to research advanced fluid mechanics by researching with it.

6.1 Impact on Future Research

The UNCC HSWT has academic plans and research initiatives starting in the summer of 2021. Two senior high school students will be teaming up with UNCC engineering students to research over the summer presented at the summer research exposition on campus.

Currently, there are three papers (two theses and an AIAA manuscript) that are being written regarding the construction of the UNCC HSWT. The AIAA abstract was accepted in April 2021. The manuscript for that abstract is due in July 2021 and presented at the AIAA virtual conference in August 2021.

The UNCC HSWT will be used as lab equipment in the Advanced Experimental Methods course for the Fall 2021 semester. Students in that course will learn how to operate that system and use the collected data to solve fluid problem statements and write reports.

6.2 Closing Remarks I: Potential Improvements

6.2.1 Heating Chamber

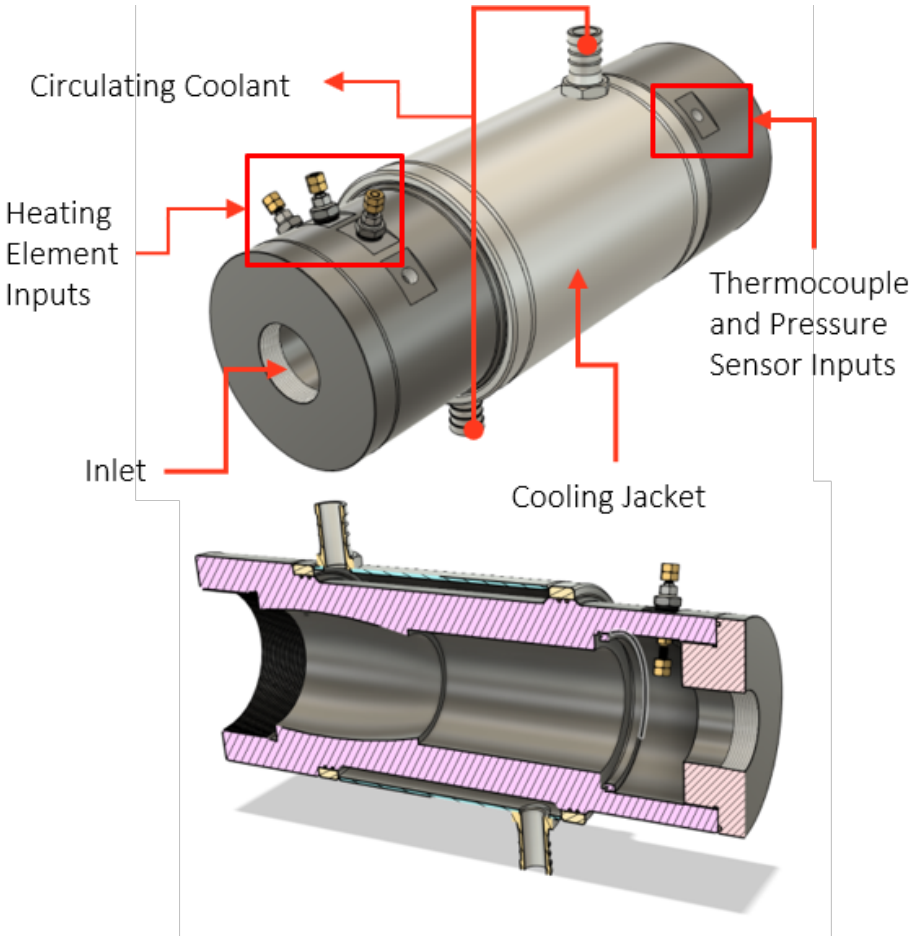

Figure 6.1: Diagram for a conceptional heat chamber design.

A Heating Chamber will be integrated into the plenum to maintain a predetermined temperature that will prevent liquefaction in the testing chamber for speeds exceeding Mach 4. Currently, the heating chamber system design is incomplete but is still in development. The heating chamber should reach temperatures up to 700 K. This required 15,000+ kW of power, which was outside of our budget. However, we can still run the system at Mach 5 without any issues.

The new conceptual design of this heating chamber is shown in figure 6.1. The plenum is made from plain carbon steel and directs heated gases into one flow from

the heating chamber to the entrance to the CD Nozzles. It utilizes a cooling jacket to help keep the exterior cooling and expedite cooling the heating chamber down after use. This concept has been outfitted with bungs for installing thermocouples, high-pressure/high-temperature pressure sensors, and the heating element inputs. The heating chamber used in the MAF facility is shown in figure 6.2. The 2019 senior design team wanted to incorporate this design, but the drawings and seeing it in person showed a high-value part outside our budget.

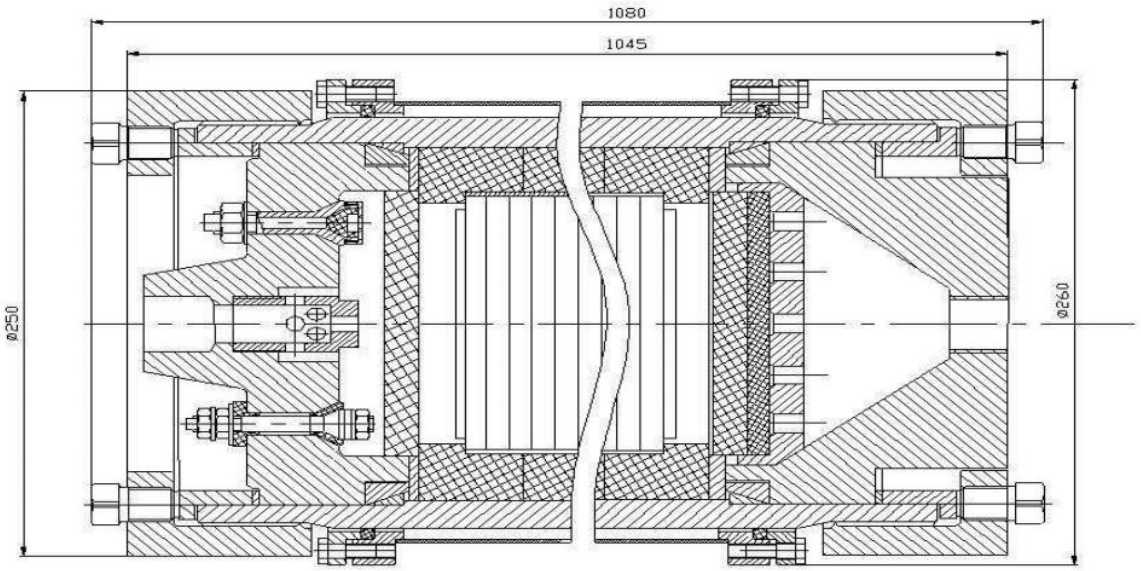

Figure 6.2: Image of John Becker with Hypersonic Wind Tunnel.

6.2.2 Consistent Data Collection

As mentioned before, the initial conditions and parameters set for each test run of the UNCC HSWT were arbitrary. Whatever pressure was reach was the pressure that was tested. In my opinion, let us take the tables from the MAF document and run the same test with the same parameters in order to make some valid data comparisons. Several Mach gauges also need to be integrated into the LabVIEW program using different system values and calculations instead of downloading raw data and transferring it into Microsoft Excel to the plot. Once these suggestions are met, I believe improving the system's functionality will be much more manageable.

6.3 Closing Remarks II: Test Chamber Failure

6.3.1 "Starting" a Hypersonic Tunnel

On April 30, 2021, my advisor and Dr. Tkacik attempted to run a tunnel test using a velocity sweeping Pitot tube and a Mach 3 CD nozzle at 1300 psi. Before running this test, assurance that the testing chamber lid was secure was done. Once the test commenced, the lid flew several feet in the air and landed about 5 feet away from the tunnel. No one was harmed or injured, and the only damage that took place was a small gouge in the concrete floor where the lid landed. The lid and the testing chamber suffered significant damage that rendered them inoperable. The following write-up explains the chain of events in full detail.

In order to reach hypersonic velocities, the tunnel needs to "START." In this process, the flow enters the test chamber from a DeLaval nozzle and exits through a diffuser outlet. If everything works correctly, boundary layers form in the exit diffuser, and when the flow reaches the expansion at the downstream end, a second throat forms and the exit reaches Mach 1 on the way out. This second shock reduces the test chamber pressure to a strong vacuum, increasing the flow through the DeLaval nozzle and "STARTS" the tunnel.

When a tunnel "STARTS," tunnel operation is referred to as "RUNNING." If the second shock is lost, the flow slows in the nozzle. This phenomenon is referred to as an "UN-START," and the tunnel stops "RUNNING." Un-starts were a common problem in the SR-71 Blackbird spy plane engines and a source of significant research studies in the 1960s.

6.3.2 Expected Upstream and Downstream Nozzle Pressure

We have run the tunnel dozens of times, recording the nozzle's pressures up to and downstream. Since the pressure storage tanks release air through pipes, our upstream pressure is recorded at the "False Heater," a pipe adapter into which the

nozzle screws. Since we were planning on a high-pressure heater but have not made it, we made an adapter and gave it the name "False Heater." Using the Mach 5 nozzle, we typically record False Heater Pressures of 700 psig for a tank pressure of 840 psig. We also see test chamber pressures of -12.5 psig (2 psia) during a run.

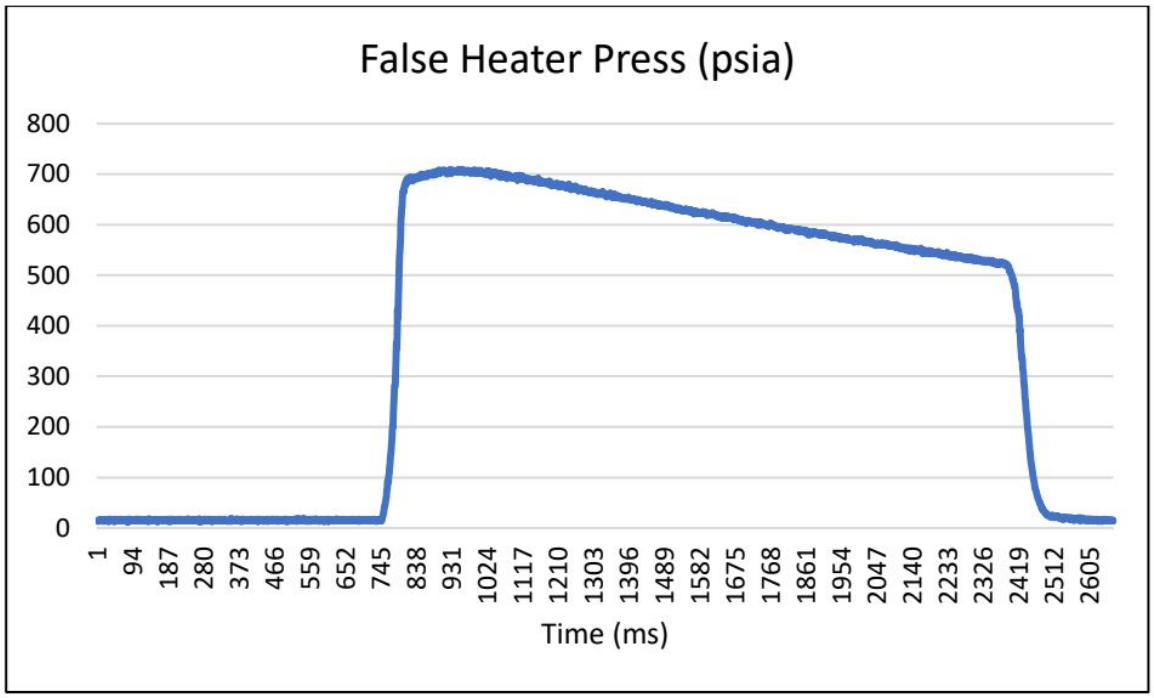

Figure 6.3: The upstream pressure was typically 700 psi.

This run was typical and performed just two days before the failure (29 April 2021).

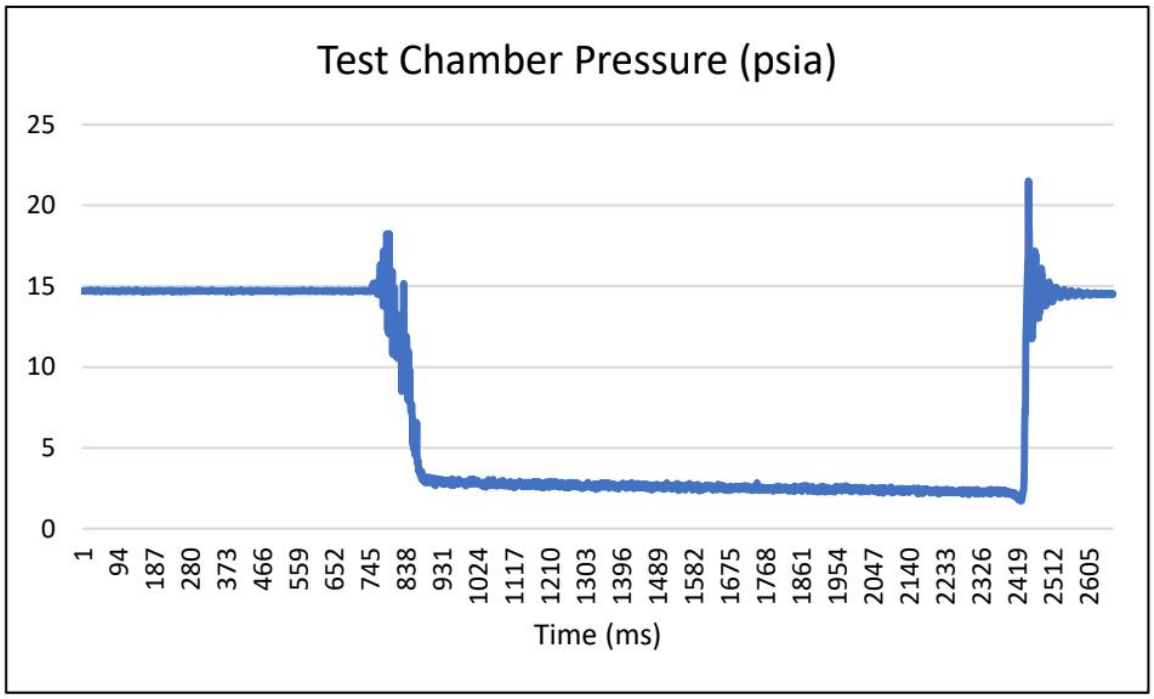

Figure 6.4: Test Chamber pressure was typically a strong vacuum of -12.5 psi.

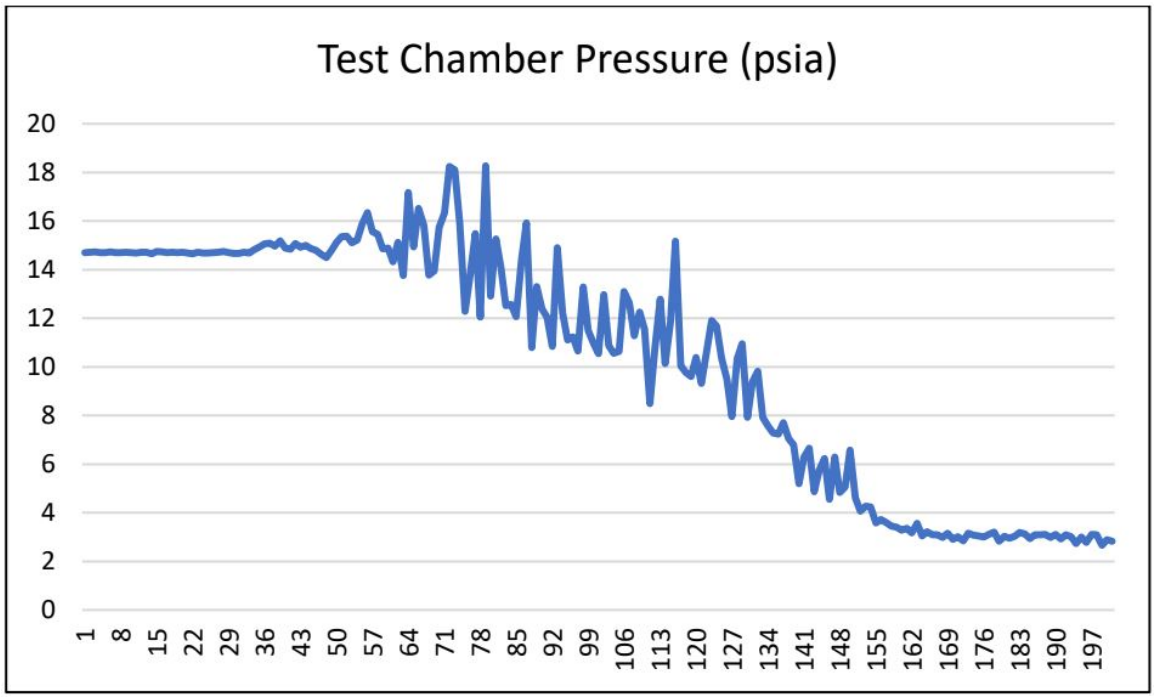

Figure 6.5: Expanded view of typical chamber pressure during first 0.1 seconds of run

6.3.3 Traversing Pitot Probe Development

In our tunnel, STARTING has been easy; however, we have installed a Pitot probe on an electronic linear actuator to traverse across and provide a position record to measure the flow field. Due to the severity of flow, we placed a support beam across the flow on a slotted track for the Pitot probe. The first probe was torn free in the strong wind, and we modified it and the support track several times in response.

The final design of the traverse support was massive considering the small 100mm circular flow field. The probe was increased from 3.2mm (1/8") diameter up to 4.8mm (3/16") and the support from 4.5mm to 7.9mm. In addition, five M6 button head screws and nuts plus washers were added to hold it all together.

With the massive traversing support blocking the flow field, we had trouble getting the tunnel to START. In response, we had just modified to streamline the fasteners to reduce the support cross-section replacing the M6 hex nuts with flat 8-32 screws and "Weld Nuts."

6.3.4 31 April 2021 Test Plan

In order to get the tunnel to START with the traverse, the plan was to use:

- A more robust 3/16" stagnation Pitot probe
- Use the slimmer support with the flat weld nuts
- Change to the slower Mach = 3 DeLaval nozzle

In addition, to hopefully help get the tunnel to start, the twelve high-pressure tanks were then charged to 1500 psi.

6.3.5 1300 psi Test Pressure

Although we have designed the pressure system to handle over 3,000 psi, we had not previously run it over 1,000 psi. The dangerous components were thought to be

the high-pressure lines that see full pressure. The test chamber typically experiences a vacuum, so this was not deemed a problem. This incident would prove to be false.

6.3.6 Test Run, the Lid Blows Off

A video recording was made inside the test chamber, and between the audio and the video, it appears that the test began smoothly for about 2 seconds. However, the tunnel did not start properly, and the test chamber pressure began to rise. The chamber sensor is rated from -14.7psig to +30 psig, and it is measured way beyond before pegging the electronics around +60 psig. If the internal pressure was 60 psig, that produces a force of (60psi x 10" x 20" = 12,000lbs) 53kN. The higher pressure would, of course, translate to an even higher force.

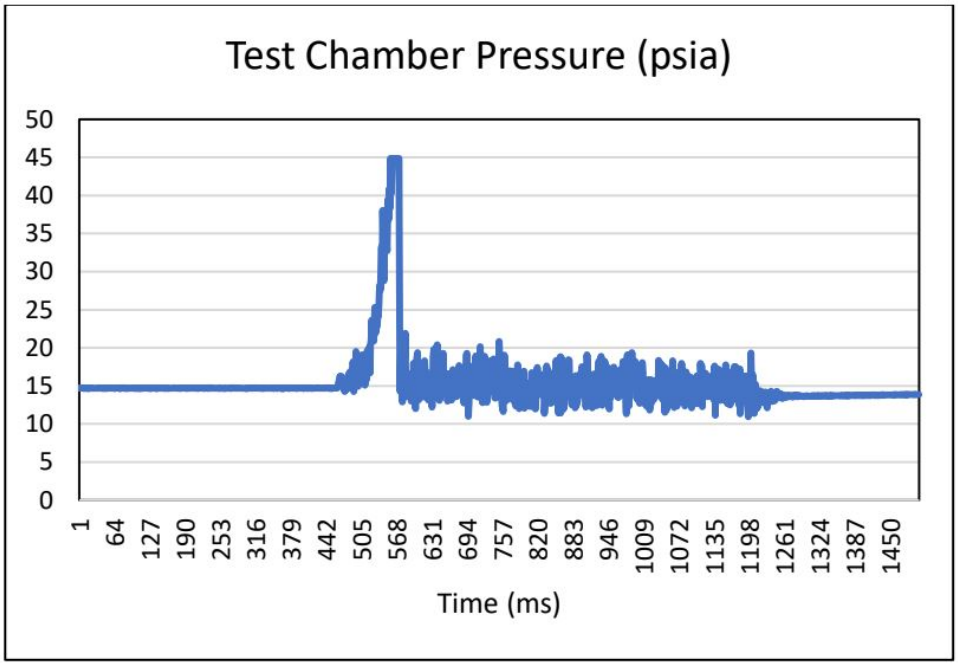

Figure 6.6: Test Chamber pressure revealing pressure spike during start of failure.

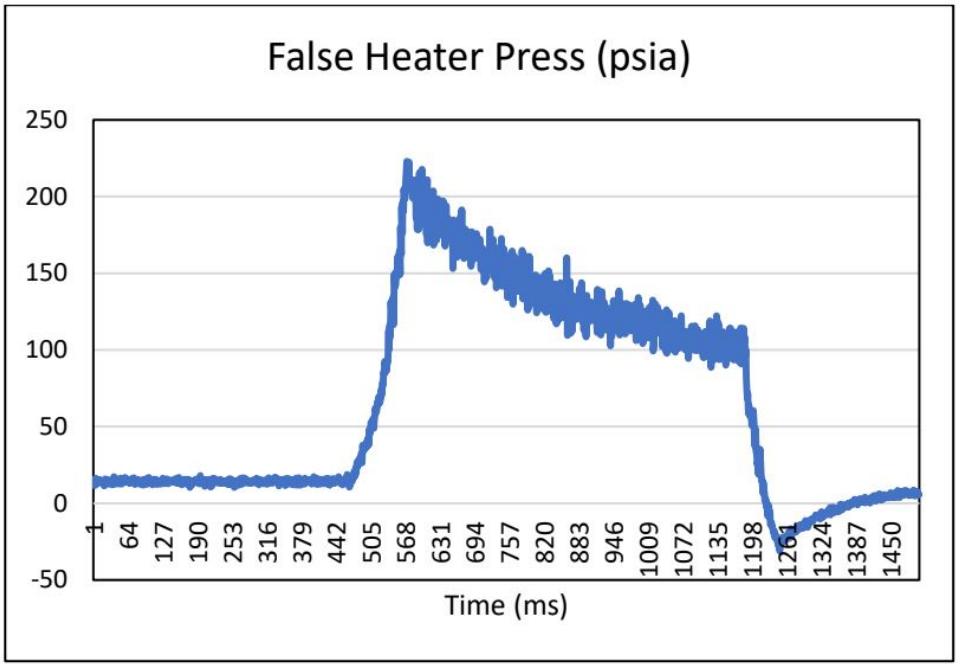

Figure 6.7: False Heater pressure data during failure event.

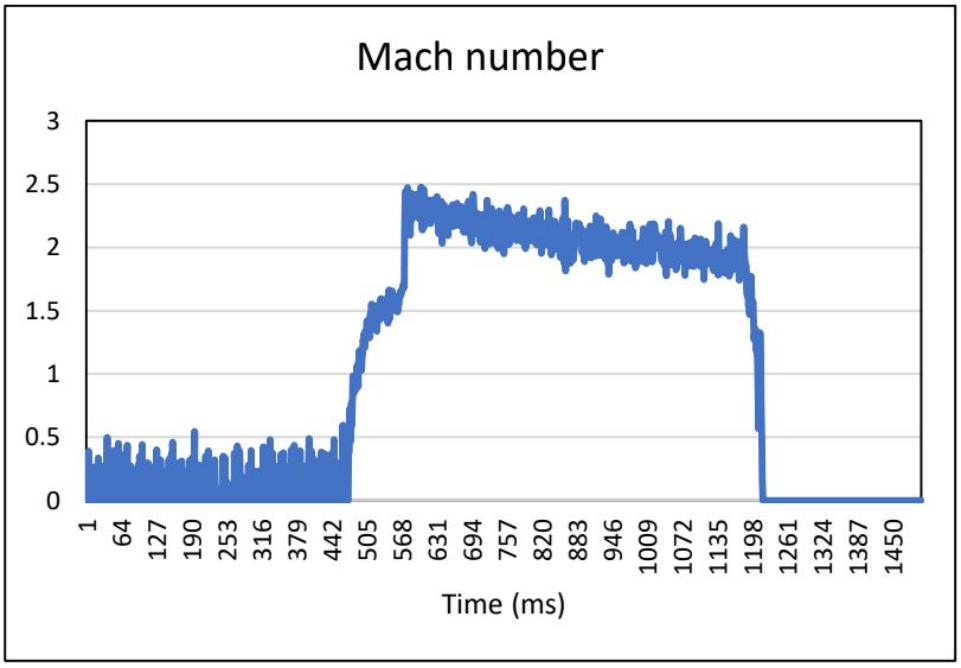

Figure 6.8: Calculated Mach number during failure event.

The 12.7mm (1/2") thick aluminum lid has seven holes and slides down over seven M5 studs. Seven stainless wing nuts are used to clamp the lid down to the chamber,

and the torque was checked just before the test. When the lid blew off, four wing nuts stripped the threads right off the studs. Two of the studs pulled apart at their base. As the lid pulled away, the final stud stayed intact and pulled sideways through the aluminum, leaving a slot in the lid.

Figure 6.9: Four of the M5 wing nuts stripped out the threads and were pulled off the M5 studs.

Figure 6.10: The last of seven studs was intake but the aluminum lid pulled laterally through it and cut a slot.

The lid flew off the top of the test chamber and hit the floor 1 meter from the frame on the water channel side, about midway down the frame. My graduate advisor (Dr. Peter Tkacik) and I were at the upstream end of the tunnel, approximately 3m away.

Figure 6.11: Shallow chip in floor approximately 25 mm in diameter.

6.3.7 The Sides Almost Blow Out

In addition, several of the M5 fasteners used to hold the sides of the test chamber together also failed. Some completely stripped the threads out of the aluminum walls and popped out. Many were very loose and had pulled threads out but had not popped out because by that time, the top had come off, and the internal pressure dropped.

Figure 6.12: Two of the side M5 fasteners pooped completely out of the chamber.

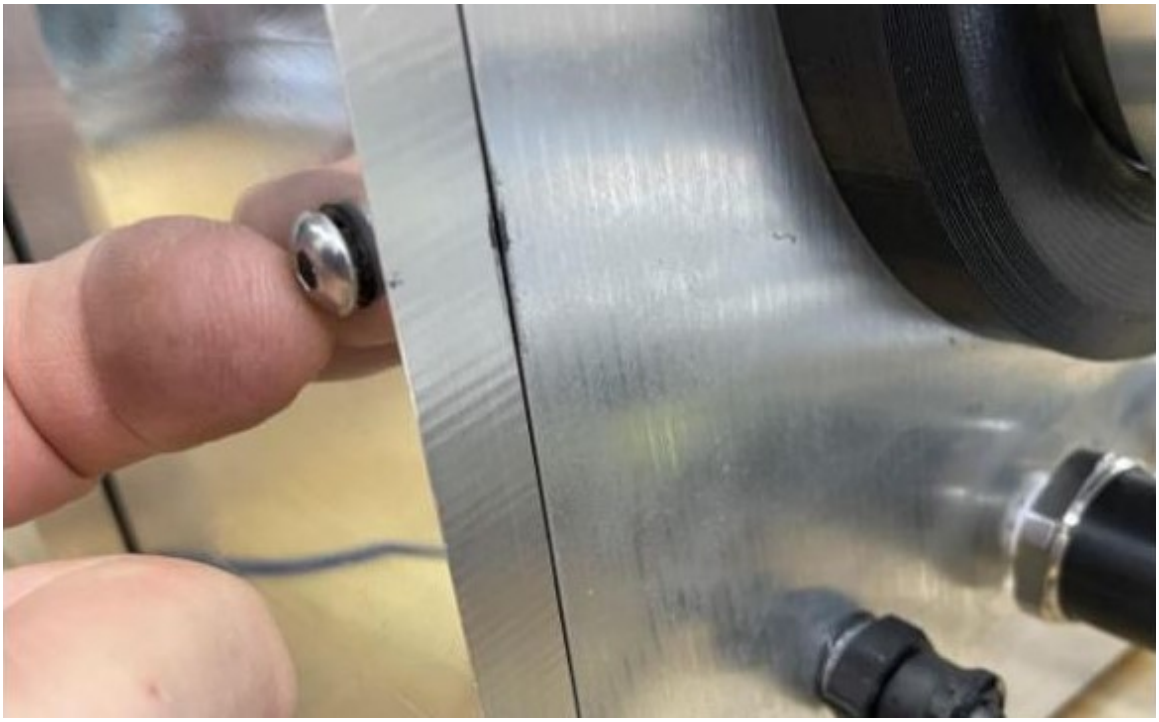

Figure 6.13: Loosened M5 Button Head cap screw in chamber wall.

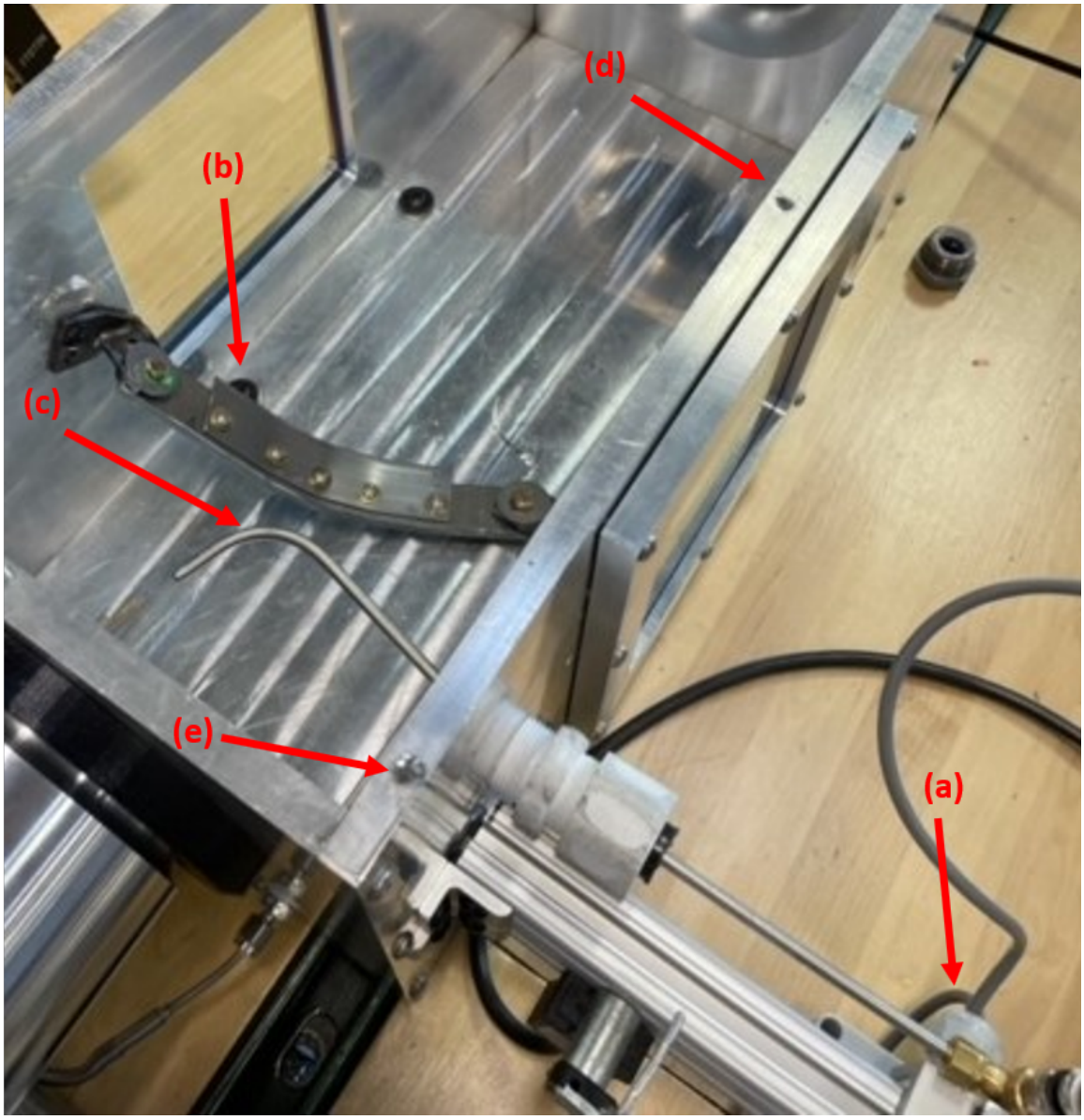

Figure 6.14: Inside of Test Chamber after failure; (a) Traverse Actuator, (b). Bent Traverse Support, (c), Bent Pitot Probe, (d) Broken off stud, (e) Stripped Stud.

6.3.8 Pressure Ratio Across the Laval Nozzle

With a high enough pressure ratio, a de Laval nozzle will go super-sonic at its exit. The equation is:

$$\frac{P_0}{P} = \left(\frac{2}{\gamma+1}\right)^{\left(\frac{\gamma}{\gamma-1}\right)} \left(\frac{1+\gamma}{1+\gamma M^2}\right) \left(1+\frac{\gamma-1}{2}M^2\right)^{\left(\frac{\gamma}{\gamma-1}\right)} \tag{6.1}$$

(ref. Hill and Peterson, "Mechanics and Thermodynamics of Propulsion" Addison Wiley publishers, equation 3-23)

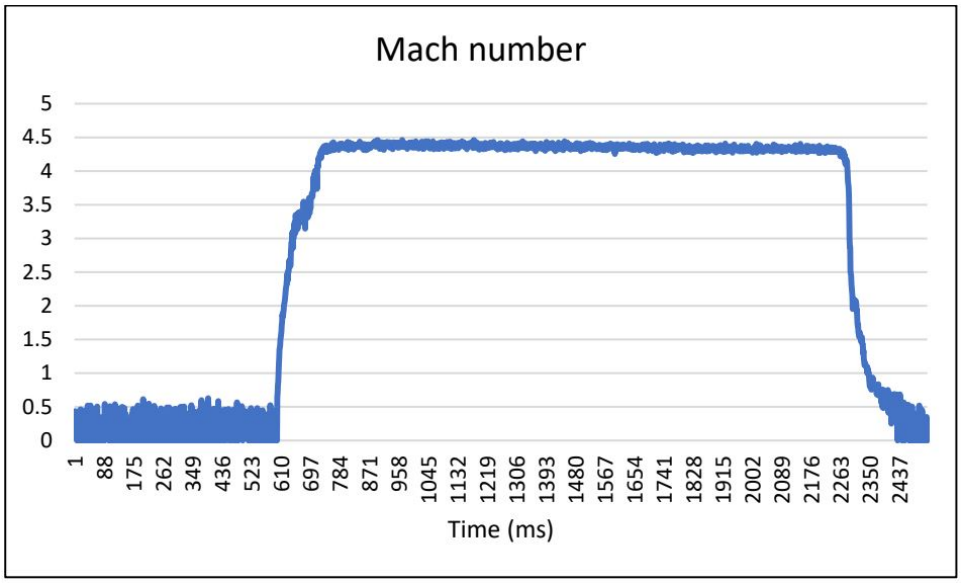

Figure 6.15: Typical Mach measurements (from 29 April 2021 data).

The measured pressure normally match the test results. The result is that the chamber produces whatever test pressure needed to reach the correct Mach number and for Mach 5 and a pressure ratio (Po/P) of 514 is needed, so for 700psi upstream, the chamber pressure is 1.36 psia.

The calculated test failure pressure should have been a vacuum. For a Mach 3 nozzle, the throat is much larger. This is because the area ratio needs to be much smaller than the higher Mach number nozzles, but they all use a 100mm diameter exit. The throat of the Mach 7 Nozzle is only about 12mm, whereas the Mach 3 nozzle is closer to 40mm. Because the Mach 3 nozzle has such a large throat, the flow is much greater, and the upstream pressure is not high.

As expected, where a Mach 5 nozzle will have an upstream pressure of 700 psi, the Mach 3 nozzle had an upstream pressure of only 150 to 200 psi.

The result is that for a Mach 3 nozzle, the pressure ratio is 33, and for an upstream pressure of 220 psia, the test chamber pressure would calculate out to be 6.65 psia or

still a vacuum.

6.3.9 So, If All the Pressures Look Okay, What Happened?

In the extreme pressure spike review on 31 April 2021, the most logical result is that there was a short-term backup of air during the initiation of flows in the diffuser. As the extreme volume of air exiting the (large throat of the) nozzle arrived in the test chamber, it needed to flow out the diffuser to exit. This required a flow pattern in the diffuser to initiate and form boundary layers and then form an exit shock. Once the exit shock was formed and the tunnel was "RUNNING," the test chamber would drop in pressure to a vacuum of 6.65 psia.

The estimation is that if the tunnel had "Started," things would have calmed down considerably.

6.3.10 Three Recommendations are Suggested

1. A Hazard Work Analysis is performed on both the equipment design and the operator procedures.

2. The long-term solution is to rebuild the testing chamber using:

   (a) Thicker Steel

   (b) Larger Fasteners

   (c) Assembly Protocols (For fastener torque and marking)

   (d) Safety Straps

3. A short-term solution is to rebuild the current test chamber:

   (a) Utilizing twice the number of fasteners.

   (b) Blue Marked M5 fasteners

   (c) Assembly Protocols

4. New protocol for short term testing.

In the case of rebuilding the current chamber, it is recommended that the tunnel be moved outdoors prior to any testing at a high pressure. That is, for the first test, and any test with a tank pressure higher than 80% of the highest test pressure, (e.g., test it at 1,000 psi and use it outdoors for any test over 800 psi).

REFERENCES

[1] D. Marren and F. Lu, "Advanced hypersonic test facilities," 2002.

[2] S. J. Beresh, K. M. Casper, J. L. Wagner, J. Henfling, R. Spillers, and B. O. Pruett, "Modernization of sandiaâs hypersonic wind tunnel," in *53rd AIAA Aerospace Sciences Meeting*, p. 1338, 2015.

[3] R. Joussot, S. Coumar, and V. Lago, "Icare, cnrs, orléans,"

[4] K. Reddy, "Hypersonic flight and ground testing activities in india," 2007.

[5] H. M. Sayler, *Hypersonic weapons: Background and issues for Congress*. Congressional Research Service, 2019.

[6] P. P. Cone, *Assessing the Influence of Hypersonic Weapons on Deterrence*. USAF Center for Strategic Deterrence Studies, Air University, 2019.

[7] T. A. Heppenheimer, *Facing the heat barrier: a history of hypersonics*, vol. 4232. Government Printing Office, 2009.

[8] R. Chen, "Computational studies of the virginia tech hypersonic wind tunnel," in *Proceedings of the Virginia Tech Symposium for undergraduate research in engineering*, Citeseer, 2004.

[9] J. V. Becker, "Results of recent hypersonic and unsteady flow research at the langley aeronautical laboratory," *Journal of Applied Physics*, vol. 21, no. 7, pp. 619–628, 1950.

[10] J. BECKER, "Studies of high lift/drag ratio hypersonic configurations," in *International Council of the Aeronautical Sciences*, p. 551, 1965.

[11] D. R. Jenkins, *X-15: Extending the Frontiers of Flight*, vol. 562. NASA, 2007.

[12] T. A. Heppenheimer, *Facing the heat barrier: a history of hypersonics*, vol. 4232. Government Printing Office, 2009.

[13] D. R. Jenkins, *Hypersonic: the story of the North American X-15*. Specialty Press, 2008.

[14] C. H. Wolowicz and T. D. Gossett, *Operational and Performance Characteristics of the X-15 Spherical, Hypersonic Flow-Direction Sensor*. National Aeronautics and Space Administration, 1965.

[15] L. McLain and M. Palitz, *Flow-field investigations on the X-15 airplane and model up to hypersonic speeds*, vol. 4813. National Aeronautics and Space Administration, 1968.

[16] R. Wiswell and R. Wiswell, "X-15 propulsion system," in *33rd Joint Propulsion Conference and Exhibit*, p. 2682, 1997.

[17] T. Smith, "The dyna-soar x-20: A historical overview," *Quest: The Magazine of Spaceflight*, vol. 3, pp. 13–18, 1994.

[18] R. F. Houchin II, *US Hypersonic Research and Development: The Rise and Fall of'Dyna-Soar', 1944-1963*. Routledge, 2006.

[19] R. G. Forman, R. J. Gillen, and R. S. Szacik, "Description and evaluation of environmental control and cryogenic supply subsystems for x-20 (dyna-soar).," tech. rep., SYSTEMS ENGINEERING GROUP WRIGHT-PATTERSON AFB OH, 1965.

[20] M. Vachon, T. Grindle, C. St. John, and D. Dowdell, "X-43a fluid and environmental systems: ground and flight operation and lessons learned," in *AIAA/CIRA 13th International Space Planes and Hypersonics Systems and Technologies Conference*, p. 3337, 2013.

[21] C. McClinton, "X-43-scramjet power breaks the hypersonic barrier: Dryden lectureship in research for 2006," in *44th AIAA aerospace sciences meeting and exhibit*, p. 1, 2006.

[22] S. A. Berry, M. DiFulvio, M. K. Kowalkowski, *et al.*, "Forced boundary-layer transition on x-43 (hyper-x) in nasa larc 31-inch mach 10 air tunnel," *NASA TM*, vol. 210315, p. 2002, 2000.

[23] P. Harsha, L. Keel, A. Castrogiovanni, and R. Sherrill, "X-43a vehicle design and manufacture," in *AIAA/CIRA 13th International Space Planes and Hypersonics Systems and Technologies Conference*, p. 3334, 2005.

[24] R. T. Voland, L. D. Huebner, and C. R. McClinton, "X-43a hypersonic vehicle technology development," *Acta Astronautica*, vol. 59, no. 1-5, pp. 181–191, 2006.

[25] E. H. Hirschel *et al.*, "Basics of aerothermodynamics," 2005.

[26] W. Hayes, *Hypersonic flow theory*. Elsevier, 2012.

[27] J. T. Blackmore, *Ernst Mach; his work, life, and influence*. Univ of California Press, 1972.

[28] E. Josyula, *Hypersonic Nonequilibrium Flows: Fundamentals and Recent Advances*. American Institute of Aeronautics and Astronautics, Inc., 2015.

[29] G. Bar-Meir, *Fundamentals of compressible flow mechanics*. PhD thesis, Open Textbook Library, 2012.

[30] P. Balachandran, *Fundamentals of compressible fluid dynamics*. PHI Learning Pvt. Ltd., 2006.

[31] R. D. Zucker, "Fundamentals of gas dynamics," *NASA STI/Recon Technical Report A*, vol. 78, p. 11956, 1977.

[32] S. Glegg and W. Devenport, *Aeroacoustics of low Mach number flows: fundamentals, analysis, and measurement*. Academic Press, 2017.

[33] V. Babu, "Quasi one dimensional flows," in *Fundamentals of Gas Dynamics*, pp. 69–102, Springer, 2021.

[34] R. Vos and S. Farokhi, *Introduction to transonic aerodynamics*, vol. 110. Springer, 2015.

[35] S. He, Z. Yang, and Y. Gu, "Nonlinear dynamics of an aeroelastic airfoil with free-play in transonic flow," *Nonlinear dynamics*, vol. 87, no. 4, pp. 2099–2125, 2017.

[36] L. Maddalena, F. Vergine, and M. Crisanti, "Vortex dynamics studies in supersonic flow: Merging of co-rotating streamwise vortices," *Physics of Fluids*, vol. 26, no. 4, p. 046101, 2014.

[37] H. Lomax, T. H. Pulliam, and D. W. Zingg, *Fundamentals of computational fluid dynamics*. Springer Science & Business Media, 2013.

[38] W. Hayes, *Hypersonic flow theory*. Elsevier, 2012.

[39] P. Orlandi, *Fluid flow phenomena: a numerical toolkit*, vol. 55. Springer Science & Business Media, 2012.

[40] M. Meyers, *Shock waves and high-strain-rate phenomena in metals: concepts and applications*. Springer Science & Business Media, 2012.

[41] A. A. Pasha and K. Sinha, "Simulation of hypersonic shock/turbulent boundary-layer interactions using shock-unsteadiness model," *Journal of Propulsion and Power*, vol. 28, no. 1, pp. 46–60, 2012.

[42] L. Duan, M. M. Choudhari, A. Chou, F. Munoz, R. Radespiel, T. Schilden, W. Schröder, E. C. Marineau, K. M. Casper, R. S. Chaudhry, *et al.*, "Characterization of freestream disturbances in conventional hypersonic wind tunnels," *Journal of spacecraft and rockets*, vol. 56, no. 2, pp. 357–368, 2019.

[43] E. S. Taskinoglu, D. D. Knight, and S. P. Schneider, "Computational fluid dynamics evaluation of bleed slot of purdue mach 6 quiet tunnel," *AIAA journal*, vol. 44, no. 6, pp. 1360–1362, 2006.

[44] J. Dino, "Ames technology capabilities and facilities," 2008.

[45] S. J. Beresh, K. M. Casper, J. L. Wagner, J. Henfling, R. Spillers, and B. O. Pruett, "Modernization of sandiaâs hypersonic wind tunnel," in *53rd AIAA Aerospace Sciences Meeting*, p. 1338, 2015.

[46] D. Wilkening, "Hypersonic weapons and strategic stability," *Survival*, vol. 61, no. 5, pp. 129–148, 2019.

[47] T. Karako and W. Rumbaugh, "Inflection point," 2020.

[48] T. S. Kocian, *Computational hypersonic boundary-layer stability and the validation and verification of EPIC*. PhD thesis, 2018.

[49] R. A. of Sciences Division: Institute of Theoretical and A. Mechanics, "The model aerodynamic facility (maf) for student's research and instructions," December 2002. Last retrieved 2019-12-10.

[50] B. Atcheson, W. Heidrich, and I. Ihrke, "An evaluation of optical flow algorithms for background oriented schlieren imaging," *Experiments in fluids*, vol. 46, no. 3, pp. 467–476, 2009.

[51] C. L. Dailey, "Supersonic diffuser instability," *Journal of the Aeronautical Sciences*, vol. 22, no. 11, pp. 733–749, 1955.

[52] N. Instruments, *SCXI - Getting Started with SCXI*, vol. 1. National Instruments, 2000.

[53] A. Direct, *DL06 Micro PLC User Manual*, vol. D0-06USER-M. Automation Direct, 2020.

[54] W. P. Eaton and J. H. Smith, "Micromachined pressure sensors: review and recent developments," *Smart Materials and Structures*, vol. 6, no. 5, p. 530, 1997.

[55] J. Berthold, W. Ghering, and D. Varshneya, "Design and characterization of a high temperature fiber-optic pressure transducer," *Journal of lightwave technology*, vol. 5, no. 7, pp. 870–876, 1987.

[56] D. D. Pollock, *Thermocouples: theory and properties*. CRC press, 1991.

[57] M. Heitor and A. Moreira, "Thermocouples and sample probes for combustion studies," *Progress in energy and combustion science*, vol. 19, no. 3, pp. 259–278, 1993.

[58] B. McKeon, J. Li, W. Jiang, J. Morrison, and A. Smits, "Pitot probe corrections in fully developed turbulent pipe flow," *Measurement science and technology*, vol. 14, no. 8, p. 1449, 2003.

[59] J. M. Allen, *Pitot-Probe Displacement in a Supersonic Turbulent Boundary Layer*, vol. 6759. National Aeronautics and Space Administration, 1972.

[60] A. Direct, *DirectSOFT6 - Programming Software User Manual*, vol. PC-DSOFT6-M. Automation Direct, 2019.

[61] N. Instruments, *LabVIEW - Getting Started with LabVIEW*, vol. 1. Automation Direct, 2013.

[62] M. A. Saad, "Compressible fluid flow," *Englewood Cliffs*, 1985.

[63] N. F. Carnahan and K. E. Starling, "Equation of state for nonattracting rigid spheres," *The Journal of chemical physics*, vol. 51, no. 2, pp. 635–636, 1969.

[64] M. Rapp, J. Gumbel, and F.-J. Lübken, "Absolute density measurements in the middle atmosphere," in *Annales Geophysicae*, vol. 19, pp. 571–580, Copernicus GmbH, 2001.

APPENDIX A: Additional UNCC HSWT CAD Drawings

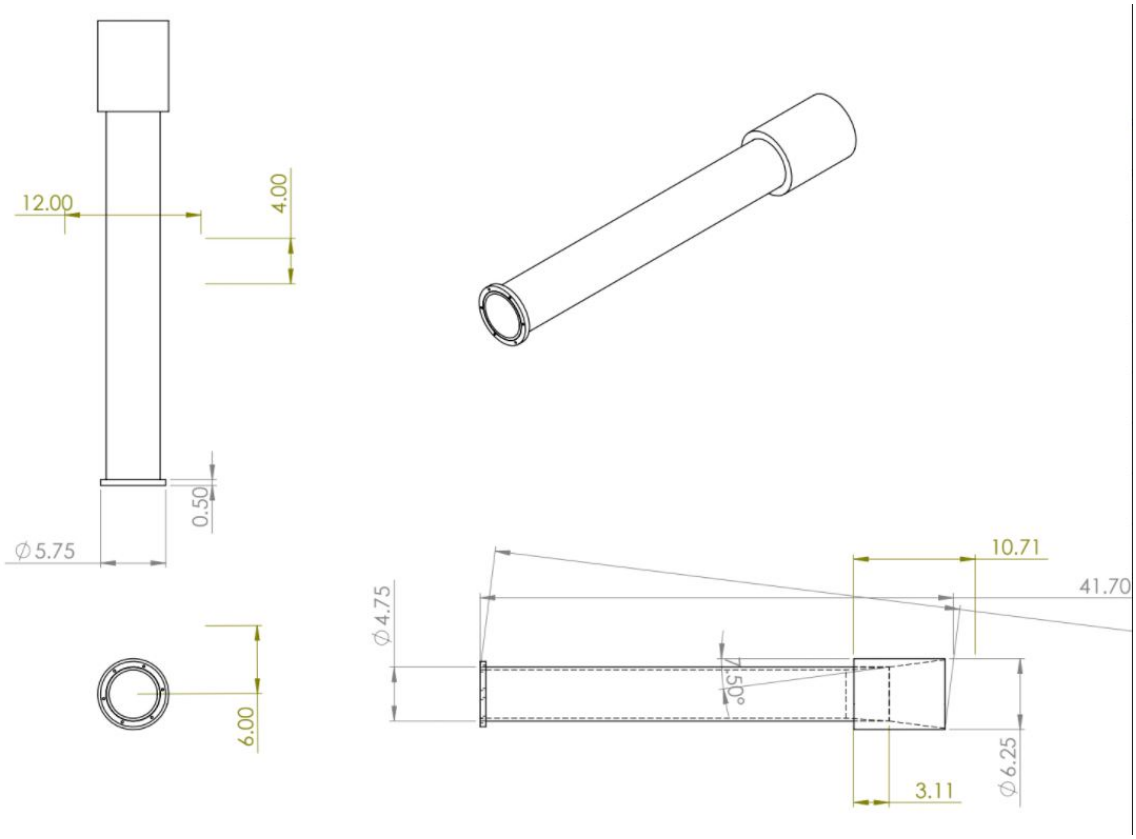

Figure A.1: Drawing of the UNCC HSWT diffuser.

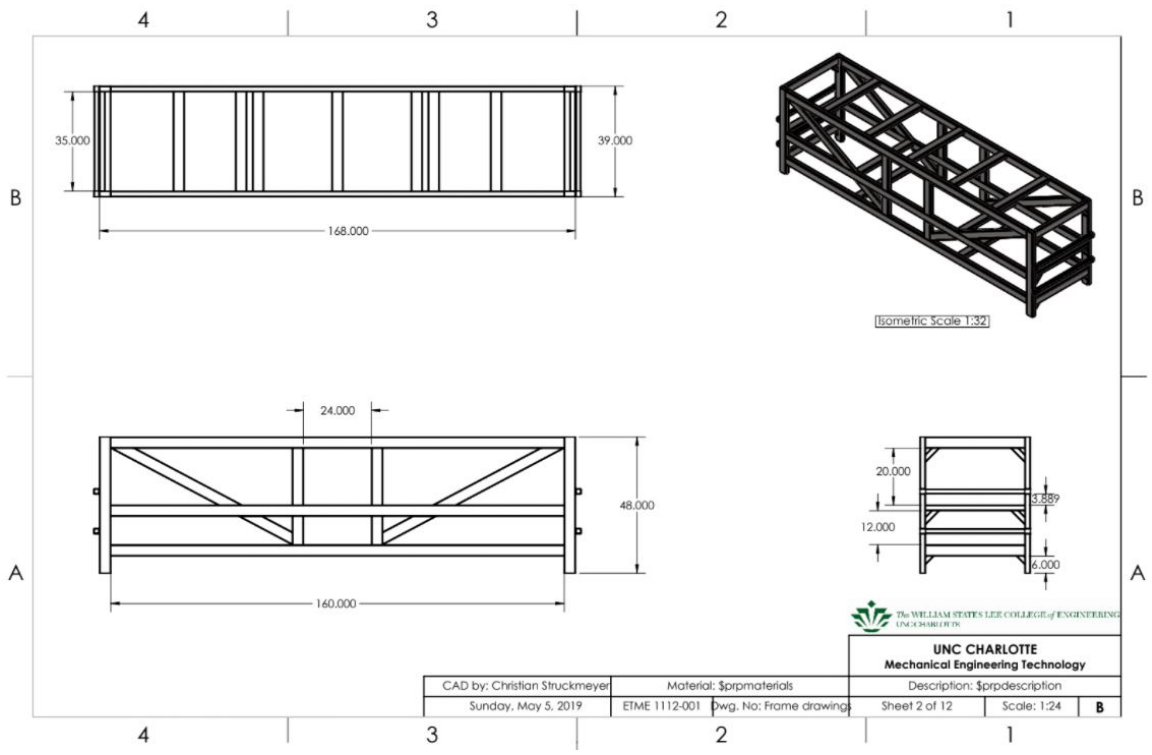

Figure A.2: Drawing of the UNCC HSWT frame.

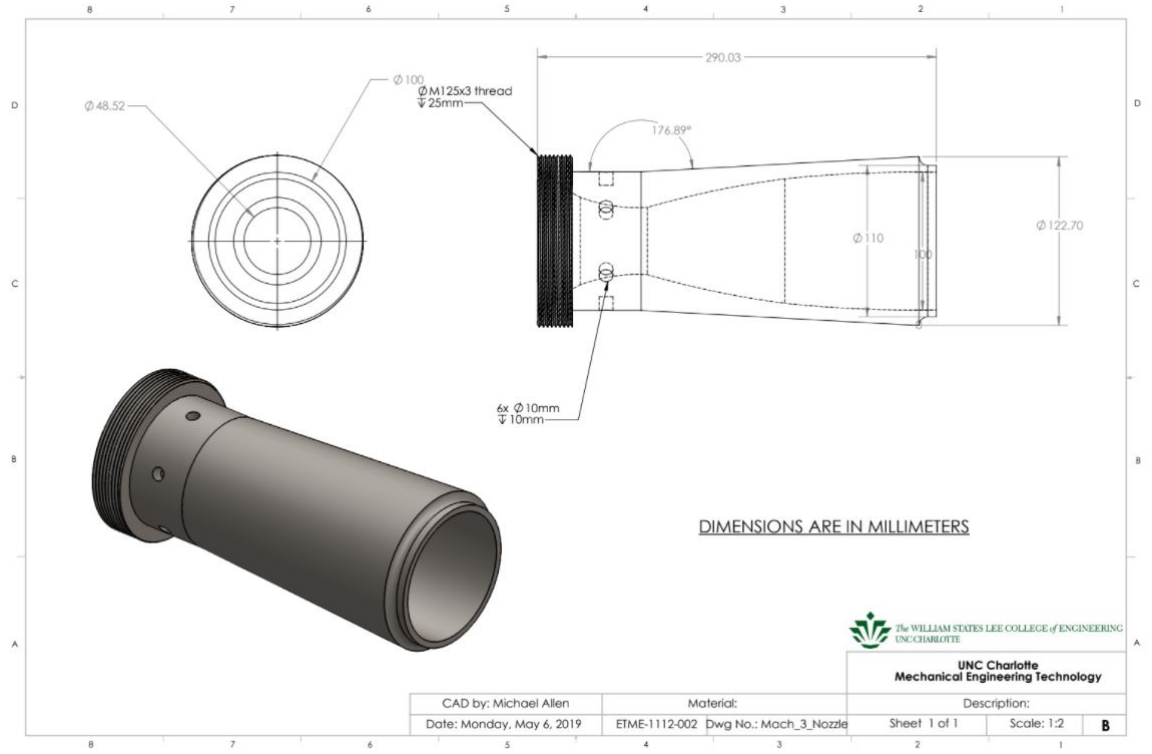

Figure A.3: Drawing of the UNCC HSWT Mach 3 nozzle.

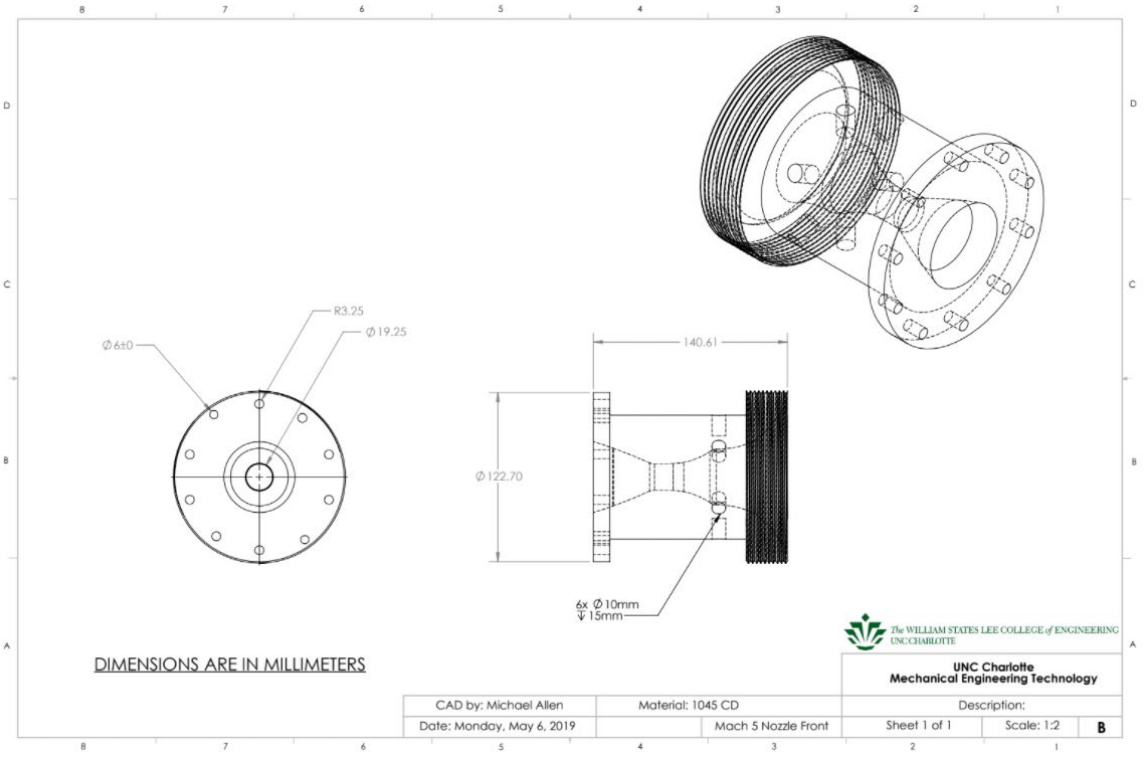

Figure A.4: Drawing of the UNCC HSWT Mach 5 nozzle outlet.

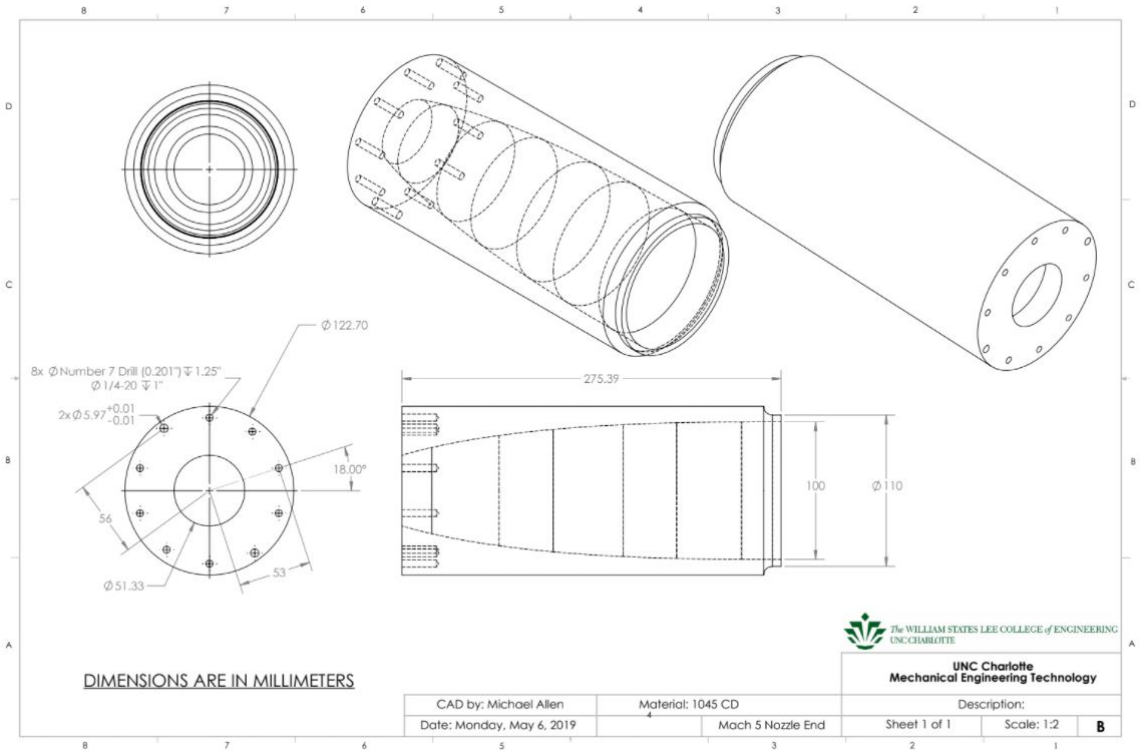

Figure A.5: Drawing of the UNCC HSWT Mach 5 nozzle inlet.

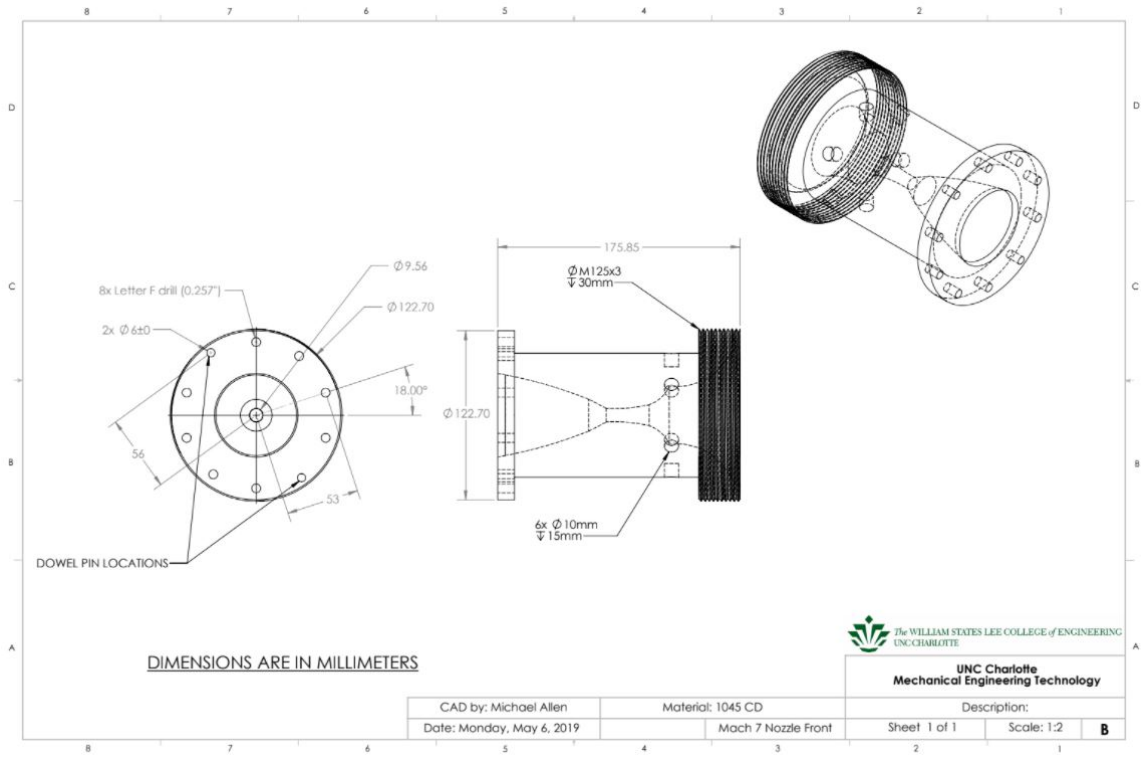

Figure A.6: Drawing of the UNCC HSWT Mach y inlet.

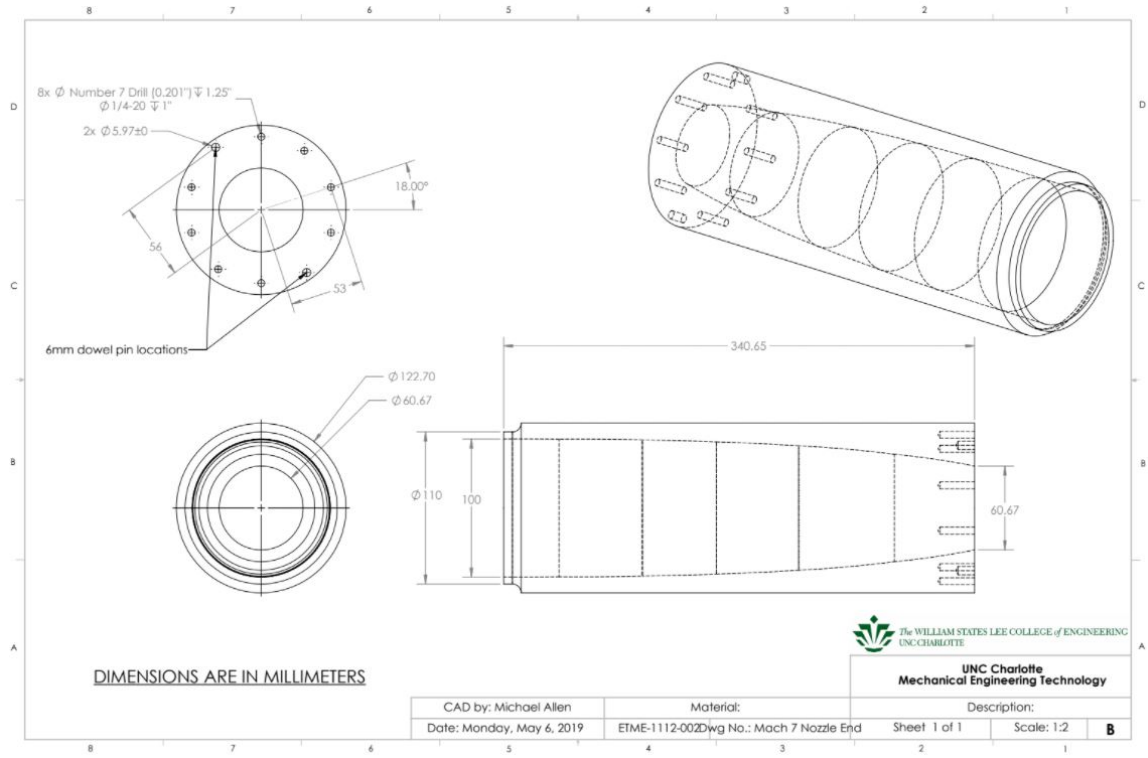

Figure A.7: Drawing of the UNCC HSWT Mach 7 outlet.

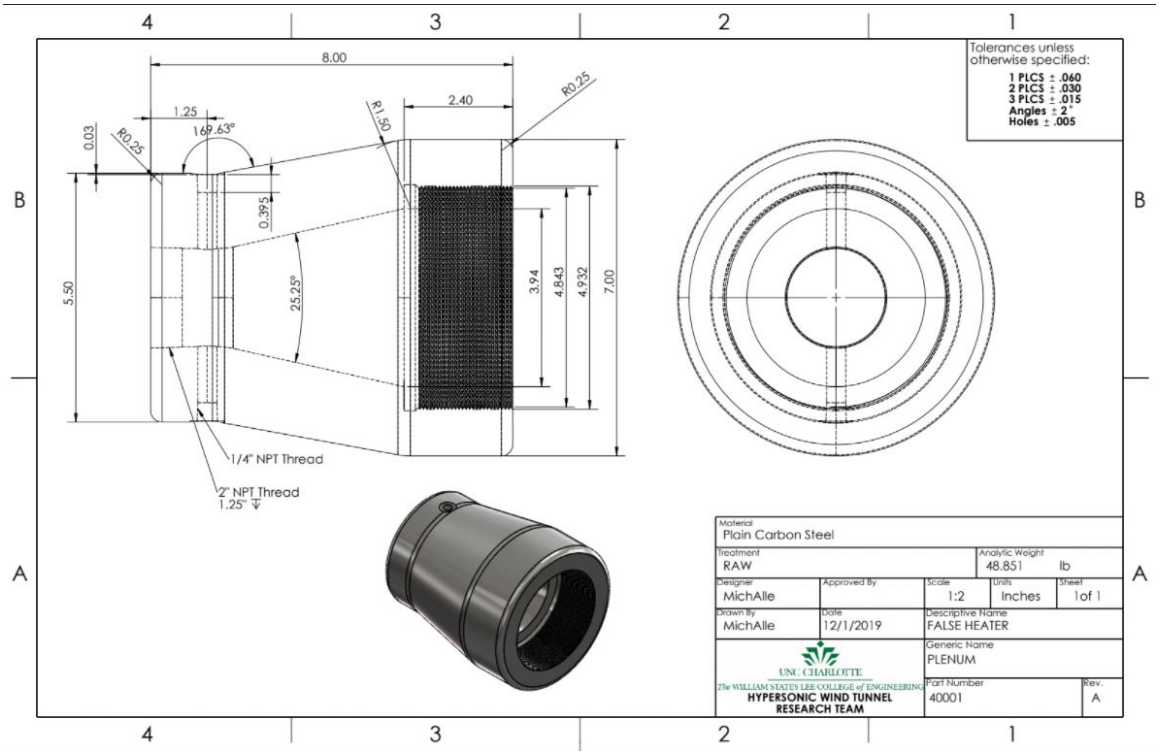

Figure A.8: Drawing of the UNCC HSWT plenum.

APPENDIX B: UNCC HSWT Operating Procedures

B.0.1 Model Installation and Removal

1. Ensure the wind tunnel is not currently operating and the E-Stop is pressed and emitting light.

2. Ensure the high-pressure tanks are de-pressurized by checking the analog pressure gauge located below the test section on the bottom row of the manifold (Figure 3.17).

3. Ensure the Fast Valve safety lock-out, located immediately next to the control solenoid on the Fast Valve, is engaged in the closed position (Figure 3.18).

4. Ensure the secondary safety ball valve underneath the table directly beneath the Fast Valve is in the closed position (Figure 3.16).

5. Remove the test section ceiling by first removing the wing-nuts. This operation requires two hands and a sturdy place to stand.

6. Install the desired test specimen on the stinger and fasten it securely.

B.0.2 Angle of Attack

To adjust the test specimen in the test chamber, make sure the angle of attack is set correctly with the test chamber ceiling. Install the test section ceiling by tightening all the wing-nuts securely.

B.0.3 Wind Tunnel Firing Set Up Operation

1. Make sure the E-Stop is still depressed.

2. Ensure the wind tunnel is in a suitable place to initiate a test run. Preferably outside or in a safe part of the building.

3. Make sure the power cable is installed securely. Make sure to turn the breakers inside the control panel to the on position.

4. Ensure the necessary data cables are hooked up to the control station, and all data and power cables are securely attached to the correct location on the control station and National Instruments SCXI.

5. Make sure the desired Mach velocity Converging-Diverging Nozzle is installed. After making sure the air valves are all closed, turn on the compressor and set it to the desired operating pressure. ***Note: The maximum pressure this system should ever be pressurized to is 2750psi, and the pressure the nozzles are designed to operate at to achieve their desired velocities is 2400psi.*** Ensure the control station has the desired LabVIEW program or another data acquisition software ready to gather data. Once the tanks are up to operating pressure, turn the compressor off.

6. Unlock the fast valve solenoid safety lock-out.

7. Slowly open the secondary valve under the table to fully arm the system.

8. After checking the surroundings and warning anyone within hearing range, the E-Stop may be released.

9. **Anyone within the building or nearby must be wearing the proper PPE**(hearing protection and eye protection minimum).

10. To initiate the data acquisition program, press RECORD. To initiate a test run of the wind tunnel, press the RUN button.

B.0.4 Quick Reference Guide

- Test Section size: 9" x 9" x 18"
- Maximum Test Section Velocity: Mach 7 2401 m/sec (5370.88 mph)

- Maximum Solid Blockage ratio defined as the projected area of the test object divided by the total cross-sectional area of the test section: 0.10
- A common Solid Blockage Ratio is 0.05. The cross-sectional area of the test section is 81in2 and the diffuser tube area is 15in^2.
- A typical test specimen mounted to the stinger should have a frontal hydraulic area of around 2in^2 if mounted in the rear 50% of the test chamber and increasing to 8in2 the farther forward the specimen is mounted. The smaller the specimen is, the less interference the results will reflect.
- Maximum tank pressure is 2750 psi, and 240 psi is recommended.

B.0.5 Safety

1. Instructor or authorized personnel must always be in the room while the power supply to the tunnel is on.
2. Keep all objects, including people, out of all parts of the wind tunnel.
3. Keep the test section and parts of the diffuser, frame, and silencer free of debris.
4. Make sure the surrounding area of the wind tunnel is free of debris.
5. Do not put any foreign objects in the test section.
6. Before installing a C-D Nozzle, make sure it is clear of potential blockages.
7. Do not pull or move any of the wires, power supplies, or instruments.
8. Do not open any port or cover on the test section while the wind tunnel is operating.
9. Make sure to step on a portion of the frame with Safety-Walk installed if a user must step on any part of the frame.

10. Make sure tank retention straps, tank retention rails, base plate bolts of the test chamber, diffuser bolts, and silencer bolts are fastened before and after every test.

11. Do not walk in front of the wind tunnel entrance or exit while the tunnel is operating.

12. Wear eye protection and hearing protection any time the wind tunnel is within one step of running.

B.0.6 Testing Guidelines

A. Physical Restrictions of the Tunnel

- Test section is 9" x 9" and 18" long.
- Test section velocity range is Mach 1 - 7.

B. Solid Blockage Ratios

A Solid blockage is the ratio of the frontal hydraulic area of the test specimen to the cross-sectional area of the test section. When a test specimen is observed in the atmosphere, the test section's walls do not affect the flow around the object, and this ratio approaches infinity. During testing of the specimen in the hypersonic wind tunnel, the test section walls affect the flow orientation and behavior around the model and alter the test results from actual real-world conditions. Blockage ratios should be below 0.10 to best avoid significant differences between testing data and real-world conditions. A blockage ratio of 0.05 would be ideal. Refer to the quick reference guide for wind tunnel area data.

C. Wall Correction Factors

Wall correction factors are a method of acknowledging and approximately correcting the presence of the test section walls and their effects on the experimental data

obtained with the testing specimen. The most common flow alteration resulting from the walls is that the streamlines around the test object are much closer together than they would be in the open atmosphere due to unpredictable pressure differences.

B.0.7 Control Panel

A. Electrical Control Panel Configuration - See Figure 3.42

This panel operates on 120 VAC for more significant components and 24 VDC for sensors, relays, solenoids, and auxiliary buttons and lights. Figure 5 shows the component breakdown.

UNQUALIFIED PERSONNEL SHOULD NOT ATTEMPT TO TROUBLESHOOT ANYTHING IN THE CONTROL PANEL UNDER ANY CIRCUMSTANCES.

The PLC is explicitly wired to control the switches and lights separately. In order to add logic to the PLC ladder logic program, follow the diagram shown in Figure 6.

Note: The thermostat is set to 90 degrees F and should be left alone.

Note: If the model or mount develops a problem during a test, immediately press the E-STOP button to end the test as quickly as possible.

B.0.8 Wind Tunnel Sensors and Instrumentation

Pressure Sensor 1 is located on the bottom row of the manifold next to the fill port and has a 0-3000psi operating range. Pressure Sensor 2 is located on the bottom of the Plenum just before the CD Nozzle and has a 0-3000psi operating range. Pressure Sensor 3 is located on the front wall of the test chamber just below the Nozzle port and has a 0-30psi operating range. Temperature Sensor 1 is located on the bottom of the Plenum just before the CD Nozzle and has a 0-500 degrees C operating range. Temperature Sensor 2 is located on the front wall of the test chamber just below the Nozzle port and has a 0-500 degrees C operating range.

B.0.9 Maintenance and Storage

This wind tunnel is designed to require very little maintenance.

The brass Safety relief valve, seen in Figure 2 next to the analog pressure gauge, should be opened periodically to ensure functionality. Poor performance or failure to open would immediately deem the wind tunnel unsafe for operation. The wind tunnel must be depressurized and a new safety pressure relief valve installed.

The threads on the CD Nozzles must be maintained meticulously and carefully cleaned before installation. Any debris must be cleaned with the appropriate cleaner or a thread file in the case of dings, dents, or galling.

High-pressure ball valves have PTFE seals packing the components tightly together to ensure a good seal. This system has three ball valves that require attention. A valve rebuild kit must be installed in even the most minor leak, or valve replacement is required immediately.

The high-pressure fill port is a scuba diving tank fill port. This fill port nipple has a high-pressure check valve built-in with a polymer seal. This seal may fail after a few years of operation. If this seal fails, it must be replaced immediately to ensure a safe pressure seal.

This wind tunnel can be stored under pressure for short periods as long as a safety barrier is established, all the air valves are closed, all the electrical breakers are off, the E-Stop button is depressed, and the pressurized status is made evident to bystanders.

APPENDIX C: Direct6SOFT Programming Panels

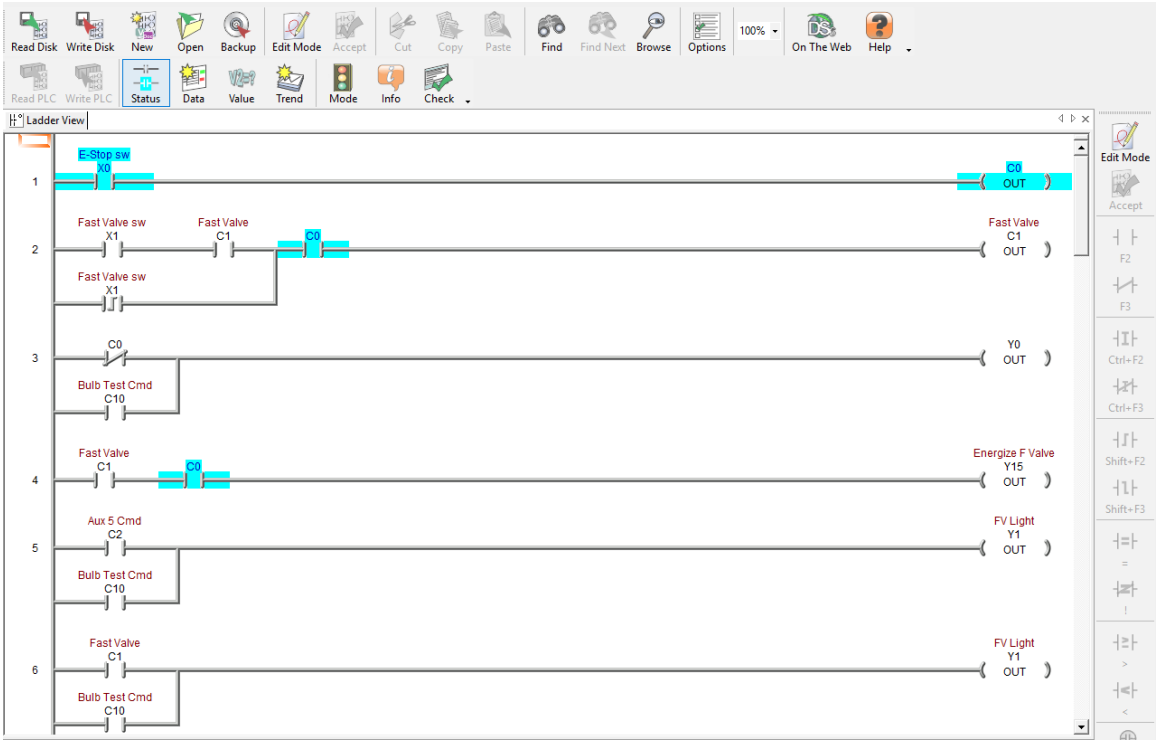

Figure C.1: Direct 6 Ladder Logic program 1.

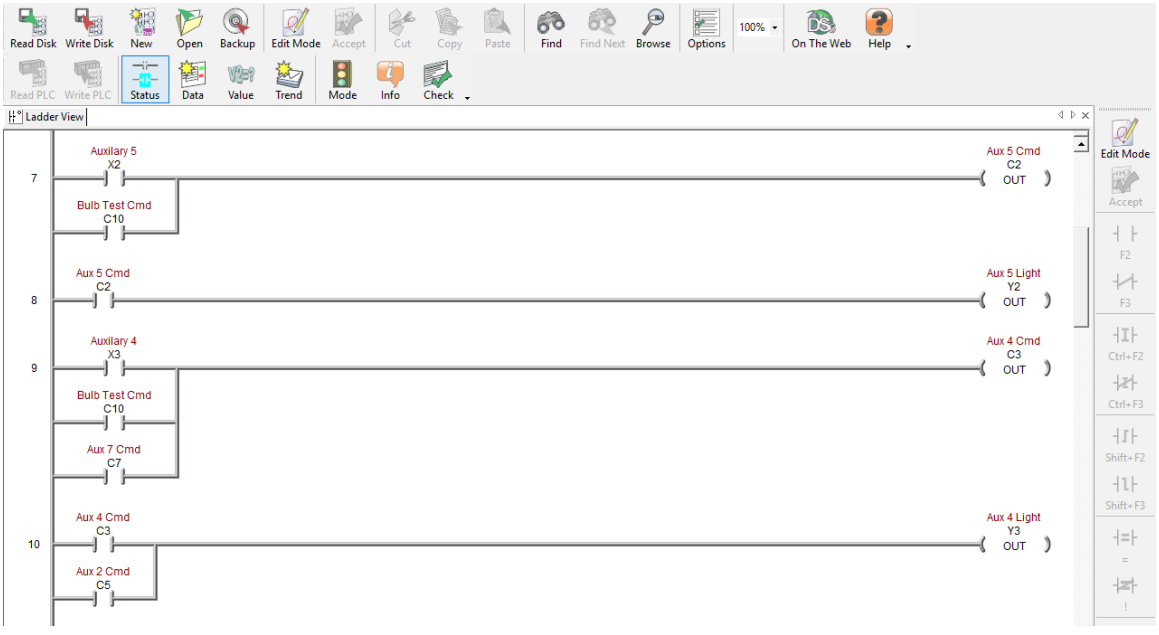

Figure C.2: Direct 6 Ladder Logic program 2.

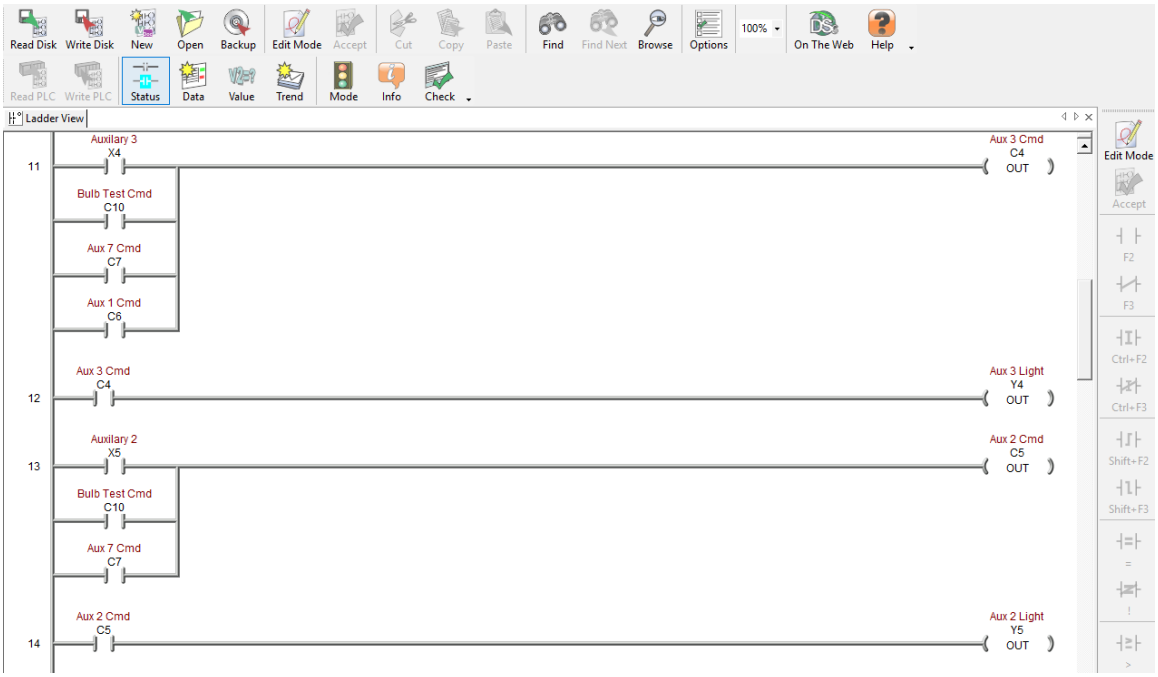

Figure C.3: Direct 6 Ladder Logic program 3.

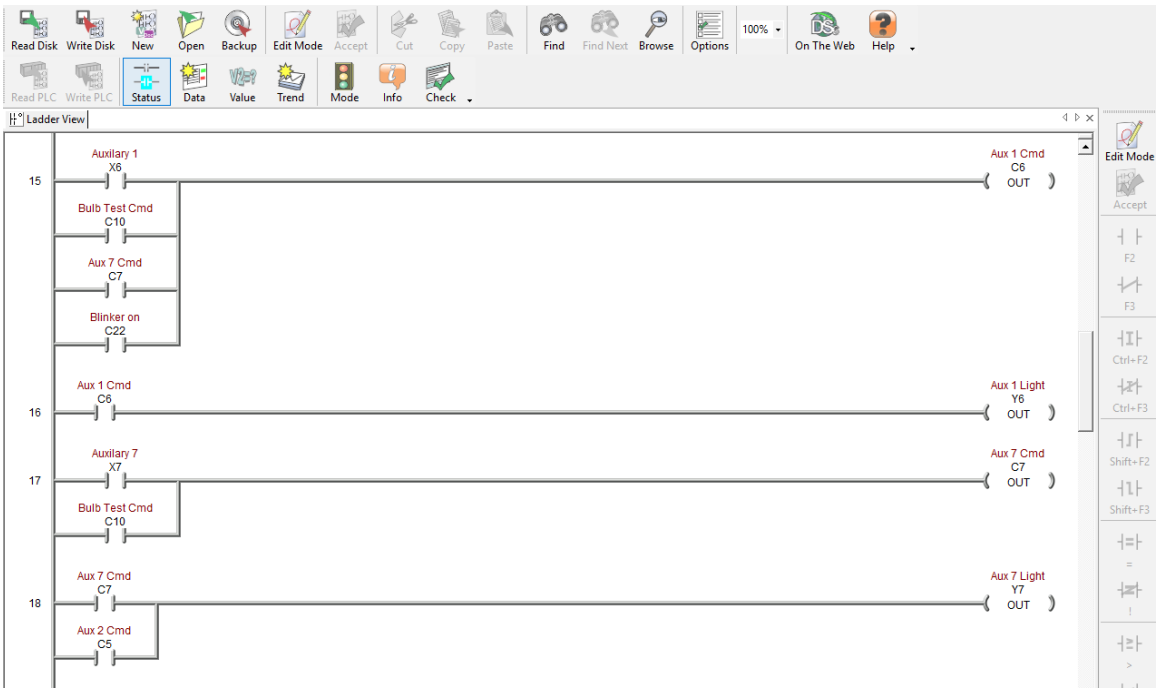

Figure C.4: Direct 6 Ladder Logic program 4.

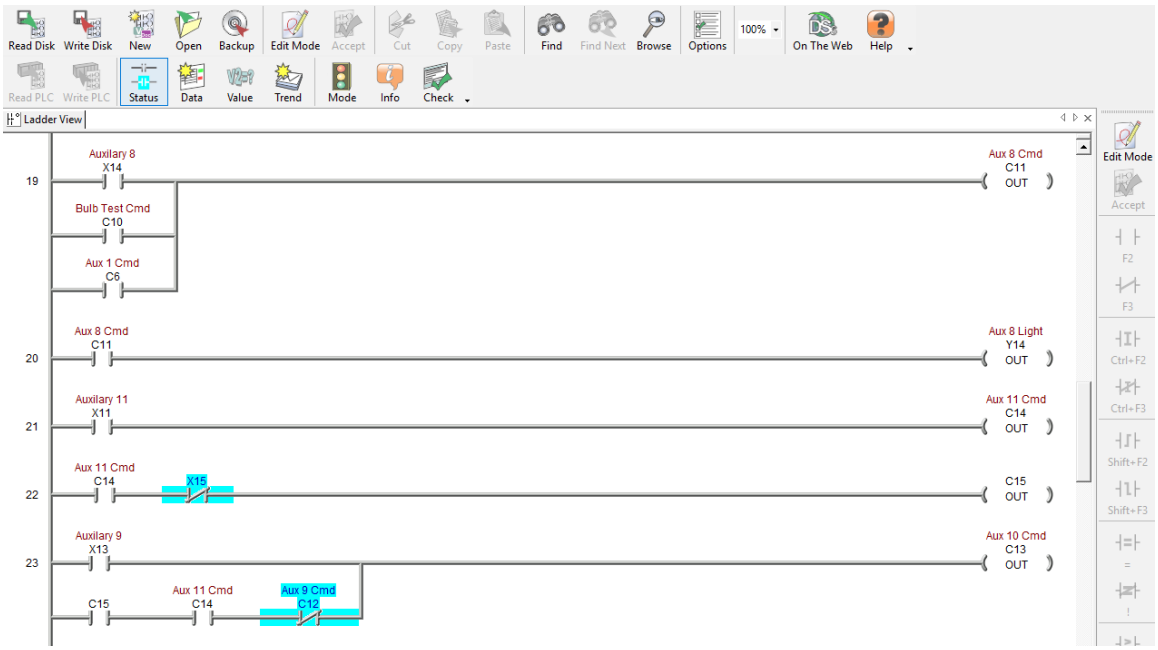

Figure C.5: Direct 6 Ladder Logic program 5.

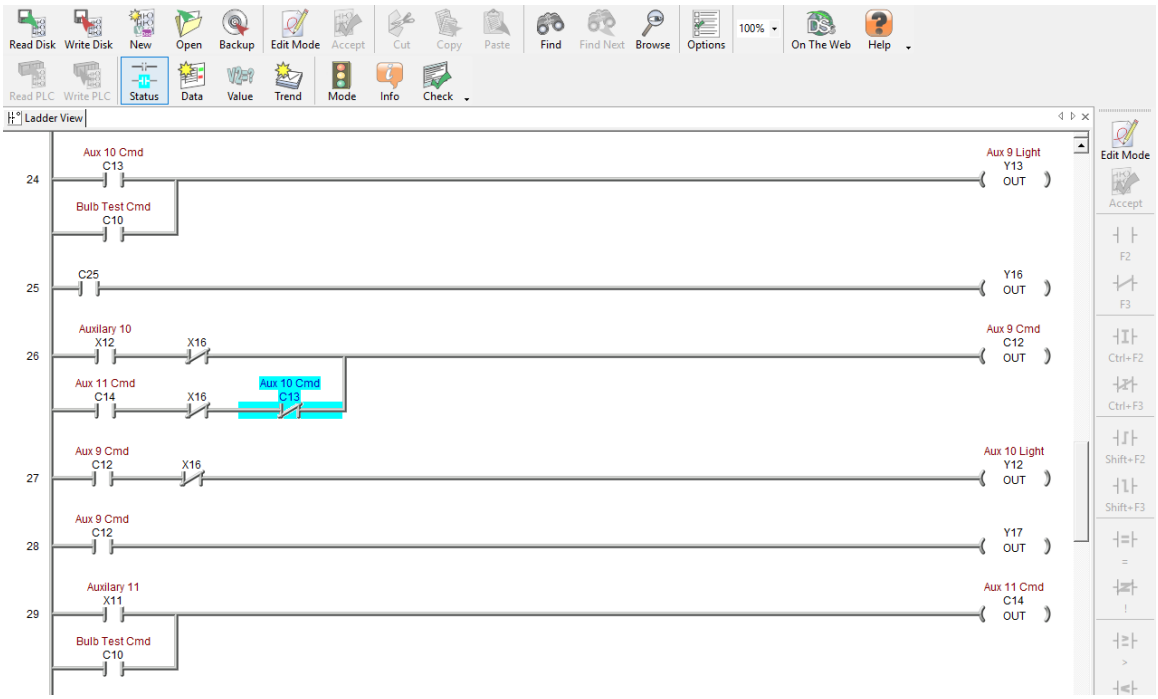

Figure C.6: Direct 6 Ladder Logic program 6.

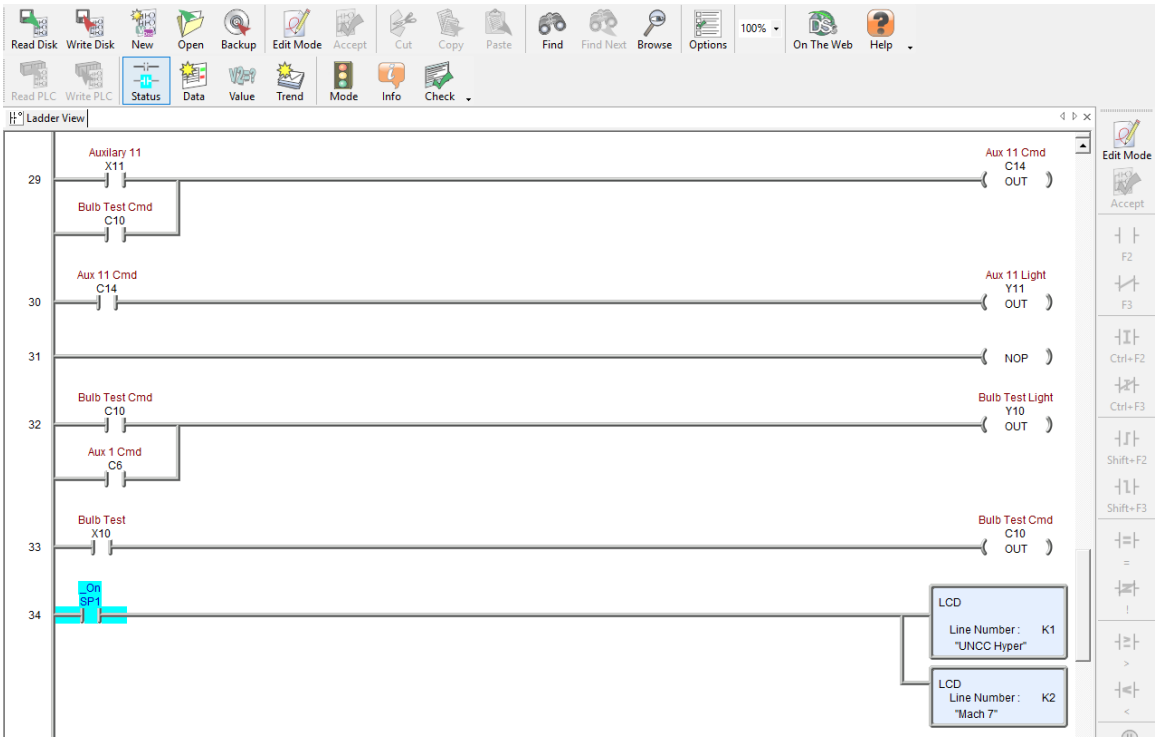

Figure C.7: Direct 6 Ladder Logic program 7.

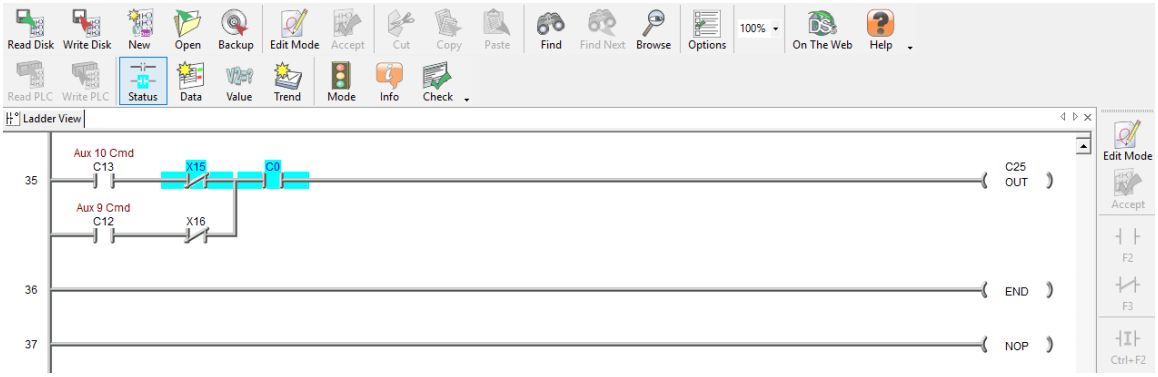

Figure C.8: Direct 6 Ladder Logic program 8.

APPENDIX D: NI LabVIEW Block Diagrams and Front Panel

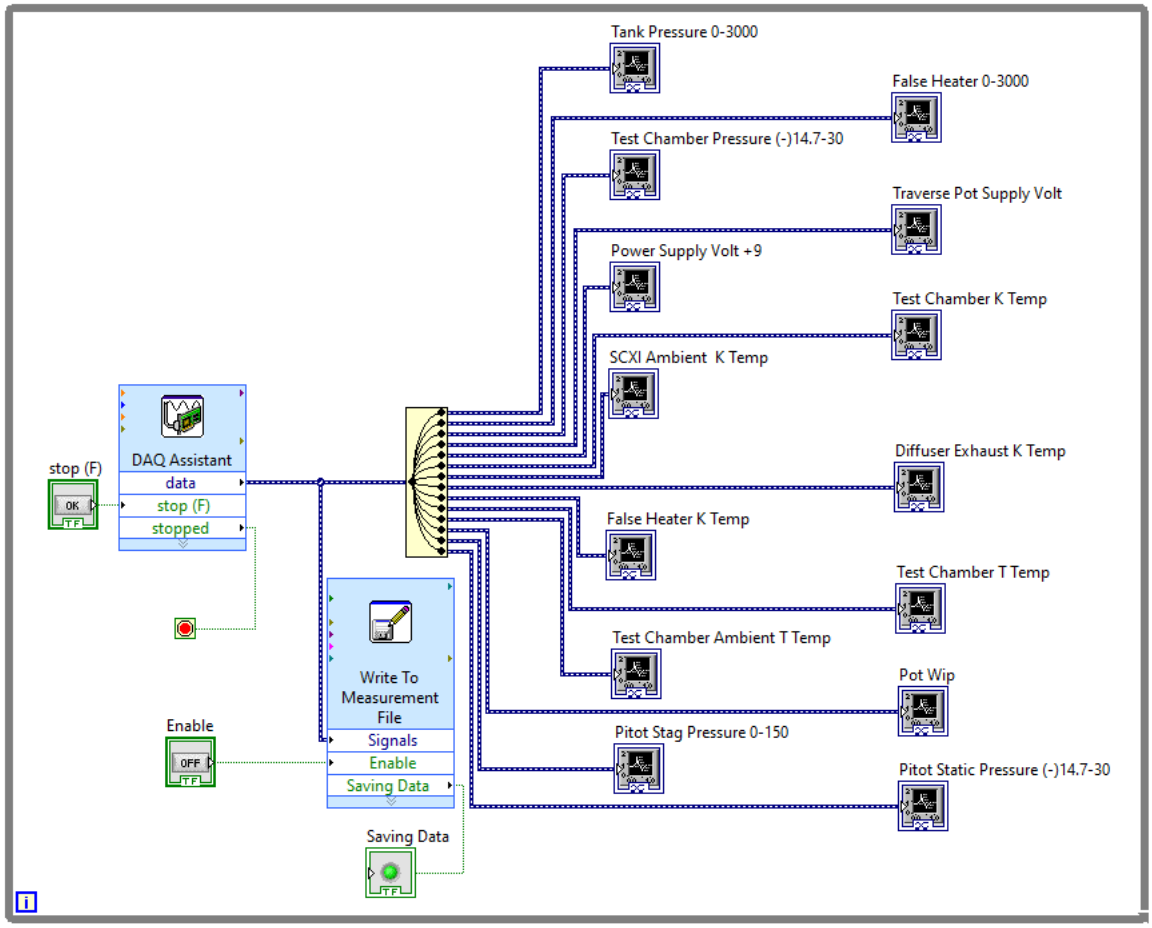

Figure D.1: Image of the UNCC LabVIEW block diagram.

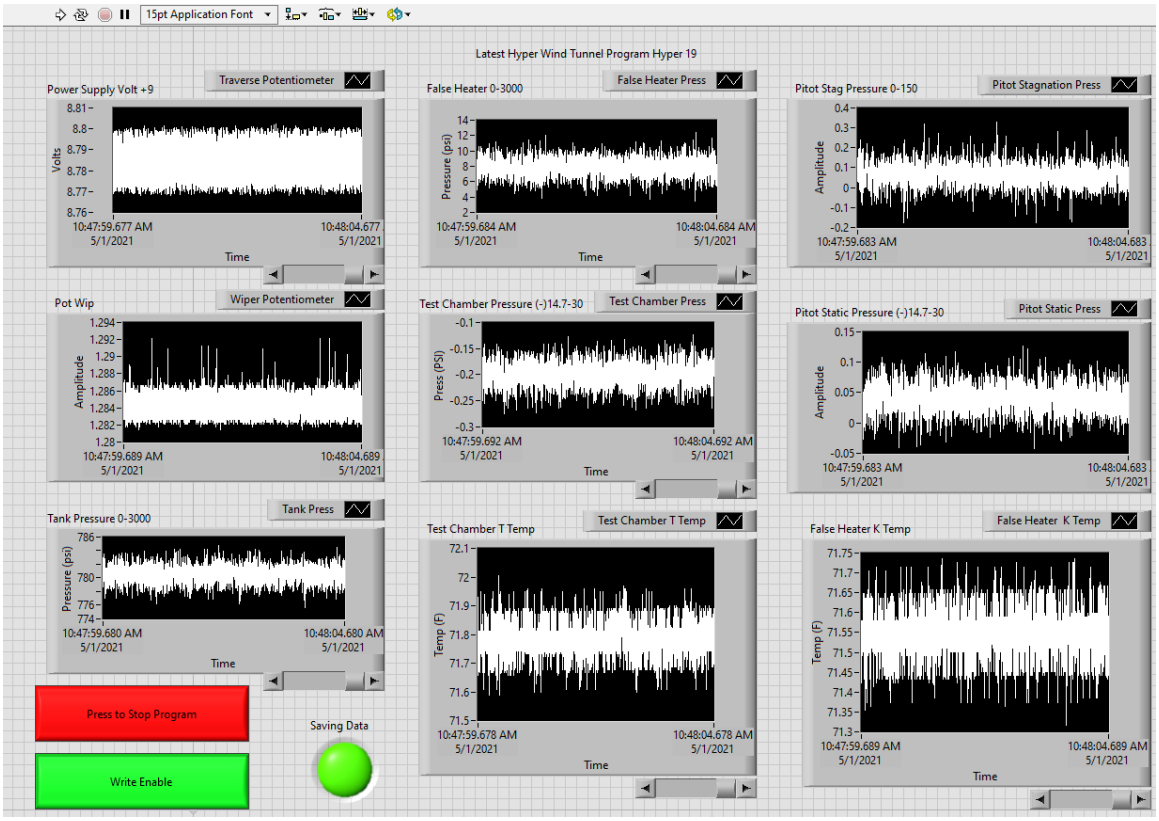

Figure D.2: LabVIEW front panel screen 1.

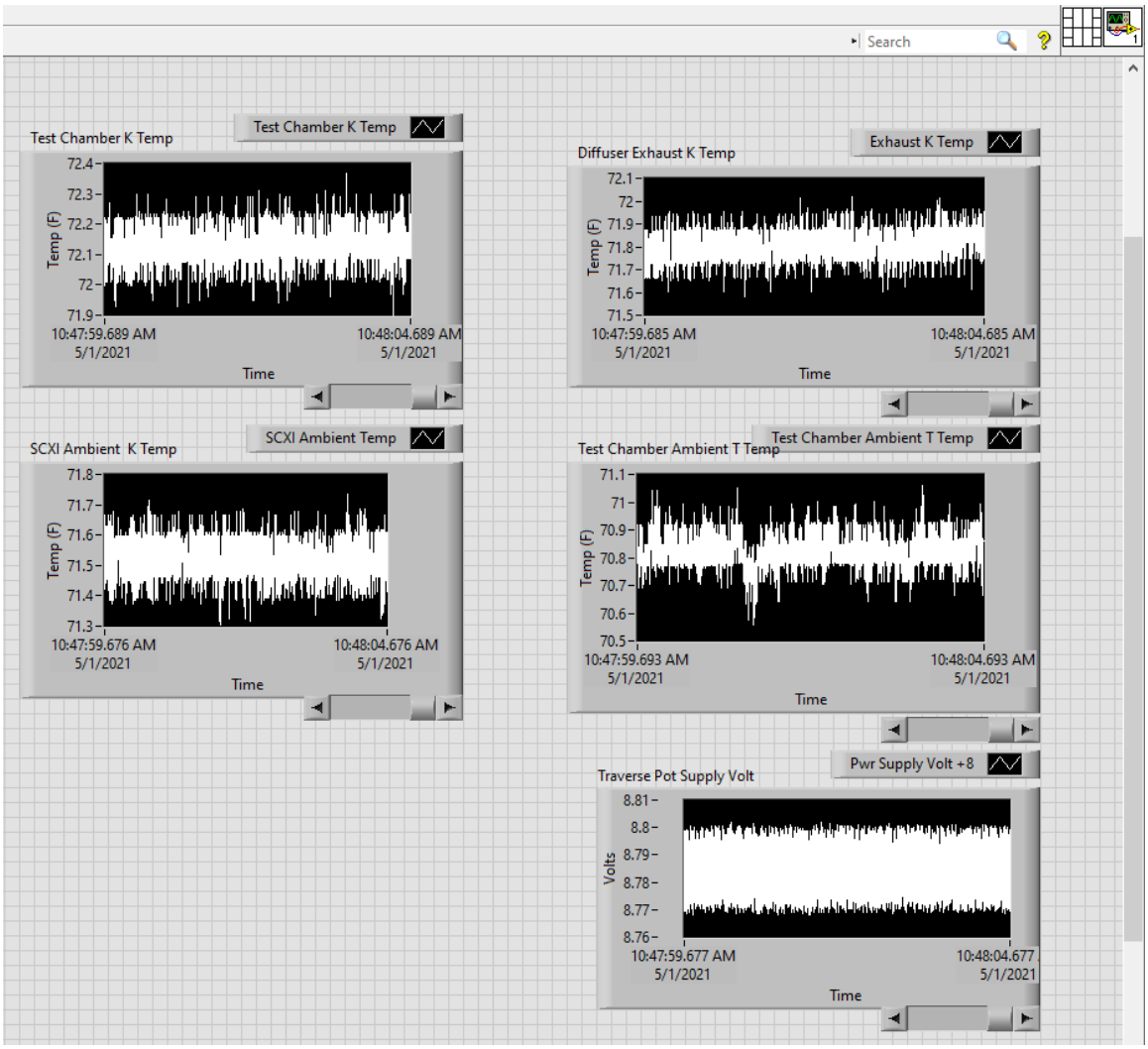

Figure D.3: LabVIEW front panel screen 2.